ANALYTICAL PREDICTIONS OF FLOW INTO AUGER HOLES AND DITCH DRAINS IN HOMOGENEOUS ANISOTROPIC SOIL

A thesis submitted to the
Indian Institute of Technology Guwahati
in partial fulfillment of the requirements for the award of the degree of

DOCTOR OF PHILOSOPHY

By

Wazir Alam

(Roll No: 08610404)

Under the supervision of

Gautam Barua

Associate Professor

DEPARTMENT OF CIVIL ENGINEERING
INDIAN INSTITUTE OF TECHNOLOGY GUWAHATI
GUWAHATI-781039, ASSAM, INDIA

AUGUST 2012

INDIAN INSTITUTE OF TECHONOLOGY GUWAHATI
Department of Civil Engineering
Guwahati -781039
Assam India

CERTIFICATE

This is to certify that the thesis entitled "***Analytical Predictions of Flow into Auger Holes and Ditch Drains in Homogeneous Anisotropic Soil***" submitted by Mr. Wazir Alam, Roll No. 08610404, to the Indian Institute of Technology Guwahati, for the award of the degree of Doctor of Philosophy in Civil Engineering is a record of bonafide research work carried out by him under my supervision and guidance. Mr. Alam has worked on these problems for a period of three and half years and the thesis is, in my opinion, worthy of consideration for the degree of Doctoral of Philosophy in accordance with the regulations of this Institute.

The results contained in this thesis have not been submitted in part or full to any other University or Institute for award of any degree or diploma.

IIT Guwahati
August, 2012

(Gautam Barua)
Associate Professor
Department of Civil Engineering
Indian Institute of Technology Guwahati
Guwahati-781039, Assam, India.

INDIAN INSTITUTE OF TECHONOLOGY GUWAHATI
Department of Civil Engineering
Guwahati -781039
Assam India

STATEMENT

I do hereby declare that the matter embodied in the thesis is a result of research work carried out by me in the Department of Civil Engineering, Indian Institute of Technology Guwahati, Guwahati, Assam, India.

In keeping with the general practice and reporting scientific observations, due acknowledgements have been made wherever the work described is based on the findings of other investigators.

IIT Guwahati
August, 2012

(Wazir Alam)
Research Scholar
Department of Civil Engineering
Indian Institute of Technology Guwahati
Guwahati-781039, Assam, India.

ACKNOWLEDGEMENTS

I express my deep sense of gratitude and indebtedness to my supervisor, Dr. Gautam Barua, Associate Professor, Department of Civil Engineering, Indian Institute of Technology Guwahati, for his valuable guidance, invaluable suggestions, effusive co-operation and help throughout the entire period of my research work. This work would not have been possible without his initiative and guidance, moral support, encouragement and help. I will be always indebted to him for his teachings, motivations and constructive suggestions which have not only developed me academically but also enriched me ethically. He has always been supportive of my efforts and strived to bring the best out of me. His teachings will always be a source of inspiration for me throughout my life.

I would also like to express my deepest sense of reverence and sincere thanks to the chairman of my Doctoral Committee, Dr. S. Talukdar, Professor, Department of Civil Engineering, IIT Guwahati, for his valuable suggestions and help at various stages of this research work.

I express my sincere thanks and deepest sense of gratitude to the members of my Doctoral Committee, Dr. S. A. Kartha, Assistant Professor, Department of Civil Engineering, IIT Guwahati and Dr. S. N. Bora, Professor, Department of Mathematics, IIT Guwahati, for their valuable suggestions, guidance, constructive criticisms and immense help at different stages of this research work. My deepest sense of gratitude and veneration to Dr. C. Mahanta, Professor, Department of Civil Engineering, IIT Guwahati, for his encouragement and indelible inspiration provided during the course of my research work.

I also take this opportunity to thank all the faculty of the Department of Civil Engineering, IIT Guwahati, for their constant support and encouragement throughout the course of this research work.

It is virtually impossible to name all my friends and well wishers with whom I shared many happy moments during my stay here at IIT Guwahati, but I would be failing in my duty, if do not take names of Ratan, Debraj, Hriday, Rajib da, Lalit and Subhadeep for their good wishes, help and support at various phases of this study.

I would also like to offer my love, admiration and respect to Ma, Abba, my family members and in-laws, for their blessings, understandings and moral support without which this work

probably would not have seen the day. Finally, I would like to offer my gratefulness and sincere thanks to my wife, Nashi, for her support, patience, encouragement and for being there with me throughout the course of this research work. Lastly, I am very much thankful to the Almighty, for blessing me with the necessary strength to carry out this study with sincerity and dedication.

August, 2012 (Wazir Alam)
IIT Guwahati

PREFACE

Drainage is essential in many irrigated regions of the world for controlling waterlogging and salinity. For sustainable agriculture, it is essential that salts carried by irrigation water are successfully flushed out from the root zones of plants and a proper soil water balance be maintained in the irrigated fields. One way of leaching salts from a soil profile is to impound the surface of the soil with good quality water in order that water moves through the root zones of crops and in the process takes away a part of the salt present in these zones, the salt rich water is then being drained by a network of equally spaced ditch drains installed for the purpose. Ditch drains are also used to control waterlogging, to provide improved circulation of air in soils and to maintain proper groundwater environment for wild life habitats. Thus, it is vital that due efforts should be made to understand the underlying hydraulics of flow into an array of ditch drains from a ponded field. Further, since a successful design of a subsurface ditch drainage network in a field requires that the directional conductivities of the soil be accurately estimated *in situ*, it is also important that suitable models for evaluation of these parameters in the field be also evolved. Numerical models are generally called upon to solve complex boundary value problems related to flow in complex domains, but for simplified geometries analytical models can also be successfully employed. In this study, an effort is being made to obtain analytical solutions to a few problems of saturated groundwater flow related to water movement to auger holes and ditch drains in a homogeneous and anisotropic soil. These solutions are important as the analytical models for the auger holes can be utilized to estimate the directional conductivities of an unconfined aquifer using results obtained from auger hole tests being performed on the aquifer, and the ponded ditch drainage solutions can be used to design ditch drainage networks for reclaiming waterlogged areas and in cleaning salt affected soils.

The thesis is broadly divided into four chapters. The first chapter gives a brief description about the importance of agricultural drainage in reclaiming salty and waterlogged soils. The chapter also highlights the importance of seeking analytical solutions to various problems related to hydrogeology. The second chapter is about development of suitable steady state auger hole seepage theories for predicting flow to fully and partially penetrating auger holes in a homogeneous and anisotropic water table aquifer underlain by an impervious layer. The

third chapter deals with the development of transient analytical models for studying hydraulics of flow into equally spaced ditch drains receiving water from a horizontal field subjected to a uniform or variable ponding field on the surface of the soil. Chapters two and three are exhaustive and complete in themselves, but still for ready reference, the salient conclusions of each of these chapters are recapitulated in chapter four. Further, there is also an appendix section where, for ease of calculations, shape factors corresponding to a few auger hole flow situations are also provided.

TABLE OF CONTENTS

LIST OF TABLES

LIST OF ABBREVIATIONS

Acad.	= Academy
Agri./Agric.	= Agricultural
Agron.	= Agronomy
Am.	= American
Analy.	= Analytical
ASAE	= American Society of Agricultural Engineer
ASCE	= American Society of Civil Engineers
B.C.	= Boundary Condition
Bull.	= Bulletin
Can.	= Canadian
cm	= Centimeter
Co.	= Company
Comm.	= Commission
Cong.	= Congress
Dan.	= Danish
Dept.	= Department
Dev.	= Development
Div.	= Division
Drain.	= Drainage
Ed.	= Edition
Eng./Engg.	= Engineering
Fig.	= Figure
Geomech.	= Geomechanics
Geophys.	= Geophysical
Ha	= Hectare
Hydrol.	= Hydrology
ICID	= International Commission on Irrigation and Drainage
IDNP	= Indo-Dutch Network Project
IIT	= Indian Institute of Technology
Irrig.	= Irrigation

ILRI	= International Institute of Land Reclamation and Soil Improvement
Inst.	= Institute
Int.	= International
ISAE	= Indian Society of Agricultural Engineers
Jour.	= Journal
kg	= Kilogram
Ltd.	= Limited
l	= Litre
mha	= Million Hectare
m	= Meter
mg	= Milligram
Mang./Manage.	= Management
min	= Minutes
No.	= Number
Numer.	= Numerical
p.	= Page
Pet.	= Petroleum
Pollut.	= Pollution
pp.	= Pages
Proc.	= Proceedings
Pvt.	= Private
Res.	= Research
Resour.	= Resources
Roy.	= Royal
s	= Second
Sci.	= Science
Soc.	= Society
Tech.	= Technology
Trans.	= Transactions

ABSTRACT

Analytical expressions are derived for predicting flow into an auger hole in an unconfined aquifer of finite horizontal and vertical extents and underlain by an impervious substratum. Solutions are provided for two cases, namely, (i) when the auger hole fully penetrates the aquifer up to the impervious base and (ii) when the hole suspends above the base layer. The validity of the developed analytical solutions are checked by drawing parallel numerical models for a few flow situations and then comparing the analytical predictions with the corresponding numerical ones. A further check on the developed equations is performed by first reducing these solutions (by letting the finite horizontal extent of the aquifer to become large) to account for a phreatic aquifer of large (theoretically infinite) horizontal extent and then comparing the analytical results obtained from them with corresponding results obtained from the analytical works of others for a few flow situations. From the study, it is seen that the zone of influence of an auger hole test in a water table aquifer underlain by an impervious layer may be considerable, particularly if the test is being carried out in an aquifer having a high anisotropy ratio (ratio of horizontal to vertical hydraulic conductivity of soil). Further, the study also reveals that the thickness of an unconfined aquifer, extent of penetration and level of water in an auger hole, play an important role in determining flow into the hole and hence due care must be taken to include these parameters in the mathematical analysis of the problem. The developed equations can be used to determine the directional conductivities of a phreatic aquifer by making use of results obtained from a typical auger hole test and can also be utilized to estimate the horizontal domain of influence associated with the test. This is important because the soil volume over which the directional conductivities of an aquifer is being sensed in a standard auger hole test is generally believed to be confined close to the centre of the hole and the existing auger hole seepage theories are not able to estimate this capture zone as these theories have been developed with the assumption of an aquifer of infinite horizontal extent. For ease of computation, shape factors (a shape factor is a coefficient which when multiplied with the rate of rise of water in a pumped auger hole, gives the hydraulic conductivity of the surrounding soil) for a wide range of auger hole flow geometries are being provided in the text so that a field practitioner can take advantage of these values in the design of an auger hole experiment. That way, a

field practitioner can make a direct use of these factors for converting a set of auger hole test data obtained from a phreatic aquifer into the directional conductivities of the aquifer as well as for estimating the horizontal extent of the disturbed zone arising due to the test, without the necessity of going through the intricate details of the developed solutions.

Analytical solutions are also provided for predicting time dependent seepage into an array of equally spaced parallel ditch drains in a homogeneous and anisotropic soil medium underlain by an impervious layer and receiving water from a ponded horizontal field of infinite extent when (i) the levels of water in the ditches are equal and the depth of ponding is uniform, (ii) the levels of water in the adjacent ditches are unequal ditches and the depth of ponding is uniform and (iii) levels of water in the adjacent ditches are unequal and the depth of ponding is non-uniform. Even though independent solution for each of these three cases are being provided in the text, the solutions of the first two cases can also be reached from the general solution obtained for the third case, a fact which is being demonstrated in the text with the help of a few examples. The validity of the developed solutions are tested by first reducing them to corresponding steady state solutions and then comparing predictions obtained from them for a few flow situations with identical predictions obtained from the analytical works of others. Further, a MODFLOW check on the general solution [case (iii)] is also being carried out. From the study, it is seen that the specific storage of soil influences the time required for a transient ditch drainage system to move to the steady state situation; a relatively longer time is required for a soil with a high specific storage coefficient than that for a soil with a low specific storage coefficient. The discharge from the top of the field as well as through the sides of the drains are found to be influenced by the directional conductivities and specific storage of soil, spacing, depth and levels of water in the ditches and depth of ponded water over the surface of the soil. The surface discharge distribution is found to show relatively greater uniformity at the early stages of simulation but with the progress of time, the extent of uniformity is found to reduce particularly for cases where the soil is subjected to a uniform depth of ponding. However, even when a soil surface is subjected to a constant depth of ponding, a high anisotropy ratio of the soil alone may lead to a marked improvement on the uniformity of the surface discharge distribution at all times in comparison to a soil having a low anisotropy ratio. A better uniformity of surface discharge may also be achieved by suitably adjusting the depths of ponding over the

soil surface – regions close to the ditches be provided with zero or negligible depths of ponding and the ponding depths may be made to progressively increase with the increase in distance from the ditch faces. It is hoped that the solutions provided herein will lead to a better and realistic design of ditch drainage networks for controlling waterlogged areas, providing a balanced subsurface water environment for the wildlife habitats and in reclaiming salt affected soils.

Keywords: Analytical models; Unconfined aquifer; Horizontal and vertical extents of aquifer; Auger hole test; Fully and partially penetrating auger hole; Hydraulic conductivity; Anisotropy; Shape factor; Ditch drains; Transient seepage; Non-uniform ponding depth; Specific storage.

CHAPTER 1

INTRODUCTION

1.1 General Background

World's food production needs to be augmented to the tune of 38 percent by 2025 and 57 percent by 2050 if global food requirements to the ever increasing population are to be maintained at the current levels (Wild, 2003). This challenge mostly is to be met by utilizing lands which have already been used for cultivation as bringing in new areas for agriculture may either be not possible in many places or, even if possible, may not be desirable (Rengasamy, 2006). Thus, the thrust is to be given to increase the productivity per unit area of the agricultural lands rather than increasing the overall area under cultivation (Rengasamy, 2006). Irrigation has played a key role in the past, and is expected to play a pivotal role in the future as well, in enhancing agricultural productivity. It is expected that the irrigation coverage of the developing countries will rise by as much as 242 million hectares by 2030 (Faures et al., 2002). In India, about 34 percent of the total arable land, amounting to 57 million hectares, is under irrigation (ICID, 2003) and this coverage is expected to rise substantially in future. The introduction of irrigation water in the agricultural fields, however, has brought in its wake the twin problems of waterlogging and salinity in many arid, semi-arid and low-lying regions of the world and about 831 million hectares of land was estimated by FAO in 2000 to be affected with the problems of soil salinity and alkalinity (Martinez-Beltran and Manzur, 2005) spanning across all the continents of the globe. In India, about 8.4 million hectares of irrigated land in the country was estimated to be afflicted with the problems of soil salinity and alkalinity, out of which about 5.5 million hectares was also waterlogged (IDNP, 2002). Further, as per CSSRI Vision 2030 (2011) document, this figure is expected to go up by about 15.5 million hectares by 2030. The chief causes of waterlogging in an irrigation command are seepage from water carrying systems, faulty water regulatory structures and silting and plant growth on the irrigation canals (Brahmabhatt et al., 2000; Datta et al., 2004). The combined effect of salinity, alkalinity, acidity, waterlogging and toxicity of soil not only has a negative influence on the quality and quantity of agricultural produce but, in the worst case, a soil may become totally unfit for cultivation (Dagar, 2005). Plants growing in waterlogged areas are also often quite vulnerable to salinity, particularly in their early stages of growth

(Barrett-Lennard, 2002). In India, due to problems of waterlogging and salinity, productivity of vast tracts of agricultural lands were found to have dwindled with time after the introduction of irrigation in these areas (Manjunatha et al., 2004; Ritzema et al., 2008).

Several experimental studies [Wesseling, et al., 1957; Rhoades, 1974; Skaggs and Van Schilfgaarde (editors), 1999; Datta et al., 2000; Datta and Jong, 2002; Manjunatha et al., 2004; Sharma and Gupta, 2006; Ritzema et al., 2008 – to name a few] have shown that subsurface drainage, carried out either through tile or ditch drains, can be successfully employed to arrest the dual problems of waterlogging and salinity in irrigated lands. The technology has already been proved to be successful in reclaiming more than 50,000 hectares of saline waterlogged soils in different parts of the country (CSSRI Vision 2030). Further, subsurface drainage has been found to have a profound impact in enhancing crop yields; the introduction of the technology has brought about an increase in yield of paddy by 45 percentage, in wheat by 111 percentage, and in cotton by a whopping 215 percentage (CSSRI Vision 2030). Reclamation of a salt affected soil often entails impounding the surface of the soil with good quality irrigation water with the intention that water moves through the soil and in the process takes away a part of the salt present in the soil profile, the salt laden water is then being drained by a system of subsurface drains installed for the purpose. Recuperation of a sodic soil is similar to that of a saline soil except that here one has to first replace the sodium ions present in the soil with that of calcium ions and then leaching out the displaced sodium ions from the soil profile. It is to be noted that the addition of a calcium containing mineral like gypsum to a sodic soil replaces the adsorbed sodium in the double layer with calcium and, in the process, makes the thickness of the double layer to decrease. This, in turn, causes the soil colloids to flocculate causing water movement through the soil to take place with relative ease (Kirkham and Powers, 1972). Ditch drains are widely used in agricultural fields for many purposes – to have a control on the water table, to provide waterlogged free environment for growing crops sensitive to water stagnation and pooling, to provide improved air circulation in soils, to reclaim salt laden soils and wet lands, to control groundwater environment for wild life habitats, to mitigate phosphorous loads of agricultural fields – to name a few (Youngs, 1994; Dils and Heathwaite, 1999; Heathwaite and Dils, 2000; Kroger et al., 2008). Because of multifarious

uses of a ditch drainage system, it is imperative that due care should be exercised to know their underlying hydraulics in detail so that efficient drainage systems for various purposes can be designed. It should be noted that, working out a suitable model of groundwater flow into ditch drains alone is not enough; efforts should also be made to see that the hydrogeological constants appearing in the model are also correctly estimated in the field, as otherwise the model's outputs may not give accurate results. The most important soil parameters which need to be estimated for successful design of a ditch drainage network are the saturated hydraulic conductivities of the soil in the horizontal and vertical directions, respectively. Thus, appropriate mathematical models for translating field measurements corresponding to various hydrogeological settings into directional conductivities of saturated soils need also be worked out.

A mathematical model is an approximate illustration of a real flow situation where, in general, a set of governing equations based on some fundamental laws of nature are being utilized to imitate the real situation (Wang and Anderson, 1982). Apart from the governing equations, a mathematical model must also embrace in its fold the boundary conditions of the flow domain proposed to be studied along with the status of the flow system at a reference time (initial condition). Mathematical models may range from a simple to a very complex one and can be utilized to study a wide many hydrogeological flow situations. Since a mathematical model is an effort to impersonate a real flow situation with the help of an equation or a set of equations, it is obvious that, for the model to succeed, the concerned differential equation or equations need to capture the actual flow situation within a reasonable degree of accuracy, as otherwise the model's outputs may differ significantly from that of real values. However, with the rapid advancement of knowledge in the field of subsurface hydrology and allied areas and the arrival of fast computing machines, solutions to many complex subsurface transport flow problems can now be obtained quite precisely. Mathematical models are basically of two types, analytical and numerical. Analytical models are generally developed for simplified geometries whereas numerical models are for more complicated situations (Walton, 1979, 1989). But with the development of newer techniques and methods, analytical models are now increasingly developed to study complex hydrogeological situations as well. Numerical models, in general, are more realistic and adaptable than analytical models but may require a large database which may be

difficult to obtain or expensive or both. Moreover, the convergence of a numerical scheme must be ensured before its predictions can be used with confidence. Analytical models, on the other hand, generally require less data than the numerical models and, if properly developed, the outputs from these models can be highly relied upon. Analytical models are also extensively used to check numerical codes and also to gain a better insight on the flow processes associated with various groundwater flow problems (Kacimov, 1997; Haitjema, 2006). Sometimes, a flow problem can also be tackled by a judicious mix of both analytical and numerical models (Nunes et al., 2002). Thus, even though analytical models are based on relatively simpler assumption and are mostly for less complicated geometries as compared to numerical models, for many flow situations they may be the most appropriate ones to apply.

An accurate estimation of various hydrogeological parameters of an aquifer in its natural state is pivotal to the understanding of various flow and transport processes through the aquifer (Dane and Topp, 2002). The most commonly used method of estimating *in situ* directional conductivities of a water table aquifer is the auger hole method. In this method, a cylindrically drilled hole in an aquifer is stressed by bailing out water from the filled hole and then relating the resultant time rate of increase of the water level in the pumped hole to the hydraulic conductivity of the encompassing aquifer soil with the aid of a suitable auger hole seepage theory. The procedure was explained in detail by Van Bavel and Kirkham (1948), Bouwer and Jackson (1974), Oosterbaan and Nijland (1994), Barua and Tiwari (1995), Smith and Mullins, (2000), among others. It should be noted that all the auger hole seepage theories currently available for the water table aquifers and developed for different hydrogeological conditions are based on the assumption of the aquifers extending to infinity in the horizontal domain. However, for artesian aquifers, Barua and Hoffmann (2005, 2007) provided the necessary auger hole theories both for the cases when the hole is being underlain by an impervious barrier and when it is being underlain by a gravel substratum, and provided appropriate shape factors for these situations. An analysis of these shape factors (Barua and Hoffmann, 2005, 2007) for an artesian aquifer for both the impervious (i.e., hole underlain by an impervious layer) and gravel (i.e., hole underlain by a gravel layer) situations shows that the change in values of these factors becomes immune to the changes in the distance of the outer layer at large distances from the centre of the hole. Thus,

if the outer layer lies at a large distance from the centre of the hole, the overall hydraulics of flow into a cylindrical hole in a confined aquifer is found to be not much impacted by this distance of the hole and the infinite horizontal extent aquifer assumption, which is often made while solving problems of this nature, appears to be a valid one for such a situation. However, incorporation of the horizontal extent of an aquifer into the mathematical framework of the auger hole solution is definitely having a very strong advantage since an application of such a solution would then enable an user to quantify the capture zone over which the conductivity of an aquifer is actually been measured in the field, a zone which would simply be not possible to locate using the conventional auger hole theories developed with the infinite aquifer assumption. There are currently no auger hole seepage models which can predict flow to an auger hole in an unconfined aquifer of finite horizontal and vertical extents and underlain by an impervious layer, both for the cases when hole fully penetrates the aquifer and rests on an impervious layer and when the hole partially penetrates the aquifer and remains suspended at a finite distance above an impervious base. There is, however, an immediate necessity of developing suitable auger hole seepage models for these flow situations as these models, once developed, can then be used to estimate both the directional conductivities as well as the capture zone associated with a typical auger hole test utilizing auger hole experimental results obtained below a water table. It should, be noted that, in general, the properties of a soil vary with space and the assumption of homogeneity of a soil may not hold strictly in practice. However, since the auger hole method actually measures the average hydraulic conductivity of a saturated soil and deals with a large soil space (Van Bavel and Kirkham, 1948; Luthin, 1957; Van Beers, 1983; Oosterbaan and Nijland, 1994), the averaging of the directional conductivity values over a representative elementary volume (REV) at a location in the saturated poro-space can be treated as representative for all the REVs of the considered poro-space without introducing much error. Infact, Dorsy (1990) found the method to be one of the most reliable methods of estimating saturated hydraulic conductivity in fields (see also Kacimov, 2000).

As mentioned before, ditch drains are widely used in many parts of the world for reclaiming waterlogged and salt affected soils. The quantity of base flow entering into ditch drains is essential to be evaluated in order to have a proper understanding on the flow and nutrient dynamics of a watershed (Goswami and Kalita, 2009, 2010). For sustaining irrigated agriculture, it is essential that the salts transported to the root zones of plants by irrigation water must not be allowed to rise above the tolerance level of the planted crops. Leaching of salt affected soils by good quality water and then disposing the salt laden water via subsurface drains, has been a commonly accepted method of reclaiming salt affected soils for quite some time now (Dielman, 1973; Martinez Beltran, 1978). In order that appropriate ditch drainage networks are being designed in the field for controlling soil salinity and waterlogging, it is imperative that the underlying hydraulics of flow to a system of subsurface ditch drains be properly understood. Numerous studies on the ponded drainage problem (Kirkham, 1950, 1960, 1965; Dielman, 1973; Martinez Beltran, 1978; Rao and Leeds-Harrison, 1991; Youngs, 1994; Barua and Tiwari, 1995; Youngs and Leeds-Harrison, 2000; Chahar and Vadodaria, 2008a, 2008b, 2011 – to name only a few) have shown that the streamline distribution in a ponded drainage scenario gets concentrated to regions close to the drains and as one moves away from the centre of the drains, the steady surface flux to the drains gets markedly reduced. This is observed to be true both for situations when a ponded field is subjected to a zero or a non-zero uniform depth of ponding at the surface of the soil. Thus, leaching of a salt affected soil vide a network of ditch drains receiving water from a ponded field of zero or a non-zero uniform depth of ponding will lead to over washing of the regions close to the drains and under washing of areas further away from the drains. One way of circumventing this problem is to drain the soil profile in stages; complete ponding followed by increasingly decreasing the area of ponding or starting from a small fractional area of ponding and then progressively extending the ponding area to the full surface area of the field, may be adopted to achieve the purpose (Rao and Leeds-Harrisson, 1991; Youngs and Leeds-Harrisson, 2000). Another way of achieving a better cleaning of a salt affected soil is to subject the soil to a variable depth of ponding with the ponding depth made to progressively increase with the increase in distance from the centre of the ditch drains. But for this procedure to be successful, it is important that a proper study analyzing flow behavior to ditch drains from a ponded field subjected to a variable depth of ponding

be carried out. There appears to be currently no in-depth study for the ponded ditch drainage problem with a variable ponding field using an analytical platform. Further, even for situations when a soil surface is imposed with a zero or non-zero uniform depth of ponding, all the available analytical models for such situations are based on the assumption of steady state flow. However, to obtain a better insight of the flow behavior to the ditches it is crucial that the transient dynamics of flow to the ditch drains be properly understood.

From the above review, it is apparent that there is a necessity to develop suitable solutions to the fully and partially penetrating auger hole problems for an unconfined aquifer of finite horizontal and vertical extents so that directional conductivities of a water table aquifer as well as the soil space over which the directional conductivities of the aquifer is being measured in a typical auger hole test, can be estimated utilizing results obtained from such a test being performed in the aquifer. It can also be seen that there exists a need to carry out a comprehensive study on the hydraulics of a ponded ditch drainage system so that efficient drainage networks for cleaning of salt affected soils as well as for reclaiming of waterlogged areas, can be designed. Considering all these in view and remembering the importance attached to analytical models, an effort has been made in this study to achieve the objectives as listed below.

1.2 Objectives

(i) To study hydraulics of an auger hole in an unconfined aquifer of finite horizontal and vertical extents both for flow situations when (a) the hole fully penetrates the aquifer and rests on an impervious layer and (b) the hole partially penetrates the aquifer and remains suspended at a finite distance above an impervious layer.

(ii) To work out analytical expressions which may be used to predict transient seepage into an array of equally spaced ditch drains fully penetrating a homogeneous and anisotropic aquifer and receiving water from a ponded field when (a) the water level heights in between the adjacent drains are equal and the ponding depth over the surface of the soil is uniform, (b) the water level heights in between the adjacent drains are unequal and the ponding depth over the surface of the soil is uniform and (c) the water level heights in between the adjacent drains are unequal and the ponding field over the surface of the soil is non-uniform.

CHAPTER 2

HYDRAULICS OF AN AUGER HOLE IN A HOMOGENEOUS AND ANISOTROPIC UNCONFINED AQUIFER OF FINITE HORIZONTAL AND VERTICAL EXTENTS

In this chapter, hydraulics of an auger hole in a homogeneous and anisotropic phreatic aquifer of finite horizontal and vertical extents is studied both for situations when the hole penetrates fully the aquifer and resides over an impervious layer and when the hole partially penetrates the aquifer and there exists an impervious layer at a finite distance from the bottom of the hole. Analytical expressions for the hydraulic head function, the stream function and the discharge rate to an auger hole, are derived for all these flow situations. Several comparison tests with other simplified models are carried out to ascertain the validity of the developed analytical models. A few numerical checks on the proposed solutions are also performed using Processing MODFLOW (Chiang and Kinzelbach, 2001). The effects of various auger hole flow parameters like geometries of an auger hole, the nature of the underlying layer below the hole, anisotropy, directional conductivities and horizontal and vertical extents of a phreatic aquifer, on the flow behavior around a stressed auger hole are also studied. The applications of the proposed solutions in estimating the directional conductivities of a phreatic aquifer utilizing results obtained from auger hole tests being performed on the aquifer, are demonstrated with the help of a few examples. Further, in these examples, the procedures to be followed for estimating the capture zone associated with an auger hole test, are also explained.

2.1 Introduction and Review of Related Work

An accurate estimation of various hydro-geological parameters of an aquifer is pivotal to the understanding of various flow and transport processes through the subsurface. A widely used and reliable method of estimating in-situ saturated hydraulic conductivity of a shallow water table aquifer is the auger hole method (Dorsey et al., 1990). The auger hole method of estimating hydraulic conductivity of a phreatic aquifer was described in detail by many, viz., Van Bavel and Kirkham (1948), Reev and Kirkham (1951), Bouwer and Jackson (1974), Oosterbaan and Nijland (1994), Barua and Tiwari (1995) – to mention a few. This method essentially consists of inducing a stress in a phreatic aquifer by bailing out a part of water

instantaneously from a cylindrically drilled hole (auger hole) of known dimension into the aquifer and then relating the consequential rate rise of water in the pumped hole to the directional conductivities of the adjoining soil medium by means of the suitable auger hole seepage theory. For an auger hole fully penetrating a water table aquifer of infinite horizontal extent and resting on an impervious base, Kirkham and Van Bavel (1948) provided a steady state theory of flow into the hole by assuming a horizontal water table around the hole and, at the same time, neglecting the capillary effects over it. Kirkham and Van Bavel (1948) also performed electric analog experiments to determine shape factors (a shape factor is a coefficient which expresses the relationship between the rate of rise of water in a pumped auger hole with the saturated hydraulic conductivity of the surrounding soil) corresponding to auger hole flow situations when the holes do not go all the way upto the impervious layer but are kept suspended above it. Ernst (1950), as reported by Van Beers (1958) and Boast and Kirkham (1971), used relaxation drawings to work out shape factors for partially penetrating auger holes in soils of infinite effective depth. Kirkham (1958) extended the earlier work of Van Bavel and Kirkham (1948) and presented a general seepage theory for predicting steady flow into a partially penetrating auger hole in an unconfined aquifer underlain by an impervious layer by splitting the flow domain into two sub-domains and then working out suitable hydraulic head expressions for each of these regions. Later, Boast and Kirkham (1971) solved the same auger hole problem as well as the one resulting due to the existence of a gravel layer at a finite distance from the bottom of auger hole, by making use of the normal equations and the Gram-Schmidt orthonormalization methods and provided suitable shape factors for a wide range of auger hole flow situations. Barua and Tiwari (1995) also offered an alternative solution to the auger hole problem for the 'impervious' case (i.e., when the hole is underlain by an impervious layer) by utilizing a different combination of Fourier series from the ones considered by Kirkham (1958) and Boast and Kirkham (1971) in their model development and argued that their solution is expected to be computationally simpler than those of Kirkham's (1958) and Boast and Kirkham's (1971) solutions, particularly when large term expansions (and hence better estimates of the conductivity values) of the involved infinite series are being carried out. Barua and Hoffmann (2005, 2007) also provided analytical expressions for predicting steady flow into a partially penetrating auger hole in a

confined aquifer of finite horizontal and vertical extents both for situations when the hole is being underlain by an impervious layer and when it is being underlain by a gravel substratum. Topp and Zebchuk (1986) reported that considerable error in the hydraulic conductivity estimates obtained vide the auger hole method may result if proper care is not taken to measure accurately the diameters of the experimental auger holes. Reeve and Kirkham (1951) reported that horizontal conductivity can be approximately sensed by performing the auger hole experiment with long and thin auger holes and the vertical conductivity may be estimated by carrying out the experiment with broad and shallow auger holes. By suitably combining the two-well method of Childs (1952) and the tube method of Kirkham (1945), Childs et al. (1957) estimated the directional conductivities of an unconfined aquifer. Talsma (1960) utilized experimental results obtained from two piezometers of varied cavity lengths to work out the directional conductivities of a phreatic aquifer. Both Child's (1957) and Talsma's (1960) methods, however, rely on the tube method for measuring the apparent hydraulic conductivity of an aquifer, which is a disadvantage since the tube method measures the apparent hydraulic conductivity of only a small volume of soil and as such the measured directional conductivities may not be a true representation of the actual field values. Healy and Laak (1973), as reported by Bouwer and Rice (1983), explored the possibility of using broad and shallow auger holes (pits) for determining the saturated hydraulic conductivity of stony soils by making use of the Thiem's equation to translate the rate of recovery of a pumped pit into the directional conductivity of the surrounding soil. Bouwer and Rice (1983), however, pointed out that Thiem's equation cannot be applied to pits that only partially penetrate an aquifer and do not go all the way up to the impervious base. They provided alternate shape factors for pits by performing an extrapolation of the piezometer theory of Youngs (1968), which may be utilized to estimate the directional conductivities of a water table aquifer using auger hole experimental results obtained from two auger holes (pits) of different geometries. These shape factors of Bouwer and Rices', however, are reported by Boast and Langebartel (1984) to be about 20 percent greater than that obtained by Bouwer and Rice (1983) from their sand tank studies on broad and shallow auger holes. By taking suitable limits to the analytical results of Boast and Kirkham (1971), Boast and Langebartel (1984) worked out suitable shape factors applicable

to broad and shallow pits for interpreting pit test results. Further, Lomen et al. (1987) presented a steady state analytical expression which may be used to infer experimental data obtained from axially symmetric auger holes and pits of arbitrary geometries. Directional conductivities of a soil column below the water table can also be estimated in the laboratory with the help of suitable devices (Kessler and Oosterbaan, 1980). The main drawback of these laboratory tests is that the volumes of soil over which the experiments are being performed are generally much smaller than those of field tests and hence, lots of experimental tests may need be performed before any significant conclusion can be arrived from these tests. It should be noted that all the auger hole seepage theories, as mentioned above, are for water table aquifers of infinite horizontal spread. For the confined situation, Barua and Hoffmann (2005, 2007) provided the necessary auger hole theories both for the cases when the hole is being underlain by an impervious barrier and when it is being underlain by a gravel substratum, and provided appropriate shape factors for these situations.

Another popular field method of estimating saturated hydraulic conductivity of soil is the Bouwer and Rice's (1976) slug test. The method of experimentation of the slug test is the same as that of the auger hole method and here also the rate of rise of water is monitored in a bore hole after a specific volume of water is instantaneously removed from the hole. It is to be noted that an auger hole may be regarded as a special case of a slug hole of zero casing length and non-restrictive bottom flow (Dagan, recovery test, 1978). Bouwer and Rice's model is based on steady well flow equation (Thiem's equation) where only the radial component of the flow is being considered. Their method actually transforms a well flow situation to an equivalent radial flow system and then linking the effective radius of the radial system with the well and aquifer geometries corresponding to the flow situation with the help of electric analog experiments. For ease of calculation, suitable empirical equations together with graphs for estimating the coefficients appearing in these equations were provided for estimating equivalent radii corresponding to a wide range of flow and aquifer configurations. The computation procedure of Bouwer and Rice's model was further simplified by Van Rooy (1988 – as reported by Yang and Yeh, 2004) and Yang and Yeh (2004) by converting their coefficient curves into corresponding polynomial functions utilizing the regression method. Because of wide scale applicability of the Bouwer and Rice's method by soil scientists and

engineers, the accuracy of the method was checked by several investigators both for the confined and unconfined aquifer conditions (Dagan, 1978; Widdowson et al., 1990; Dawson and Istok, 1991; Brown and Narasimhan, 1995; Hyder et al., 1994; Hyder and Butler, 1995; Zlotnik et al., 2010). Brown and Narasimhan (1995) commented from their numerical study of the slug test method that Bouwer and Rice's procedure should be used with caution for tests performed in unconfined aquifers, particularly for situations where the well screen starts from the water table (i.e., for auger hole flow situations) itself, as considerable deviation from the radial flow approximation may then occur. This observation is in line with the observations of Bouwer (1989), Hyder and Butler (1995), Zlotnik et al. (2010) for similar flow configurations. Further, Bouwer and Rice's model does not seem to work very well for homogeneous anisotropic soils (Zlotnik, 1994; Hyder and Butler, 1995; Zlotnik et al., 2010).

Dagan (1978) developed semi-analytical solutions, using Green's function, for predicting flow to partially penetrating slug holes in a phreatic aquifer corresponding to various slug test scenarios under steady state condition. These solutions assume the aquifer to be of infinite horizontal extent and the water table to be flat; however, one notable feature of these solutions is their ability to handle the non-uniform flow at the well screen which Dagan achieved by resorting to a well screen discretization procedure. This procedure was also followed by others (Selim and Kirkham, 1974; Gringarten and Ramey, 1975; Lee and Damiata, 1995; Chang and Chen, 2002, 2003; Perina and Lee, 2006) to solve various other well hydraulics problems in the past. A particular configuration of the slug hole (recovery test) considered by Dagan (1978) coincides with the auger hole problem of Kirkham (1958) and Boast and Kirkham (1971) and as such Dagan's solution for such a situation is expected to work for an auger hole as well. This is, however, not exactly true as Dagan's auger solution (recovery test) does not consider flow through the bottom of an auger hole as do Kirkham's (1958) and Boast and Kirkham's (1971) models. Further, Dagan's model has also been observed to run into numerical difficulties when the active length of a slug hole is taken small as compared to the radius (Widdowson et al., 1990; Yang and Yeh, 2004) of the hole. However, numerical work on the multi-level slug test problem (Braester and Thunvik, 1984, Widdowson et al., 1990; Melville et al., 1991) showed that Dagan's solution does give results

comparable with those obtained by numerical means for flow situations where the active length of a slug is much higher than that of the radius of the hole. Widdowson et al. (1990) provided numerical solution to the slug test problem and presented dimensionless curves which can be used to interpret slug test results for various slug geometries under both confined and unconfined aquifer conditions. Their analysis also showed that aquifer storage has negligible influence on the hydraulics of a slug hole in a phreatic aquifer, particularly if the storage coefficient of the aquifer is low and a stressed slug hole in an unconfined aquifer quickly goes into a quasi-steady mode during a slug test.

According to Van Beers (1958), the auger hole method measures the average saturated hydraulic conductivity of a soil column extending 30 to 50 cm radially from the centre of the hole and a few decimeters below the bottom of the hole. Bouwer and Jackson (1974) reported that the auger hole method measures saturated hydraulic conductivity of a soil volume equal to about $0.4 \times$ *depth of auger hole below the water table* m^3, where the depth is expressed in metres. Oosterbaan and Nijland (1994), however, observed that the radial influence of the method to be about 30 cm and the vertical influence to be about 20 cm below the bottom of the hole, or should there be a relatively impermeable layer within 20 cm below the bottom of the hole, the vertical influence would be extending up to it. The capture zones associated with a pumping well for both confined and unconfined aquifers are found to be influenced, among other variables, by the degree of penetration of the well (Haitjema and Kramer, 1988; Faybishenko et al., 1995; Schafer, 1996) as well as by the anisotropy ratio (the ratio of horizontal to vertical hydraulic conductivity) of the aquifer material (Bair and Lahm, 1996; Schafer, 1996; Zlotnik, 1997). There appears to be currently no analytical model which can be used to trace the capture zone associated with an auger hole test in an unconfined aquifer. This is because there is right-now no analytical model which can be used to simulate flow into an auger hole dug in a phreatic aquifer of finite horizontal and vertical extents, even though, as mentioned before Barua and Hoffmann (2005, 2007) provided the relevant models for a partially penetrating auger hole in an artesian aquifer for both the cases when the bottom of the hole rests above an impervious barrier and also when it rests above a gravel substratum. For an auger hole fully penetrating a water table aquifer and resting on an impervious layer, Kirkham and Power (1972) provided a series solution for it but, in their

analysis, they assume the outer layer to be a Neumann boundary (i.e., a no-flow boundary) rather than a Dirichlet one (i.e., a constant head boundary). The Neumann boundary under-estimates the flow to the auger holes whereas the Dirichlet one over-estimates it. Thus the two provide bounds between which the true value lies, both approaching the true value as the outer boundary extends outwards. As flow to a stressed auger hole takes place both from the top water table as well as from the side boundaries, a solution to the problem obtained by imposing a Neumann condition at the outer boundary may be considerably different from that of the one developed by considering a Dirichlet condition at the outer boundary, particularly for flow situations where the anisotropy ratio of the experimental aquifers is high. It is worth mentioning in this context that, for most sediment deposits, anisotropy is more of a common phenomenon rather than an exception (Maasland, 1957; Bair and Lahm, 1996; Schafer, 1996; Zlotnik, 1997) and the water transmitting capacity along the bedding planes of the deposits (i.e., along the horizontal direction) has generally been observed to be higher than that along perpendicular to the planes (i.e., along the vertical direction).

From the above review, it is apparent that there is a necessity to develop suitable solutions to the different variants of the auger hole problem for a phreatic aquifer of finite horizontal and vertical extents so that directional conductivities of a water table aquifer as well as the soil space over which the directional conductivities of the aquifer is being measured, can be estimated utilizing results obtained from a typical auger hole test being performed on the aquifer. Taking these in view, a study is being undertaken here to achieve the following objectives.

2.2 Objectives

To develop equations for the hydraulic head function, the stream function and the discharge rate, for steady groundwater seeping into an auger hole in a saturated, homogeneous and anisotropic water table aquifer of finite horizontal and vertical extents when

(i) the auger hole fully penetrates the aquifer and rests on an impervious layer and

(ii) the auger hole partially penetrates the aquifer and rests above an impervious layer.

2.3 A General Solution to the Steady State Continuity Equation of Flow into an Auger Hole in a Homogeneous and Anisotropic soil Medium

In order to obtain analytical expressions to the boundary value problems considered for study, it is necessary that we first develop a general solution to the differential equation governing flow into an auger hole in a homogeneous and anisotropic aquifer. The steady state continuity equation of flow into an auger hole for a homogeneous and anisotropic aquifer can be represented as

$$K_r \frac{\partial^2 \phi}{\partial r^2} + \frac{K_r}{r} \frac{\partial \phi}{\partial r} + K_z \frac{\partial^2 \phi}{\partial z^2} = 0, \tag{2.1}$$

where ϕ is the hydraulic head, K_r and K_z are the horizontal and vertical hydraulic conductivities of the aquifer and r and z are the radial and vertical coordinates, respectively. A general solution of Eq. (2.1) may be attempted by making use of the separation of variable method (Kirkham, 1972). Dividing Eq. (2.1) by K_z, we have

$$\frac{K_r}{K_z} \frac{\partial^2 \phi}{\partial r^2} + \frac{K_r}{K_z} \frac{1}{r} \frac{\partial \phi}{\partial r} + \frac{\partial^2 \phi}{\partial z^2} = 0. \tag{2.2}$$

Substituting

$$(K^a)^2 = \frac{K_r}{K_z}, \tag{2.3}$$

in Eq. (2.2), we get

$$(K^a)^2 \frac{\partial^2 \phi}{\partial r^2} + \left(K^a\right)^2 \frac{1}{r} \frac{\partial \phi}{\partial r} + \frac{\partial^2 \phi}{\partial z^2} = 0. \tag{2.4}$$

Let

$$\phi = R(r)Z(z), \tag{2.5}$$

be a solution of Eq. (2.4), where $R(r)$ is a function of r only and $Z(z)$ is a function of z only. Applying Eq. (2.5) to Eq. (2.4) and separating the variables out, we get

$$(K^a)^2 \frac{R''(r)}{R(r)} + \left(K^a\right)^2 \frac{1}{r} \frac{R'(r)}{R(r)} = -\frac{Z''(z)}{Z(z)}. \tag{2.6}$$

Here, L.H.S. of the Eq. (2.6) is a function of r only and the R.H.S. of the Eq. (2.6) is a function of z only; thus both these expressions can be equated to a constant, say α^2 ($\alpha^2 > 0$). Hence Eq. (2.6) can be expressed by

$$(K^a)^2 \frac{R''(r)}{R(r)} + \left(K^a\right)^2 \frac{1}{r}\frac{R'(r)}{R(r)} = -\frac{Z''(z)}{Z(z)} = \alpha^2. \tag{2.7}$$

That is,

$$Z''(z) + \alpha^2 Z(z) = 0 \tag{2.8}$$

and

$$r^2 R''(r) + rR'(r) - \frac{r^2\alpha^2}{\left(K^a\right)^2} R(z) = 0. \tag{2.9}$$

A solution of Eq. (2.8) can be represented as

$$Z(z) = \sum_{n=1}^{N_0} \left[A_n \sin(\alpha_n z) + B_n \sin(\alpha_n z)\right], \tag{2.10}$$

where α_n, A_n and B_n are arbitrary constants and N_0 is any positive integer. It should be noted that in Eq. (2.10), the property that the sum of solutions of a differential equation is also its solution, is used. Also, a solution of Eq. (2.9) can be expressed as

$$R(r) = \sum_{n=1}^{N_0} \left[C_n I_0\left(\frac{\alpha_n r}{K^a}\right) + D_n K_0\left(\frac{\alpha_n r}{K^a}\right)\right], \tag{2.11}$$

where $I_0(.)$ and $K_0(.)$ are the zero-order modified Bessel's function of first kind and second kind, respectively, and C_n and D_n are any arbitrary constants.

Substituting Eqs. (2.10) and (2.11) in Eq. (2.5) and observing that a constant is also a solution of Eq. (2.1), a general solution, thus, of the steady state continuity equation in cylindrical coordinate can be expressed as [see also Eq. (A10), Barua and Bora, 2010]

$$\phi = \sum_{n=1}^{N} \left\{ \left[C_n I_0\left(\frac{\alpha_n r}{K^a}\right) + D_n K_0\left(\frac{\alpha_n r}{K^a}\right)\right] \left[A_n \sin(\alpha_n z) + B_n \cos(\alpha_n z)\right] \right\} + T. \tag{2.12}$$

Eq. (2.12) forms the basis of the analytical solutions that we propose to obtain for the flow problems considered for study in this chapter. Here T is any arbitrary constant.

2.4 Mathematical Formulation and Solution

2.4.1 Case 1: Theory of seepage into a fully penetrating auger hole in an unconfined aquifer of finite domain

Fig. 2.1 shows the geometry of an auger hole of radius a fully penetrating a homogeneous and anisotropic unconfined aquifer and resting on an impervious layer. The depth of the impervious layer is taken as h and the water level in the auger hole is taken as H_1, all distances being measured from the water table as shown in the figure. The aquifer is underlain by an impervious layer. The flow profile of interest is the one obtained by invoking a sudden lowering of water level in the hole, the water in the hole been previously standing flush with the surrounding water table. In order to ascertain the horizontal domain of influence of a typical auger hole test, the hydraulic head on a concentric cylindrical surface located at a distance b from the centre of the hole is assigned a value of zero, the head being measured with respect to the origin O as shown in the figure. Due to axial symmetry, the flow region on the right of the vertical axis is only considered for analysis. For convenience, the z-axis is taken as positive vertically downward and the r-axis positive towards the right. Further, in our analysis here, we assume the water table to be flat during an experimental run with negligible capillary effects above it, flow to be steady, water and aquifer materials to be incompressible and the principal directions of anisotropy to coincide with the horizontal and vertical directions, respectively. It is to be observed that, since the volume of water involved in a slug test is small, the assumption of a flat water table during a slug test in a phreatic aquifer can be treated as a valid one for most field test conditions (Kirkham and Van Bavel, 1948, Kirkham, 1958; Boast and Kirkham, 1971; Dagan, 1978; Lomen et al., 1987; Widdowson et al., 1990; Kacimov, 2000; Zlotnik et al., 2010). Further, the numerical study of Widdowson et al. (1990) also shows that the steady state assumption, which is being generally made in analyzing flow behavior around a pumped auger hole, is a justifiable one judging from the fact that a stressed slug hole in an unconfined aquifer immediately goes into a quasi-steady state, particularly when the storage coefficient of the aquifer is low.

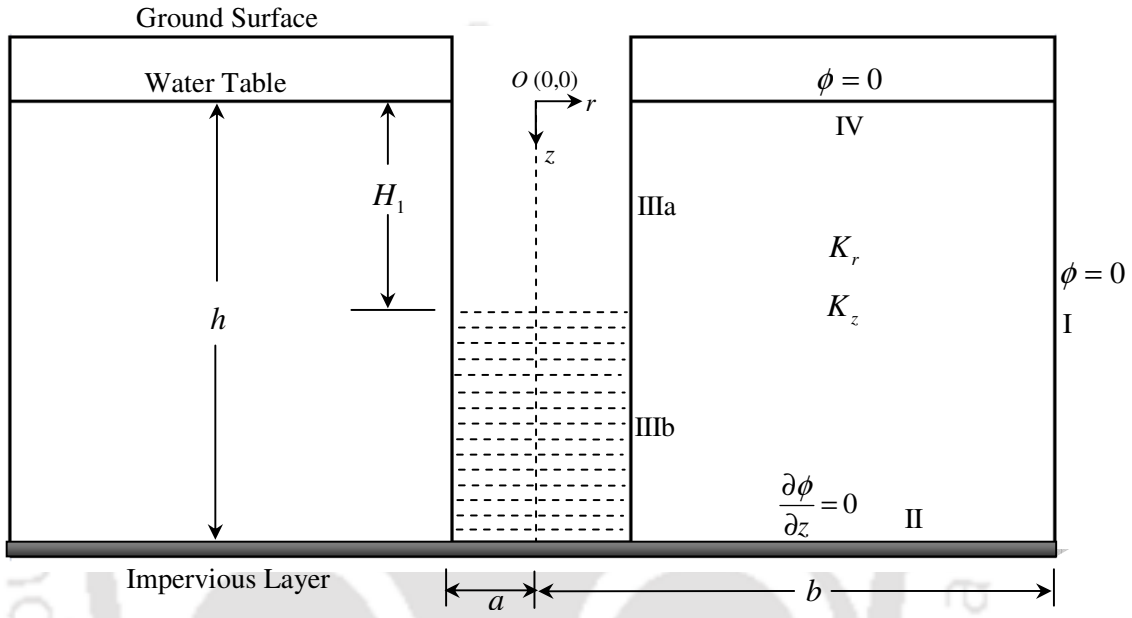

Fig. 2.1. Geometry of the flow system of an auger hole resting on an impervious layer in an unconfined aquifer of finite horizontal and vertical extents

The solution to the flow problem shown in Fig. 2.1 thus then dictates that Eq. (2.1) need be solved subject to the boundary conditions as given below

$$\phi = 0, \qquad r = b, \qquad 0 < z < h, \tag{I}$$

$$\frac{\partial \phi}{\partial z} = 0, \qquad z = h, \qquad a < r < b, \tag{II}$$

$$\phi = -z, \qquad r = a, \qquad 0 < z \le H_1, \tag{IIIa}$$

$$\phi = -H_1, \qquad r = a, \qquad H_1 \le z < h, \tag{IIIb}$$

$$\phi = 0, \qquad z = 0, \qquad a < r < b, \tag{IV}$$

where ϕ is the hydraulic head, as measured from the origin *O*. The problem considered here may be pictured as an extension of the fully penetrating auger hole problem of Kirkham and Van Bavel (1948) and Barua and Tiwari (1995) for a phreatic aquifer of infinite horizontal extent to that of a similar type of aquifer of finite horizontal extent.

In order that Eq. (2.12) straightway absorbs boundary conditions I, II and IV in its fold, the constants appearing in the equation may be appropriately adjusted to yield

$$\phi = \sum_{m=1}^{M} C_m \left[\frac{K_0\left(\frac{-N_m b}{K^a}\right) I_0\left(\frac{-N_m r}{K^a}\right) - K_0\left(\frac{-N_m r}{K^a}\right) I_0\left(\frac{-N_m b}{K^a}\right)}{K_0\left(\frac{-N_m b}{K^a}\right) I_0\left(\frac{-N_m a}{K^a}\right) - K_0\left(\frac{-N_m a}{K^a}\right) I_0\left(\frac{-N_m b}{K^a}\right)} \right] \sin(N_m z), \tag{2.13}$$

where

$$N_m = \left[\left(\frac{1\text{-}2\text{m}}{2} \right) \frac{\pi}{h} \right], \tag{2.14}$$

M is any positive integer, i.e., $M = 1, 2, 3 \ldots$, *m* is a summation index and C_m are constants to be determined utilizing the remaining boundary conditions.

Applying boundary conditions IIIa and IIIb to Eq. (2.13), we get, at $r = a$

$$\sum_{m=1}^{M} C_m \sin(N_m z) = -z, \qquad 0 < z \le H_1, \tag{2.15}$$

and

$$\sum_{m=1}^{M} C_m \sin(N_m z) = -H_1, \qquad H_1 \le z < h. \tag{2.16}$$

Letting $M \to \infty$ in the above relations and running a Fourier series in the interval $0 < z < h$, the constants C_m can then be evaluated as

$$C_m = \frac{2}{h}\left[\int_0^{H_1}(-z)\sin(N_m z)dz + \int_{H_1}^{h}(-H_1)\sin(N_m z)dz\right]. \tag{2.17}$$

Eq. (2.17), upon simplification, gives

$$C_m = \frac{-2}{h(N_m)^2}\sin(N_m H_1). \tag{2.18}$$

Hence, from Eqs. (2.14) and (2.18), we have

$$C_m = \left[\frac{-8h}{(1-2m)^2\pi^2}\right]\sin\left[\left(\frac{1-2m}{2}\right)\frac{\pi H_1}{h}\right]. \tag{2.19}$$

We would like to point out here that this is the same expression for the Fourier coefficients as has been obtained by Barua and Tiwari [see their Eq. (11), 1995] in their solution to the fully penetrating auger hole problem for an aquifer of infinite horizontal extent. This is understandable as the nature of the Fourier series considered by Barua and Tiwari (1995) is the same as has been taken here but we would like to emphasize that, because of inclusion of the additional variable *b* in our flow problem to account for the horizontal finiteness of our aquifer here as compared to the radially infinite aquifer auger hole problem considered by Barua and Tiwari (1995), the ensuing hydraulic head functions in both these solutions are coming out to be quite different – there, we were dealing with two Bessel functions only [see Eq. (12) Barua and Tiwari, 1995] but here, on the other hand, we are dealing with as many as eight Bessel functions as can be seen in Eq. (2.13) above.

Substituting C_m from Eq. (2.19) in Eq. (2.13), the expression for the hydraulic head function for the flow problem finally works out to be

$$\phi = \sum_{m=1}^{M}\left[\frac{-8h}{(1-2m)^2\pi^2}\right]\sin\left[\left(\frac{1-2m}{2}\right)\frac{\pi H_1}{h}\right]$$

$$\times\left[\frac{K_0\left(\frac{-N_m b}{K^a}\right)I_0\left(\frac{-N_m r}{K^a}\right) - K_0\left(\frac{-N_m r}{K^a}\right)I_0\left(\frac{-N_m b}{K^a}\right)}{K_0\left(\frac{-N_m b}{K^a}\right)I_0\left(\frac{-N_m a}{K^a}\right) - K_0\left(\frac{-N_m a}{K^a}\right)I_0\left(\frac{-N_m b}{K^a}\right)}\right]\sin(N_m z). \tag{2.20}$$

Now, to get the Stoke's stream function, ψ, from the developed hydraulic head function, we apply the relations (Bear, 1972)

$$K_r \frac{\partial \phi}{\partial r} = \frac{1}{r} \frac{\partial \psi}{\partial z} \tag{2.21}$$

and

$$K_z \frac{\partial \phi}{\partial z} = -\frac{1}{r} \frac{\partial \psi}{\partial r}, \tag{2.22}$$

connecting the two in case of axis-symmetric flow for a homogeneous anisotropic soil – the resulting expression for the stream function, after simplification, turns out to be

$$\psi = \sum_{m=1}^{M} r\sqrt{K_r K_z}\, C_m \left[\frac{K_0\left(\frac{-N_m b}{K^a}\right) I_1\left(\frac{-N_m r}{K^a}\right) + K_1\left(\frac{-N_m r}{K^a}\right) I_0\left(\frac{-N_m b}{K^a}\right)}{K_0\left(\frac{-N_m b}{K^a}\right) I_0\left(\frac{-N_m a}{K^a}\right) - K_0\left(\frac{-N_m a}{K^a}\right) I_0\left(\frac{-N_m b}{K^a}\right)} \right] \cos(N_m z), \tag{2.23}$$

where $I_1(.)$ and $K_1(.)$ are the first-order modified Bessel functions of first and second kinds, respectively, and the other symbols have already been defined. It is to be noted that, in Eq. (2.23), the constant of integration has been taken as zero as the quantity of interest is the flow in between two streamlines rather than their absolute values. To have a better picture of flow around a stressed auger hole, the stream function given by Eq. (2.23) can be first normalized before being used for plotting as under

$$\psi^n = \left[1 - \frac{\psi(r,z)}{\psi(a,0)} \right]. \tag{2.24}$$

Eq. (2.24) has been used to plot normalized streamlines for a few flow situations of Fig. 2.1 as can be seen in Figs. 2.7 and 2.8, respectively.

The quantity of water, Q_f, entering the auger hole can now be readily obtained by an application of the Darcy's law at the well face of the hole, that is

$$Q_f = 2\pi a K_z \int_0^h \left(\frac{\partial \phi}{\partial r} \right)_{r=a} dz. \tag{2.25}$$

Now

$$\left(\frac{\partial\phi}{\partial r}\right)_{r=a} = \sum_{m=1}^{M} -C_m\left(\frac{N_m}{K^a}\right)\left[\frac{K_0\left(\frac{-N_m b}{K^a}\right)I_1\left(\frac{-N_m a}{K^a}\right)+K_1\left(\frac{-N_m a}{K^a}\right)I_0\left(\frac{-N_m b}{K^a}\right)}{K_0\left(\frac{-N_m b}{K^a}\right)I_0\left(\frac{-N_m a}{K^a}\right)-K_0\left(\frac{-N_m a}{K^a}\right)I_0\left(\frac{-N_m b}{K^a}\right)}\right]\sin(N_m z).$$

Using the above expression in Eq. (2.25) and integrating within the specified limit, we get

$$Q_f = -2\pi a\sqrt{K_r K_z}\sum_{m=1}^{M} C_m\left[\frac{K_0\left(\frac{-N_m b}{K^a}\right)I_1\left(\frac{-N_m a}{K^a}\right)+K_1\left(\frac{-N_m a}{K^a}\right)I_0\left(\frac{-N_m b}{K^a}\right)}{K_0\left(\frac{-N_m b}{K^a}\right)I_0\left(\frac{-N_m a}{K^a}\right)-K_0\left(\frac{-N_m a}{K^a}\right)I_0\left(\frac{-N_m b}{K^a}\right)}\right]. \tag{2.26}$$

2.4.2 Case 2: Theory of seepage into an auger hole underlain by an impervious layer in an unconfined aquifer of finite horizontal and vertical extents

We now seek a solution to the flow problem of Fig. 2.2 for the case when the hole does not go all the way up to the impervious layer but suspends above it. Fig. 2.2 shows the geometry of such a flow situation where a partially penetrating auger hole penetrates up to a depth of H_3 of a water table aquifer of thickness h, the other variables being same as those already defined for the fully penetrating problem of Fig. 2.1. For ease of solution, we divide the flow domain of Fig. 2.2, as in Kirkham (1958, 1959) and Barua and Tiwari (1995), into two sub-domains R-I and R-II, as shown in the figure. The hydraulic head function in R-I is designated as ϕ_1 and in R-II as ϕ_2. The solution to the boundary value problem thus requires that $\phi_{1(i)}$ and $\phi_{2(i)}$ must be suitably evaluated such that the governing equations

$$K_r\frac{\partial^2\phi_1}{\partial r^2}+\frac{K_r}{r}\frac{\partial\phi_1}{\partial r}+K_z\frac{\partial^2\phi_1}{\partial z^2}=0, \tag{2.27}$$

for R-I, and

$$K_r\frac{\partial^2\phi_2}{\partial r^2}+\frac{K_r}{r}\frac{\partial\phi_2}{\partial r}+K_z\frac{\partial^2\phi_2}{\partial z^2}=0, \tag{2.28}$$

for R-II,

need be satisfied along with the following boundary and interfacial conditions.

$$\frac{\partial \phi_1}{\partial r} = 0, \qquad r = 0, \qquad H_3 < z < h \tag{I}$$

$$\phi_1 = -H_1, \qquad z = H_3 \qquad 0 < r < a, \tag{II}$$

$$\phi_1 = \phi_2, \qquad r = a, \qquad H_3 < z < h, \tag{IIIa}$$

$$K_{r1}\frac{\partial \phi_1}{\partial r} = K_{r2}\frac{\partial \phi_2}{\partial r}, \qquad r = a, \qquad H_3 < z < h, \tag{IIIb}$$

$$\frac{\partial \phi_1}{\partial z} = 0, \qquad z = h, \qquad 0 < r < a, \tag{IV}$$

$$\phi_2 = -z, \qquad r = a, \qquad 0 < z \le H_1, \tag{Va}$$

$$\phi_2 = -H_1, \qquad r = a, \qquad H_1 \le z < H_3, \tag{Vb}$$

$$\phi_2 = 0, \qquad z = 0, \qquad a < r < b, \tag{VI}$$

$$\phi_2 = 0, \qquad r = b, \qquad 0 < z < h, \tag{VII}$$

$$\frac{\partial \phi_2}{\partial z} = 0, \qquad z = h, \qquad a < r < b. \tag{VIII}$$

Again, in view of Eq. (2.12), ϕ_1 and ϕ_2 for R-I and R-II of Fig. 2.2, can be expressed as

$$\phi_1 = \sum_{m=1}^{M} A_m \frac{I_0\left(\frac{-N_m r}{K^a}\right)}{I_0\left(\frac{-N_m a}{K^a}\right)} \sin\left[N_m (z - H_3)\right] - H_1 \tag{2.29}$$

and

$$\phi_2 = \sum_{n=1}^{N} B_n \left[\frac{K_0\left(\frac{-N_n b}{K^a}\right) I_0\left(\frac{-N_n r}{K^a}\right) - K_0\left(\frac{-N_n r}{K^a}\right) I_0\left(\frac{-N_n b}{K^a}\right)}{K_0\left(\frac{-N_n b}{K^a}\right) I_0\left(\frac{-N_n a}{K^a}\right) - K_0\left(\frac{-N_n a}{K^a}\right) I_0\left(\frac{-N_n b}{K^a}\right)} \right] \sin(N_n z), \tag{2.30}$$

where

$$N_m = \left[\frac{(1-2m)\pi}{2(h - H_3)}\right], \tag{2.31}$$

and

$$N_n = \left[\frac{(1-2n)\pi}{2h}\right], \tag{2.32}$$

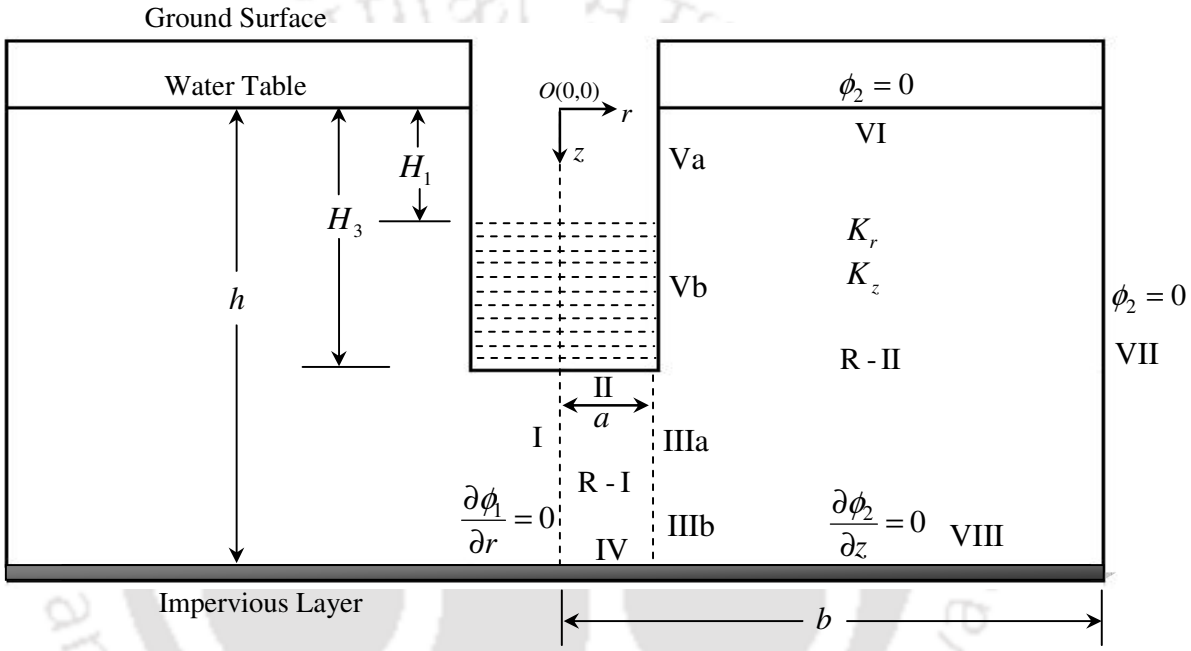

Fig. 2.2. Geometry of the flow system of an auger hole underlain by an impervious layer in an unconfined aquifer of finite horizontal and vertical extents

N is any integer, i.e., $N = 1, 2, 3 ...,$ n is a summation index and the other symbols have already been explained in the solution of the fully penetrating problem.

As can be seen, ϕ_1 and ϕ_2, by their very way of definition, satisfy boundary conditions I, II, IV, VI, VII and VIII, respectively. We now seek to determine the Fourier constants A_m and B_n appearing in Eqs. (2.29) and (2.30) by making use of the remaining boundary and interfacial conditions.

Applying Va, Vb and IIIa to Eqs. (2.29) and (2.30), respectively, we get

$$\sum_{n=1}^{N} B_n \sin(N_n z) = -z, \qquad 0 < z \le H_1, \tag{2.33}$$

$$\sum_{N=1}^{n} B_n \sin(N_n z) = -H_1, \qquad H_1 \le z < H_3 \tag{2.34}$$

and

$$\sum_{n=1}^{N} B_n \sin(N_n z) = \sum_{m=1}^{M} A_m \sin[N_m (z - H_3)] - H_1, \qquad H_3 < z < h. \tag{2.35}$$

Allowing M and N to go to ∞ and drawing a Fourier series in the interval $0 < z < h$, the constants B_n can then be determined as shown

$$B_n = \frac{2}{h}\left\{\int_0^{H_1} (-z)\sin(N_n z)dz + \int_{H_1}^{H_3} (-H_1)\sin(N_n z)dz + \int_{H_3}^{h} (-H_1)\sin(N_n z)dz + \right.$$
$$\left. + \int_{H_3}^{h} \sum_{m=1}^{M} A_m \sin[N_m (z - H_3)]\sin(N_n z)dz\right\}. \tag{2.36}$$

Integrating the above and simplifying, we get, for $N_m^2 \neq N_n^2$

$$B_n = \frac{-2}{h(N_n)^2}\sin(N_n H_1) + \sum_{m=1}^{M} \frac{A_m}{h}\left\{\frac{\sin[(N_m - N_n)h - N_m H_3]}{(N_m - N_n)} - \frac{\sin[(N_m + N_n)h - N_m H_3]}{(N_m + N_n)}\right.$$
$$\left. - \frac{\sin[(N_m - N_n)H_3 - N_m H_3]}{(N_m - N_n)} + \frac{\sin[(N_m + N_n)H_3 - N_m H_3]}{(N_m + N_n)}\right\}. \tag{2.37}$$

and for $N_m = N_n$

$$B_n = \frac{-2}{h(N_n)^2}\sin(N_n H_1) + \sum_{m=1}^{M}\frac{A_m}{h}\Big\{(h-H_3)\cos(N_m H_3) + \frac{1}{2N_m}\sin(N_m H_3) - \frac{1}{2N_m}\sin\left[N_m(2h-H_3)\right]\Big\}. \tag{2.38}$$

Eqs. (2.37) and (2.38) yield a set of relations expressing the constants B_n in terms of the constants A_m. To generate the same number of A_m as that of B_n, we take at this point

$$M = N. \tag{2.39}$$

We now rely on condition IIIb to provide us with a second set of relations linking A_m and B_n and hence their individual values; IIIb, when being applied to Eqs. (2.29) and (2.30), gives

$$\sum_{m=1}^{M} A_m \sin\left[N_m(z-H_3)\right] = \sum_{n=1}^{N} B_n P_{nm}\sin(N_n z), \tag{2.40}$$

where

$$P_{nm} = \left[\left(\frac{N_n}{N_m}\right)\frac{I_0\left(\frac{-N_m a}{K^a}\right)}{I_1\left(\frac{-N_m a}{K^a}\right)}\right]\left[\frac{K_0\left(\frac{-N_n b}{K^a}\right)I_1\left(\frac{-N_n a}{K^a}\right) + K_1\left(\frac{-N_n a}{K^a}\right)I_0\left(\frac{-N_n b}{K^a}\right)}{K_0\left(\frac{-N_n b}{K^a}\right)I_0\left(\frac{-N_n a}{K^a}\right) - K_0\left(\frac{-N_n a}{K^a}\right)I_0\left(\frac{-N_n b}{K^a}\right)}\right]. \tag{2.41}$$

Applying a Fourier run in the interval $H_3 < z < h$, in view of the fact that M and $N \to \infty$, the constants A_m can, thus, be evaluated as

$$A_m = \left[\frac{2}{(h-H_3)}\right]\int_{H_3}^{h}\sum_{n=1}^{N} B_n P_{nm}\sin(N_n z)\sin\left[N_m(z-H_3)\right]dz. \tag{2.42}$$

Integration of the above gives, for $N_m^2 \neq N_n^2$

$$A_m = \sum_{n=1}^{N}\frac{B_n P_{nm}}{(h-H_3)}\Big\{\frac{\sin\left[(N_m-N_n)h - N_m H_3\right]}{(N_m-N_n)} - \frac{\sin\left[(N_m+N_n)h - N_m H_3\right]}{(N_m+N_n)} + \frac{\sin\left[(N_m+N_n)H_3 - N_m H_3\right]}{(N_m+N_n)} - \frac{\sin\left[(N_m-N_n)H_3 - N_m H_3\right]}{(N_m-N_n)}\Big\}, \tag{2.43}$$

and for $N_m = N_n$

$$A_m = \sum_{n=1}^{N} \frac{B_n P_{nm}}{(h - H_3)} \left\{ (h - H_3)\cos(N_n H_3) + \frac{1}{2N_n}\sin(N_n H_3) - \frac{1}{2N_n}\sin\left[N_n(2h - H_3)\right] \right\}. \quad (2.44)$$

Linear equations arising out of Eqs. (2.37), (2.38), (2.43) and (2.44) can now be solved by a Gauss elimination or by some other suitable method (Scarborough, 1966) to evaluate the desired Fourier coefficients A_m and B_n. Once these coefficients are being evaluated, the hydraulic head functions ϕ_1 and ϕ_2 can next be easily determined using Eqs. (2.29) and (2.30), respectively. Thus, our boundary value problem stands solved.

To derive the stream functions from the derived hydraulic head functions, we simply need to apply, like before, Eqs. (2.21) and (2.22) to Eqs. (2.29) and (2.30), respectively – the resulting stream function expressions, ψ_1 for R-I and ψ_2 for R-II, work out to be

$$\psi_1 = \sum_{m=1}^{M} r A_m \sqrt{K_r K_z} \frac{I_1\left(\frac{-N_m r}{K^a}\right)}{I_0\left(\frac{-N_m a}{K^a}\right)} \cos\left[N_m (z - H_3)\right] \quad (2.45)$$

and

$$\psi_2 = \sum_{n=1}^{N} r\sqrt{K_r K_z} B_n \left[\frac{K_0\left(\frac{-N_n b}{K^a}\right) I_1\left(\frac{-N_n r}{K^a}\right) + K_1\left(\frac{-N_n r}{K^a}\right) I_0\left(\frac{-N_n b}{K^a}\right)}{K_0\left(\frac{-N_n b}{K^a}\right) I_0\left(\frac{-N_n a}{K^a}\right) - K_0\left(\frac{-N_n a}{K^a}\right) I_0\left(\frac{-N_n b}{K^a}\right)} \right] \cos(N_n z), \quad (2.46)$$

respectively, where, like in the fully penetrating case, we have taken the constants of integration as zero for convenience. To have a better picture of flow behavior around the hole, the stream functions are generally being first normalized before being used for plotting. In normalized form, the stream function for the sub-domain R-I may be expressed as

$$\psi_1^{(n)} = \left[1 - \frac{\psi_1(r,z)}{\psi_2(a,0)} \right] \quad (2.47)$$

and for the sub-domain R-II as

$$\psi_2^{(n)} = \left[1 - \frac{\psi_2(r,z)}{\psi_2(a,0)} \right]. \quad (2.48)$$

Eqs. (2.47) and (2.48) are being used to trace the normalized streamlines in Figs. 2.9-2.12 corresponding to a few flow situations of Fig. 2.2.

The quantity of water seeping though the sides, Q_s, of the auger hole can be determined by applying the Darcy's law at the face of the auger hole – the relevant expression turns out to be

$$Q_s = 2\pi a K_r \int_0^{H_3} \left(\frac{\partial \phi_2}{\partial r}\right)_{r=a} dz. \tag{2.49}$$

Differentiation Eq. (2.30) with respect to *r*, we have, at $r = a$

$$\left(\frac{\partial \phi_2}{\partial r}\right)_{r=a} = \sum_{n=1}^{N} B_n \left(\frac{-N_n}{K^a}\right) \left[\frac{K_0\left(\frac{-N_n b}{K^a}\right) I_1\left(\frac{-N_n a}{K^a}\right) + K_1\left(\frac{-N_n a}{K^a}\right) I_0\left(\frac{-N_n b}{K^a}\right)}{K_0\left(\frac{-N_n b}{K^a}\right) I_0\left(\frac{-N_n a}{K^a}\right) - K_0\left(\frac{-N_n a}{K^a}\right) I_0\left(\frac{-N_n b}{K^a}\right)}\right] \sin(N_n z). \tag{2.50}$$

Carrying out the integration in Eq. (2.49) using Eq. (2.50), we get

$$Q_s = 2\pi a \sqrt{K_r K_z} \sum_{n=1}^{N} B_n \left[\frac{K_0\left(\frac{-N_n b}{K^a}\right) I_1\left(\frac{-N_n a}{K^a}\right) + K_1\left(\frac{-N_n a}{K^a}\right) I_0\left(\frac{-N_n b}{K^a}\right)}{K_0\left(\frac{-N_n b}{K^a}\right) I_0\left(\frac{-N_n a}{K^a}\right) - K_0\left(\frac{-N_n a}{K^a}\right) I_0\left(\frac{-N_n b}{K^a}\right)}\right] [\cos(N_n H_3) - 1]. \tag{2.51}$$

To get the discharge component through the bottom of the hole, Q_b, we simply need to apply the Darcy's law on the bottom face of the hole – the required expression now works out to be

$$Q_b = 2\pi K_z \int_0^{a} r \left(\frac{\partial \phi_1}{\partial z}\right)_{z=H_3} dr. \tag{2.52}$$

Now

$$\left(\frac{\partial \phi_1}{\partial z}\right)_{z=H_3} = \sum_{m=1}^{M} A_m N_m \frac{I_0\left(\frac{-N_m r}{K^a}\right)}{I_0\left(\frac{-N_m a}{K^a}\right)}. \tag{2.53}$$

Solving the integral of Eq. (2.52) using Eq. (2.53), we get the expression of quantity of water entering through the bottom of the auger hole as

$$Q_b = -2\pi a\sqrt{K_r K_z}\sum_{m=1}^{M} A_m \frac{I_0\left(\frac{-N_m a}{K^a}\right)}{I_0\left(\frac{-N_m a}{K^a}\right)}. \tag{2.54}$$

Thus, the total discharge, Q_p, to the partially penetrating auger hole can be calculated as

$$Q_p = Q_s + Q_b. \tag{2.55}$$

It should be noted that the nature of the hydraulic head function, ϕ_1, proposed here is the same as that obtained by Barua and Hoffmann (2005) in their solution of the auger hole problem for the confined aquifer situation. Mathematically speaking, however, these expressions are quite different in that the former is related to flow into an auger hole in a confined aquifer whereas the one developed here deals with flow to an auger hole in an unconfined aquifer. The nature of ϕ_1 turns out to be the same in both these solutions simply because the domain decomposition adopted by Barua and Hoffmann (2005) in their solution and the one considered here is the same, as a result of which the region below the bottom of the hole and extending up to the impervious layer (i.e., the region R-I of Fig. 2.2) is turning out to be identical in both these solutions. However, we would like to emphasize once again that the boundary value problems considered by Barua and Hoffmann (2005) and the one considered here are essentially quite different and so are the corresponding solutions.

As mentioned before, a shape factor expresses the relationship between the rate of recovery of a pumped auger hole and the hydraulic conductivity of the surrounding soil medium; thus, in equation form, it may be represented as [see Eqs. (42) and (45), Barua and Hoffmann, 2005]

$$K = -C\frac{dH_1}{dt}, \tag{2.56}$$

where C is given by

$$C = \frac{\pi a^2 K}{Q_p} \times 864. \tag{2.57}$$

It should be noted that, in Eq. (2.57), K is expressed in m/day and the rate of rise of water in the hole dH_1/dt in cm/s. We give in appendix a table of shape factors corresponding to a few flow geometries of Fig. 2.2 estimated using Eqs. (2.55) and (2.57). We have also given an

example (Example 3 in field applications) showing how this shape factor table can be used to estimate directly the hydraulic conductivity of an aquifer by utilizing data obtained from a standard auger hole test.

2.5 Verification of the Proposed Models and Discussion

In order to ascertain the accuracy of our developed equations, we now first compare a few of our results obtained from our proposed models with corresponding values obtained from the analytical works of others. Fig. 2.3 shows the comparison of Q_f / KH_1 and a/h profiles as obtained from our solution of the problem of Fig. 2.1 at a few b/a ratios with the corresponding profiles obtained from the analytical solution of Kirkham and Van Bavel (1948), these profiles being drawn for an auger hole of 5 cm radius, both for the cases when the hole is half full and when it is empty (see Fig. 4, Van Bavel and Kirkham, 1948). As may be observed, in both of these cases, our predicted curves are found to be closely approaching the corresponding curves obtained from Kirkham and Van Bavel's model with the increase of b/a ratio and at about b/a equal to 50 or more, a near perfect matching is obtained. It should be noted that, as mentioned before, Kirkham and Van Bavel solved the boundary value problem of Fig. 2.1 by assuming an aquifer of infinite horizontal extent and hence our solution, being developed for a finite aquifer, should also then approach to that of Kirkham and Van Bavel's solution as *b* is allowed to increase indefinitely. The fact that our predicted curves actually approach to the identical curves obtained from Kirkham and Van Bavel's analytical model here at large *b* for the compared flow scenarios shows that our developed analytical model of the flow problem of Fig. 2.1 is a correct one. Fig. 2.4 shows the variation of $Q_p / KH_1 a$ with $h - H_3 / H_3$ ratios as obtained from the analytical solution of Boast and Kirkham (see Fig. 6, Boast and Kirkham, 1971) for a few flow situations of Fig. 2.2 with similar curves obtained from the proposed analytical model of the boundary value problem of Fig. 2.2 for a few specified *b/a* ratios. Here also we observe that, with the increase of the *b*/*a* ratio, the predictions coming out of our solution are fast approaching to those obtained from Boast and Kirkham's model and at about b/a equal to 30 or more, a very good matching is obtained. As Boast and Kirkham solved the flow problem of Fig. 2.2 for an aquifer of infinite horizontal extent (i.e., $b \to \infty$ in their model), the matching of our results with those coming out of their model at large *b* shows that our solution for the partially penetrating auger hole

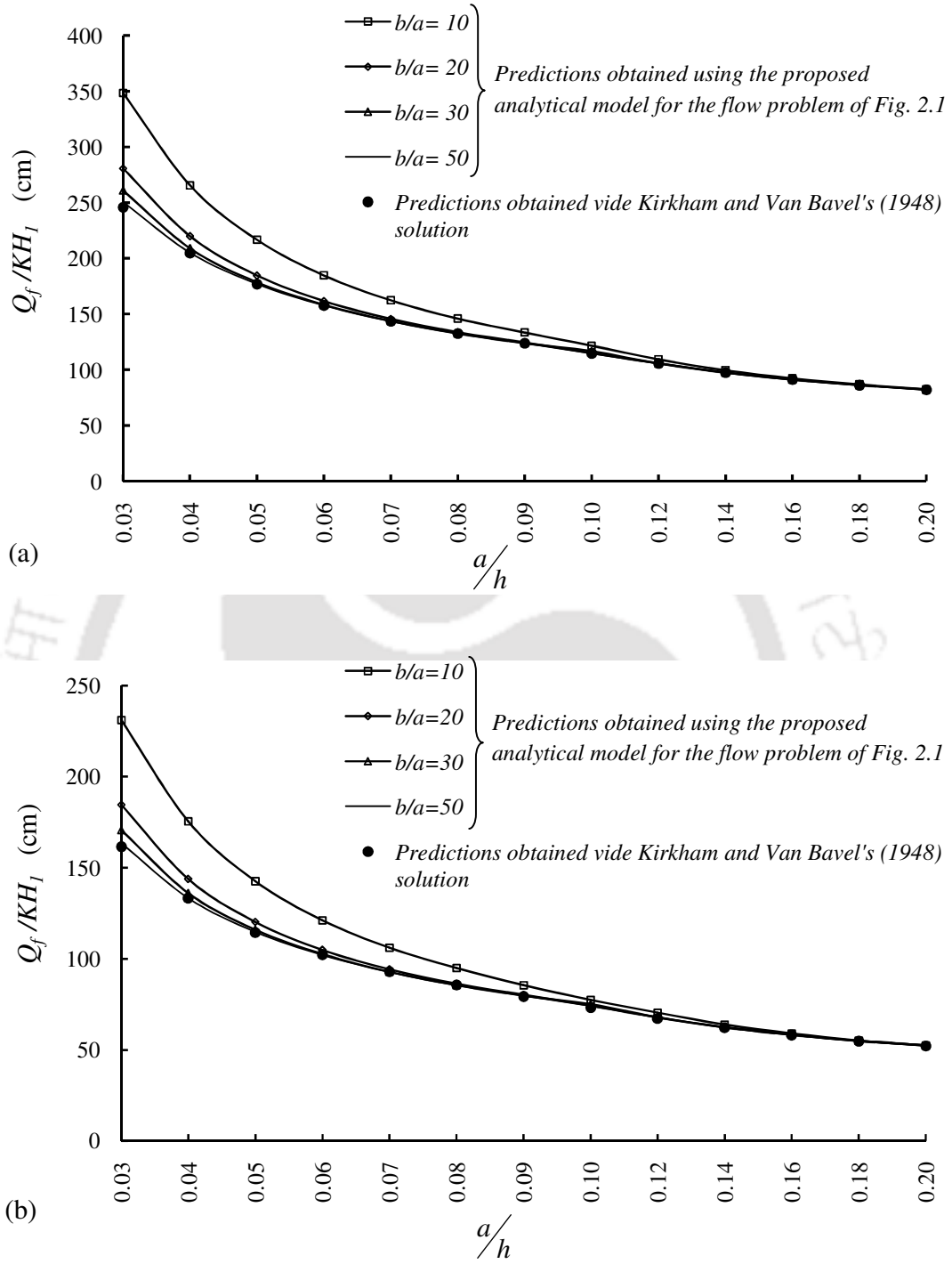

Fig. 2.3. Comparison of Q_f/KH_1 and a/h profiles as obtained from the proposed solution of the flow problem of Fig. 2.1 for different b/a ratios with the corresponding profiles obtained from the analytical works of Kirkham and Van Bavel (1948) when the other parameters of the problem are taken as $a = 5$ cm and (a) $H_1/h = 0.5$ and (b) $H_1/h = 1$

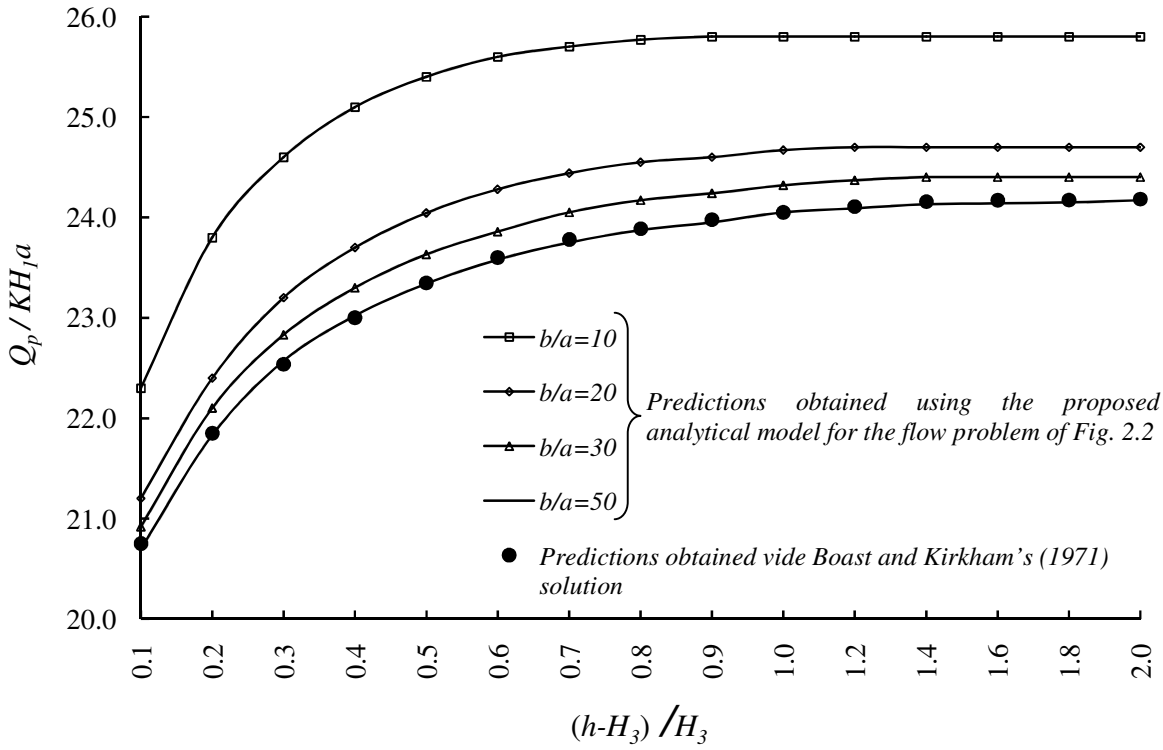

Fig. 2.4. Comparison of $Q_p / KH_1 a$ and $(h - H_3)/H_3$ curves as obtained from the proposed solution of the flow problem of Fig. 2.2 for different b/a ratios with the corresponding curves obtained from the analytical works of Boast and Kirkham (1971) when the other parameters of the problem are taken as $H_1/a = 10$ and $H_1/h = 0.75$

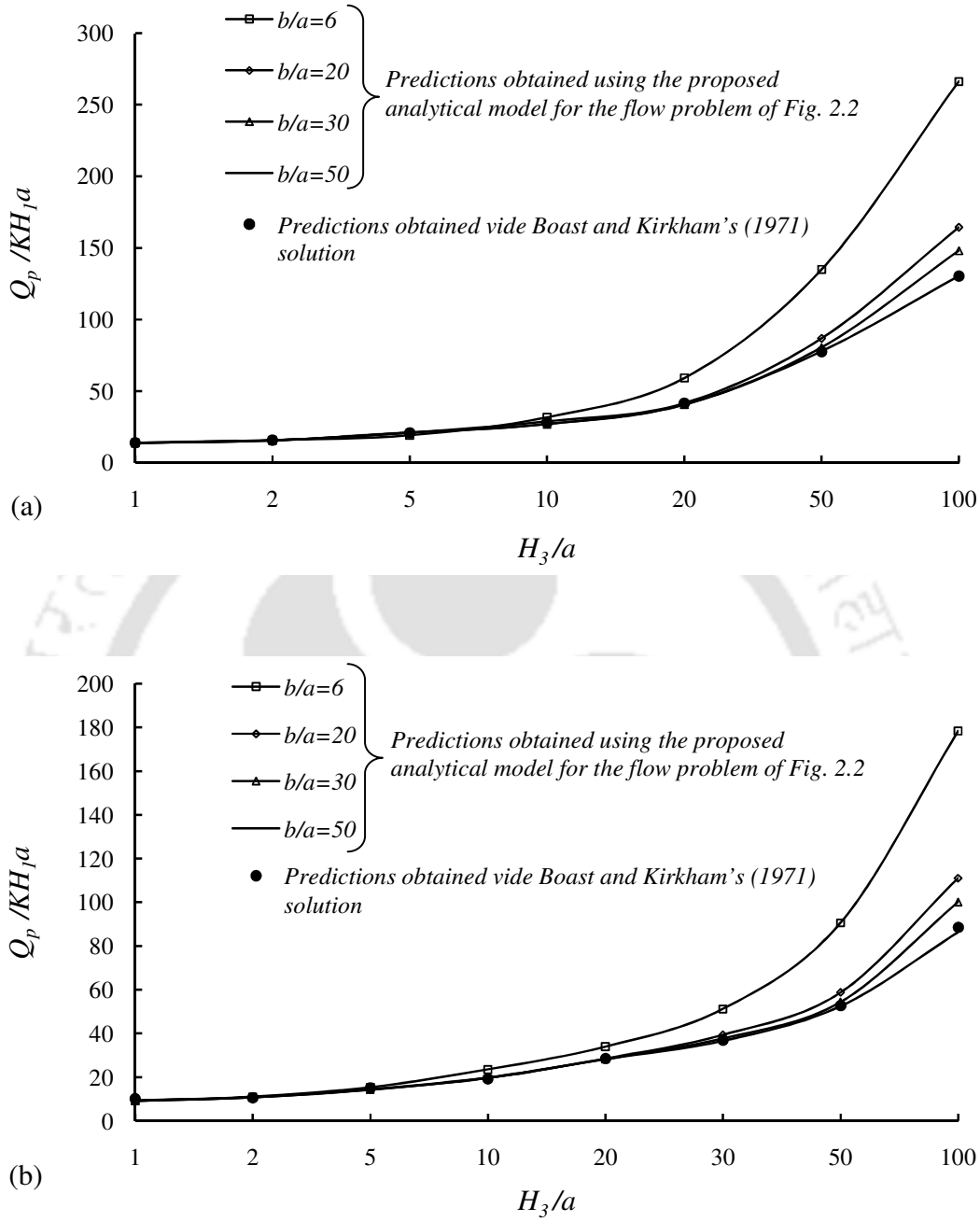

Fig. 2.5. Comparison of estimated Q_p / KH_1a values as obtained from the proposed solution of Fig. 2.2 for different b/a ratios with the corresponding values obtained from the analytical solution of Boast and Kirkham (1971) at different H_3/a ratios when the other parameters of the problem are taken as $h/H_3 = 100$ (h theoretically tends to infinity) and (a) $H_1/H_3 = 0.5$ and (b) $H_1/H_3 = 1$

has been rightly developed. Fig. 2.5 shows $Q_p / KH_1 a$ versus H_3 / a plots as obtained from our solution of the partially penetrating problem here at different *b*/*a* ratios with the corresponding curves (see Fig. 8, Boast and Kirkham, 1971) coming out of Boast and Kirkham's solution for a few flow geometries of Fig. 2.2 where it has been assumed that the bottom impervious layer lies at a very large distance (theoretically infinite) from the water table. By choosing a relatively high value of *h* along with a high *b*/*a* ratio in our model, here also we could successfully reproduce the identical plots generated out of Boast and Kirkham's solution thereby proving once again the accuracy of our developed analytical model for the partially penetrating case.

As a further check on our proposed analytical models for both the fully and partially penetrating auger problems as shown in Figs. 2.1 and 2.2, respectively, we next compare a few of our predictions (by choosing a high *b*/*a* ratio every time) with corresponding results obtained from the analytical works of Dagan (recovery test, see his Table 1, 1978) for a few flow geometries of Figs. 2.1 and 2.2, respectively. Table 2.1 shows such a comparison. As may be observed, the $Q_f / 2\pi KhH_1$ ratios as obtained from our solution for the fully penetrating case (i.e., $h / H_3 = 1$) are in exact agreement with the corresponding figures obtained from Dagan's solution and for the partially penetrating situations the (i.e., $h / H_3 = 1.1$ and 1.2) $Q_p / 2\pi KhH_1$ ratios seem to vary only very slightly (in the third places of decimals) from the corresponding values obtained vide Dagan's solution. A slight difference in results among the predictions obtained from the proposed solution for the partially penetrating auger hole with corresponding predictions obtained from Dagan's solution is understandable since Dagan's solution is based on the assumption of negligible flow through the bottom of a partially penetrating auger hole whereas in the present analysis, bottom flow has been accounted for in the analysis of the flow problem of Fig. 2.2.

In order to run a numerical check on our analytical procedure and also to ascertain the effect of specific storage on the overall hydraulics of flow around a stressed auger hole, a MODFLOW (Chiang and Kinzelbach, 2001) simulation was also carried out for a particular flow situation of Fig. 2.2 at three different storage coefficients and for each of these cases, the time required for the system to go into steady state mode was noted. A hypothetical aquifer of 5 m by 5 m surface area and thickness 1 m was modeled by drawing a grid network compri-

Table 2.1. Comparison of $Q_f/2\pi KhH_1$ and $Q_p/2\pi KhH_1$ ratios as obtained from the proposed solution of the flow problems of Figs. 2.1 and 2.2 with the corresponding values obtained from the analytical model of Dagan (1978) for a few flow situations of Figs. 2.1 and 2.2, respectively

H_3/a	$Q_f/2\pi KhH_1$		$Q_p/2\pi KhH_1$			
	$h/H_3=1$		$h/H_3=1.1$		$h/H_3=1.2$	
	Values obtained from Dagan' s solution	Values obtained from the proposed theory	Values obtained from Dagan' s solution	Values obtained from the proposed theory	Values obtained from Dagan' s solution	Values obtained from the proposed theory
100	0.239	0.236	0.251	0.256	0.256	0.261
500	0.172	0.172	0.178	0.179	0.181	0.183
1000	0.154	0.154	0.159	0.160	0.161	0.163
1500	0.145	0.145	0.149	0.149	0.151	0.153
2000	0.139	0.139	0.143	0.144	0.144	0.145

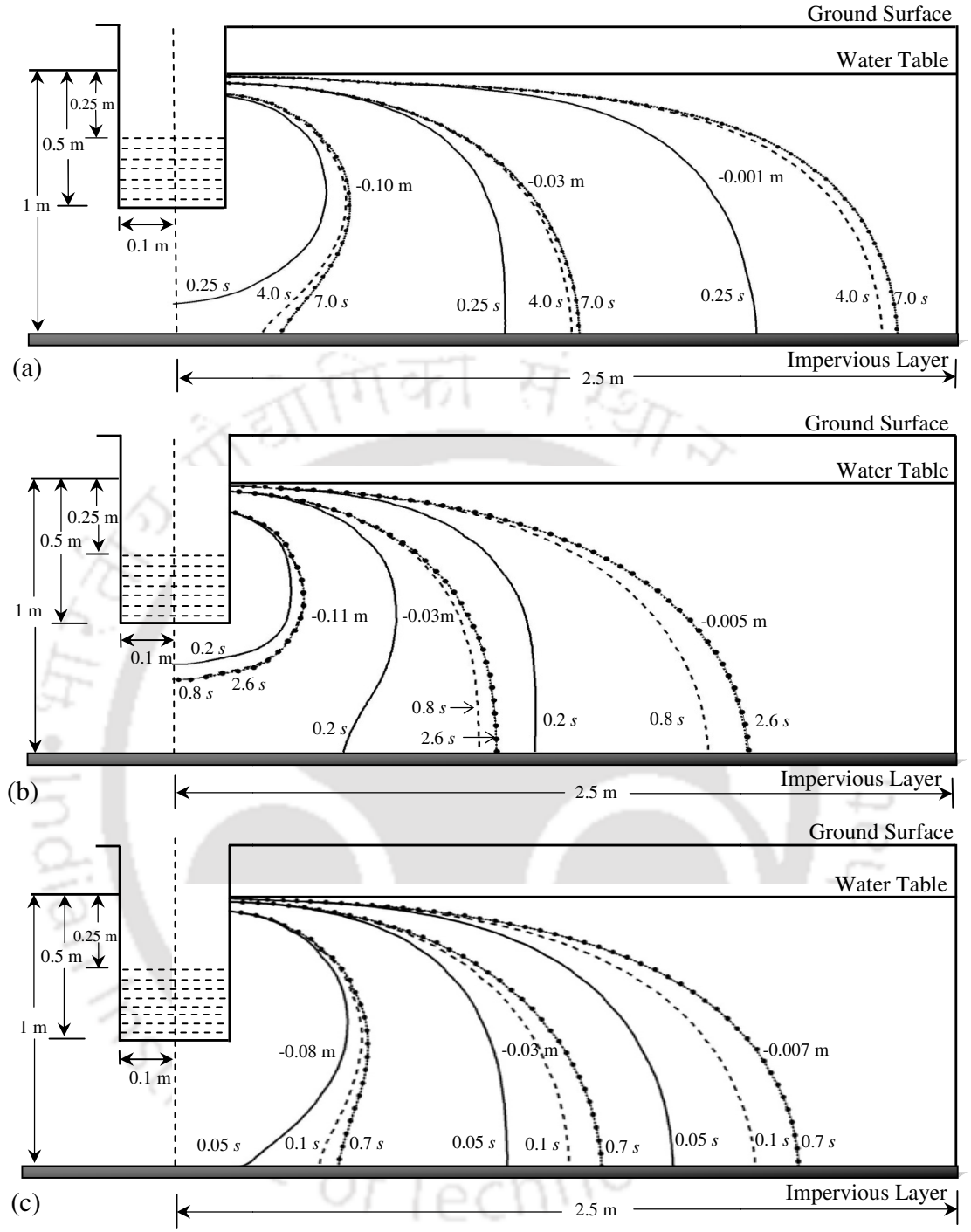

Fig. 2.6. Hydraulic head contours as obtained vide transient MODFLOW simulation of the auger hole problem of Fig. 2.2 at different times for a few flow situations of the problem and the comparison of the steady state MODFLOW generated contours with the corresponding contours obtained from the proposed analytical model of the flow problem of Fig. 2.2 when $K = 9.50$ m/day and (a) $S_s = 0.001\,\text{m}^{-1}$, (b) $S_s = 0.0001\,\text{m}^{-1}$ and (c) $S_s = 0.00001\,\text{m}^{-1}$

-sing of 52 rows, 52 columns and 22 layers. The area of each grid cell was taken as 0.1 m × 0.1 m and the depth of each layer as 0.05 m. The top row and the outermost columns were given a zero head and the imperviousness at the bottom layer was achieved by making all the cells in that layer ineffective. For representing approximately a circular auger hole of radius 0.1 m at the centre of the flow domain, four centrally located grid cells were further refined and copied down to the eleventh layer to achieve a partial penetration of 0.5 m from the top of the water table and then starting with -0.05 m in the 2nd layer and progressively decreasing by -0.05 m in each layer from the value of the preceding layer, head values up to the 11th layer were assigned using constant head cells. Thus, in that way, a head distribution ranging from 0 m in the 1st layer to -0.5 m in the 11th layer was achieved. It should be noted that all these heads were measured with respect to the origin *O* in the water table as can be seen in Fig. 2.2. The aquifer was assumed as isotropic and a constant hydraulic conductivity of 0.00011 m/s (9.5 m/day) was assigned to all the grid cells. With the above inputs, a transient simulation was carried out for three different storage coefficients, viz., $0.001\,m^{-1}$, $0.0001\,m^{-1}$ and $0.00001\,m^{-1}$, respectively, and the generated hydraulic head contours obtained at a few time intervals were noted as depicted in Fig. 2.6. The storage coefficient of an incompressible soil is zero and the head profiles shown in Fig. 2.6 instantaneously assume the steady state values. Further, to check the accuracy of our developed solution of the flow problem of Fig. 2.2, the steady state contours obtained from the MODFLOW runs were also compared with the corresponding values as predicted by our model. As may be observed, these numerically obtained steady state contours for all the tested flow situations are found to be matching completely with our analytical counterparts thereby showing again that the developed analytical solution for the flow problem of Fig. 2.2 is a correct one. It is also interesting to note from Fig. 2.6 that flow of water into a stressed auger hole quickly goes into a steady state mode and hence the steady state assumption commonly being made [Kirkham and Van Bavel, 1948; Kirkham, 1958; Dagan (recovery test), 1978] in the analysis of auger hole flow situations is expected not to make any serious error in reading actual auger hole flow scenarios. A similar observation was also made by Widdowson et al. (1990) from their numerical study on slug tests conducted in an unconfined aquifer where they reported that the effect of aquifer storage during a slug test in a phreatic aquifer may be quite insignifi-

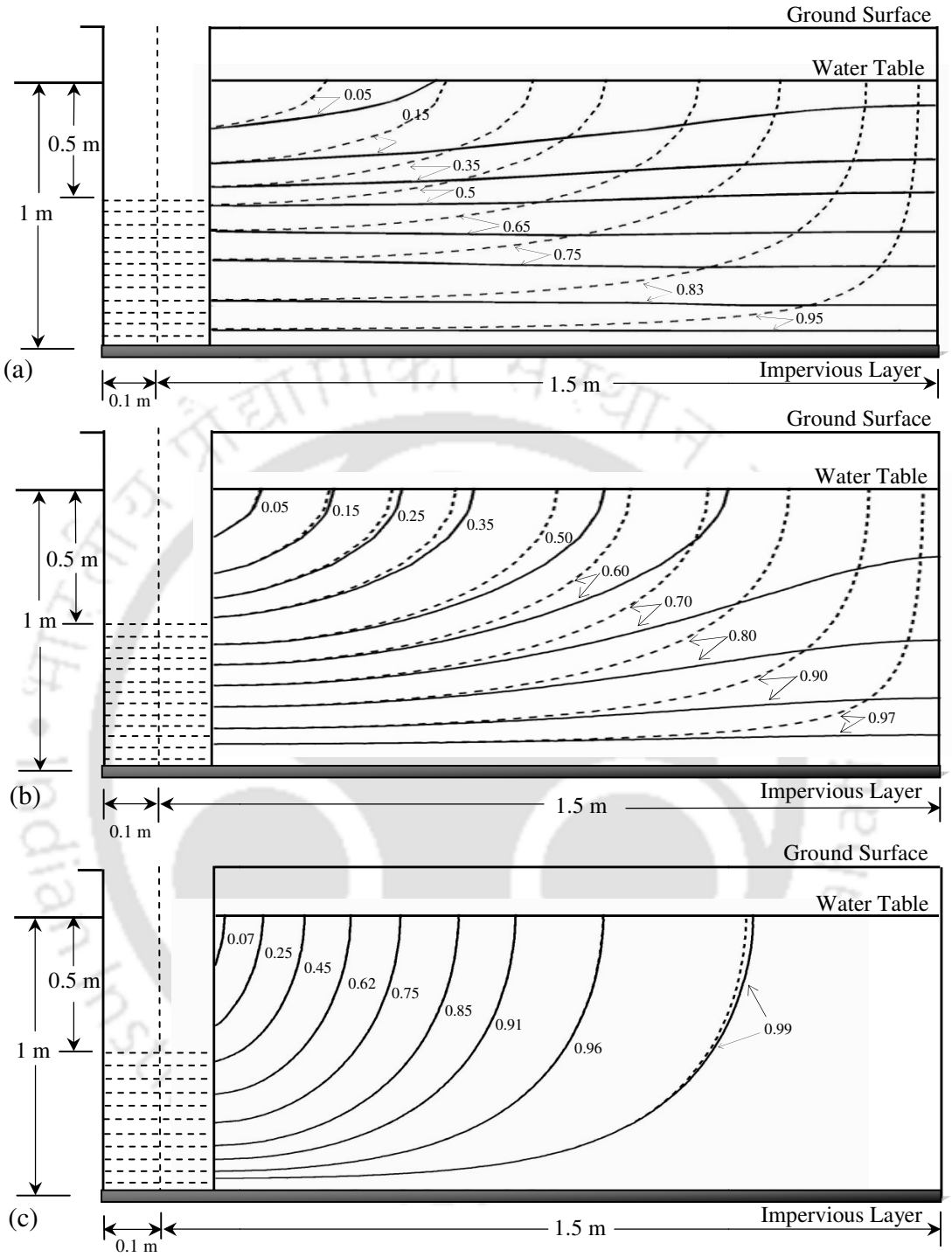

Fig. 2.7. Comparison of normalized streamlines as obtained from the proposed solution of the flow problem of Fig. 2.1 with corresponding streamlines obtained from the analytical solution of Kirkham and Powers (1972) when $b = 1.5$ m and the other parameters of the problem are taken as shown and (a) $K_r/K_z = 10/1$, (b) $K_r/K_z = 1/1$ and (c) $K_r/K_z = 1/10$

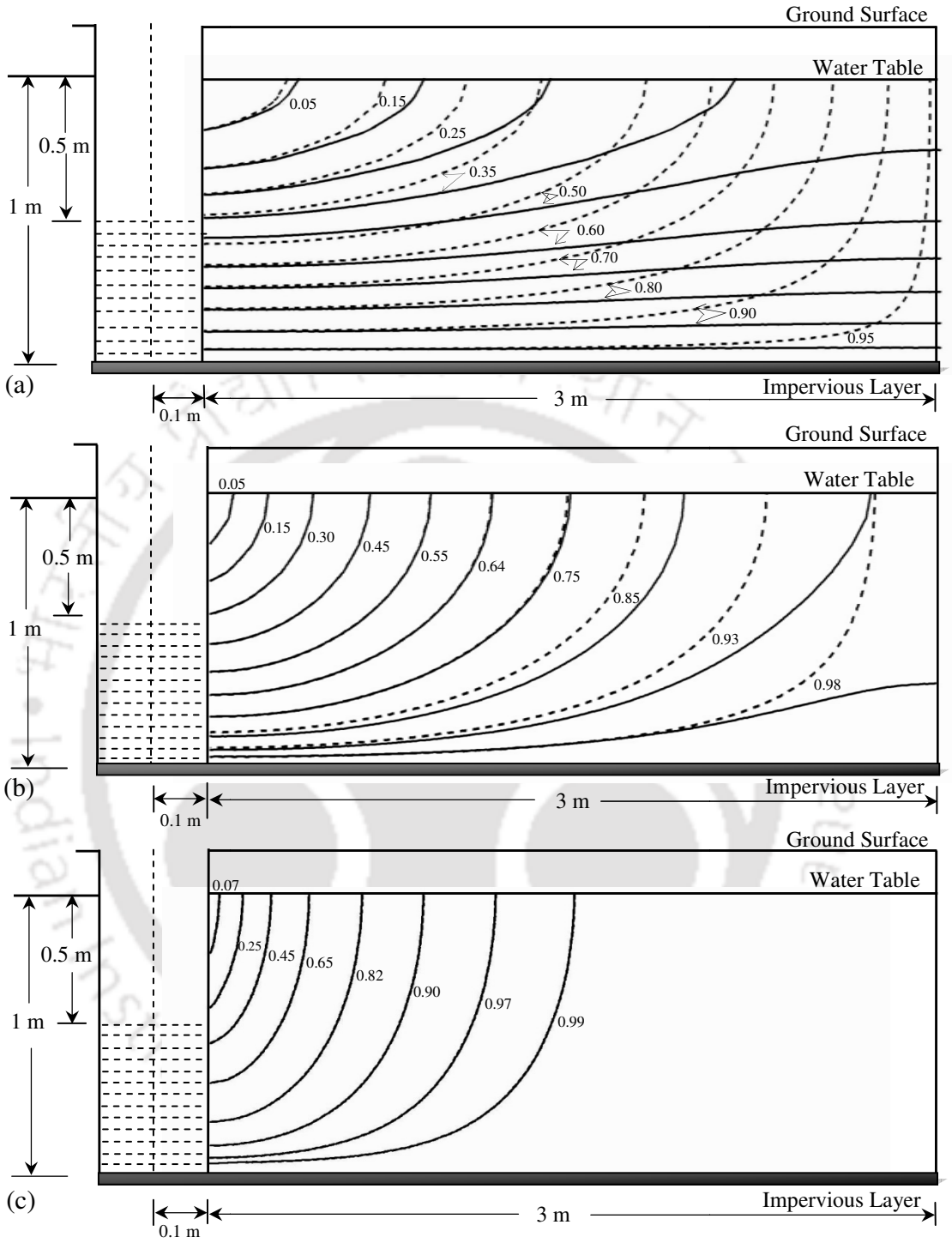

Fig. 2.8. Comparison of normalized streamlines as obtained from the proposed solution of the flow problem of Fig. 2.1 with corresponding streamlines obtained from the analytical solution of Kirkham and Powers (1972) when $b = 3$ m and the other parameters of the problem are taken as shown and (a) $K_r/K_z = 10/1$ (b) $K_r/K_z = 1/1$ and (c) $K_r/K_z = 1/10$

-cant in view of the fact that the flow around a slug hole immediately returns into a quasi-steady state after water is being allowed to flow into the stressed slug hole. This is particularly true for an unconfined aquifer having a low storage coefficient.

We would like to point out here that Kirkham and Powers (1972) obtained an analytical solution to the boundary value problem shown in Fig. 2.1 by assuming the boundary I of Fig. 2.1 as a no-flow (Neumann) one instead of the equal hydraulic head (Dirichlet) outer boundary considered here. These two solutions, however, are quite different from one another and the predicted flow behaviors around a stressed auger hole obtained from them may differ considerably from one another, particularly if the stressed auger hole lies in an unconfined aquifer with a high anisotropy ratio and/or the outer boundary lies at a relatively close distance from the centre of the stressed hole, as has been aptly demonstrated in Figs. 2.7 and 2.8, respectively. However, for an aquifer with a low anisotropy ratio, the flow behavior around a stressed hole predicted by both these solutions may be quite close to each other, provided the distance of the outer boundary is relatively large. As anisotropy ratios of most of the natural deposits are generally higher than one and also the fact that flow to a bailed auger hole takes place not only from the top water table but also from the outer boundary surface as well, the solution proposed here for the fully penetrating auger hole is expected to be more realistic than the one obtained by Kirkham and Powers for the same by imposing a no-flow boundary condition at the outer surface.

From Fig. 2.9, we see that, like in the case of fully penetrating auger hole, anisotropy of soil plays a dominant role in deciding flow behavior around a stressed auger hole partially penetrating an unconfined aquifer – among other factors remaining constant, a high anisotropy ratio of the aquifer causes the flow domain to expand and a low anisotropy ratio causes the domain to shrink in the horizontal direction. It can also be observed from Figs. 2.9 and 2.10 that, with the increase of the distance of the outer layer, most of the flow to an auger hole gets originated from the water table, particularly if the anisotropy ratio of the aquifer is low. It is also clear from the shape factor table (Table A.1, Appendix) that the effect of the distance of the outer boundary from the centre of the hole on flow to a stressed auger hole diminishes with the increase of this distance and beyond a certain value, depending on a flow situation, the radial extent of the outer boundary is having negligible impact on the overall

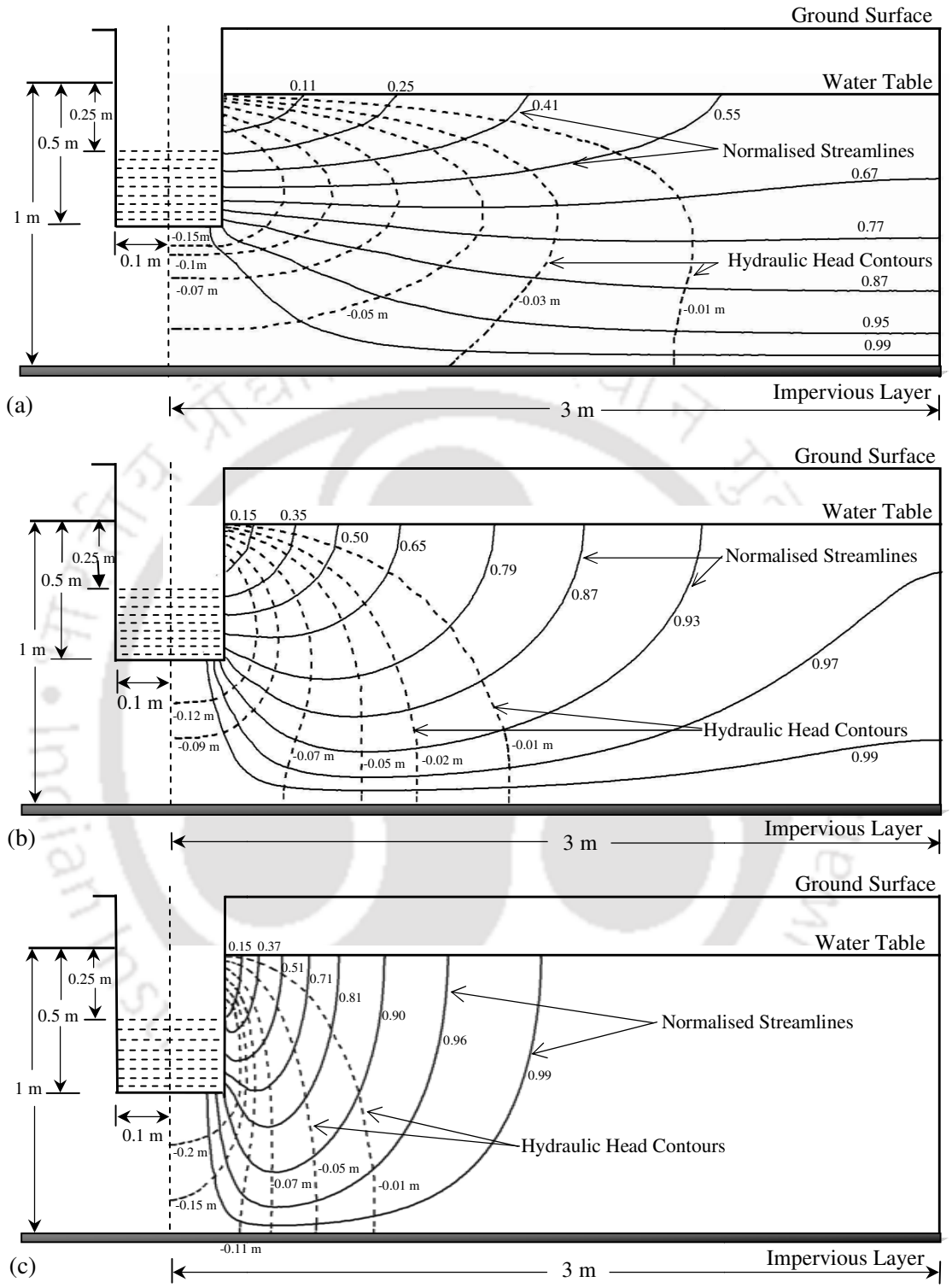

Fig. 2.9. Lines of equal hydraulic head and normalized streamlines corresponding to Fig. 2.2 when the flow geometries are as shown and (a) $K_r/K_z = 10/1$, (b) $K_r/K_z = 1/1$ and (c) $K_r/K_z = 1/10$

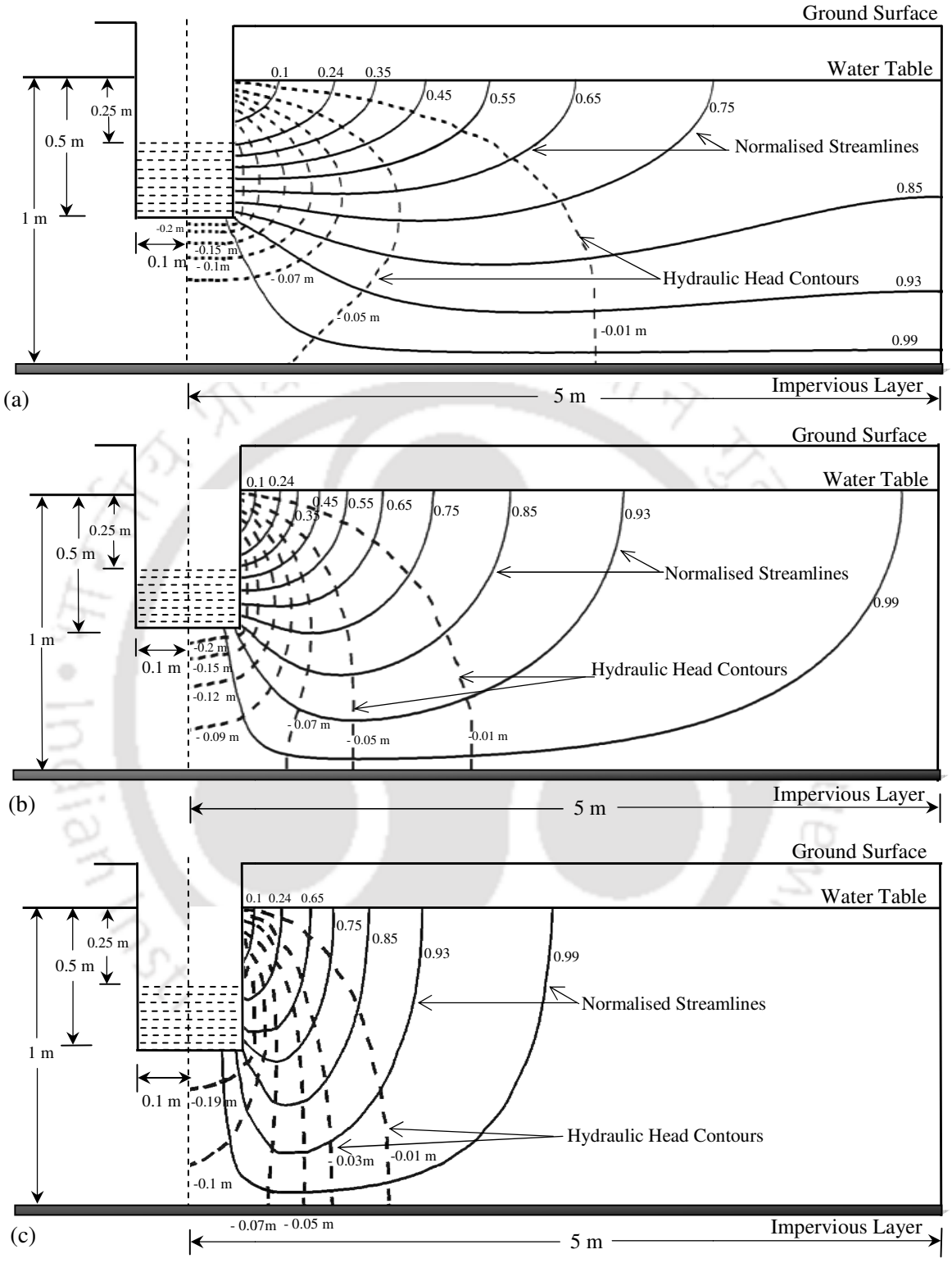

Fig. 2.10. Lines of equal hydraulic head and normalized streamlines corresponding to Fig. 2.2 when the flow geometries are as shown and (a) $K_r/K_z = 10/1$, (b) $K_r/K_z = 1/1$ and (c) $K_r/K_z = 1/10$

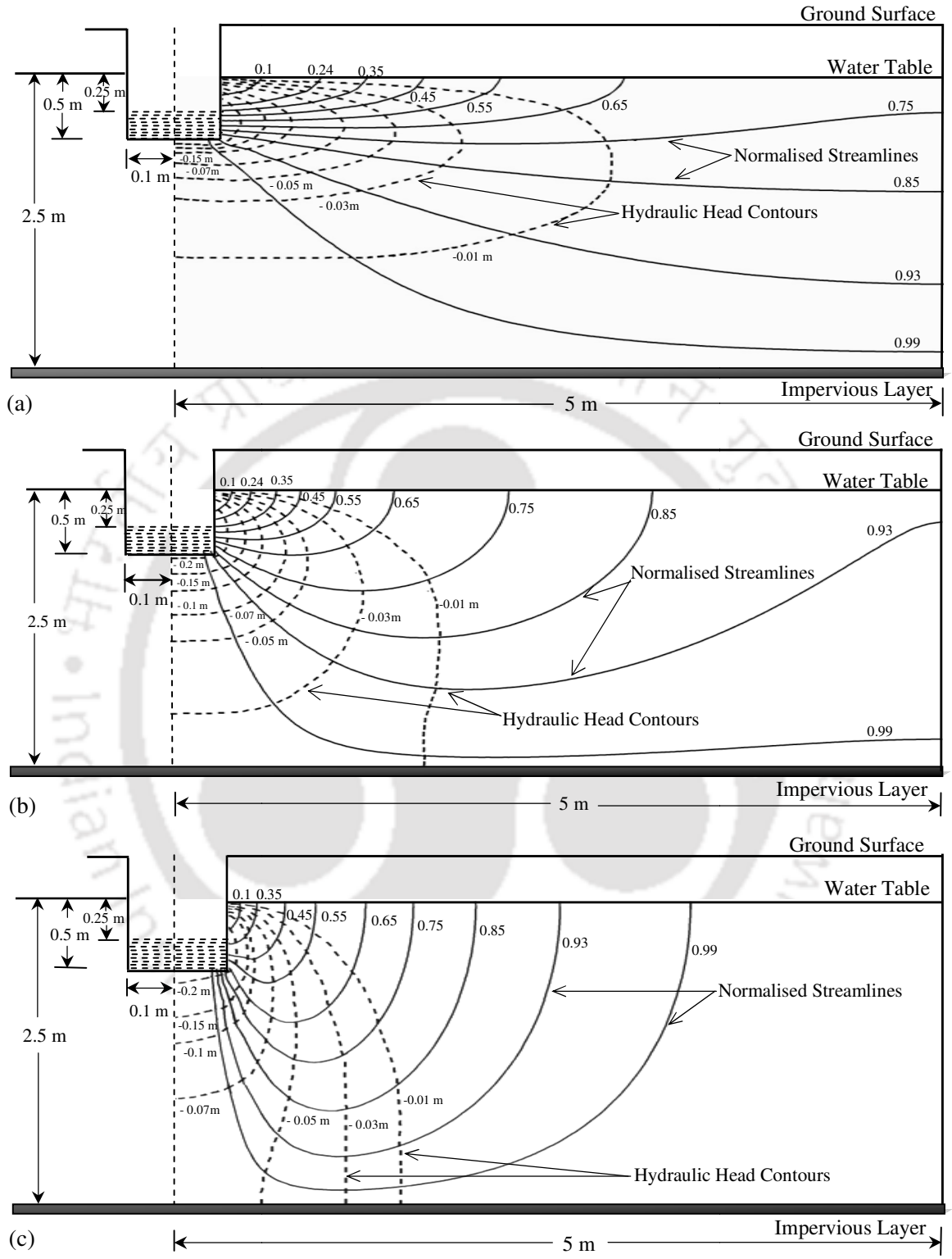

Fig. 2.11. Lines of equal hydraulic head and normalized streamlines corresponding to Fig. 2.2 when the flow geometries are as shown and (a) $K_r/K_z = 10/1$, (b) $K_r/K_z = 1/1$ and (c) $K_r/K_z = 1/10$

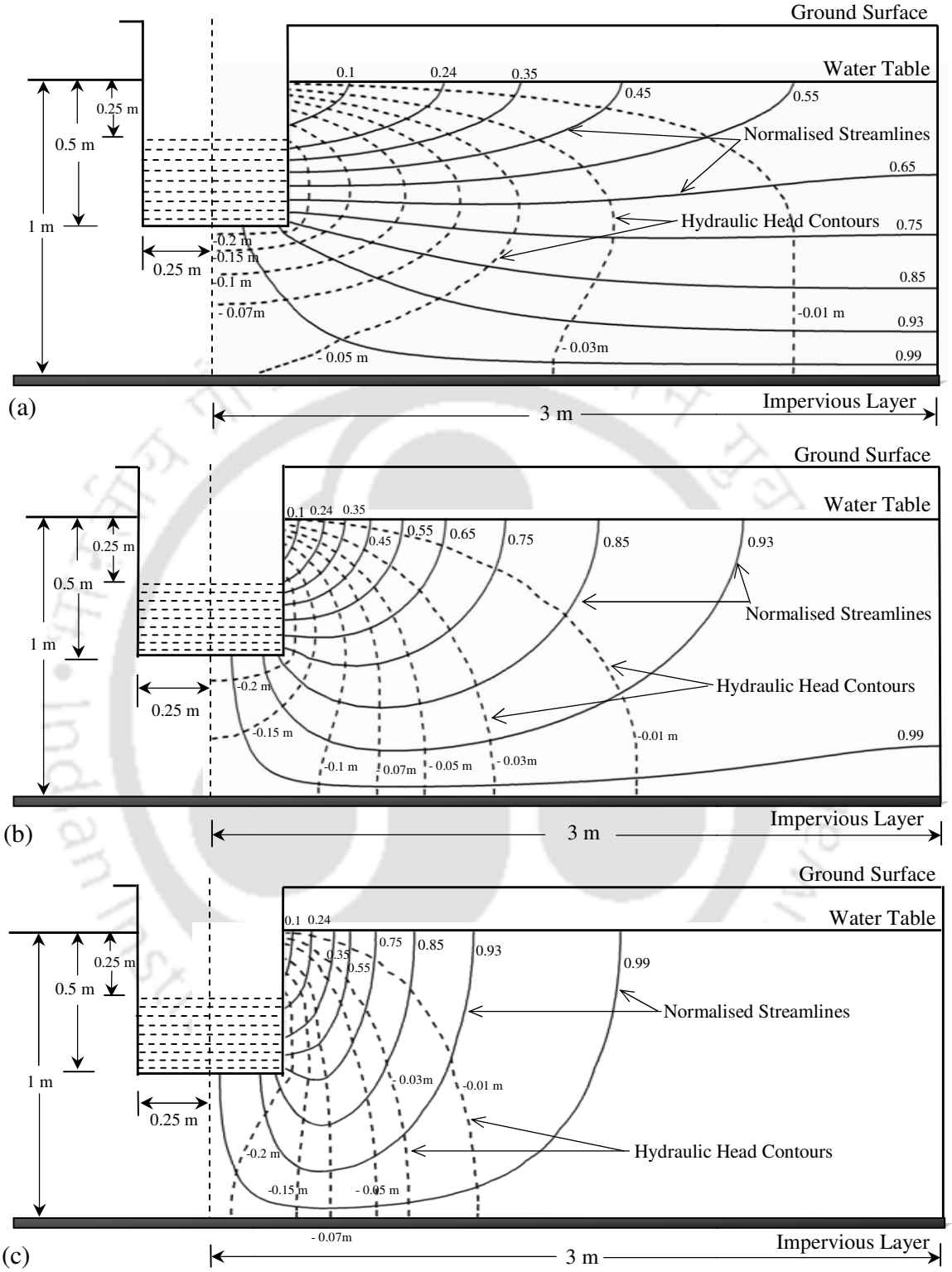

Fig. 2.12. Lines of equal hydraulic head and normalized streamlines corresponding to Fig. 2.2 when the flow geometries are as shown and (a) $K_r/K_z = 10/1$, (b) $K_r/K_z = 1/1$ and (c) $K_r/K_z = 1/10$

hydraulics around the hole. As may be observed from this table, same observation can also be made in relation to the distance of the impervious layer as measured from the top of the water table. It may also be seen in Figs. 2.9 to 2.11 that, among other factors remaining the same, the increase of depth of the impervious layer from the water table causes the streamlines to uncoil and may also lead to a considerable increase in the fraction of bottom flow to an auger hole, mainly if the hole is being laid in a soil with a low anisotropy ratio. Also, Fig. 2.12 reveals that bottom flow may account for a considerable portion of the total flow to an auger hole, particularly if the diameter of the hole is large and is being dug in a soil having a low anisotropy ratio.

2.6 Field Applications

The analytical models proposed here can be utilized to estimate the directional conductivities of an unconfined aquifer as well as the horizontal domain of influence of the perturbed zone arising out of an auger hole test, using auger hole experimental data below a water table. If the anisotropy ratio of the tested aquifer is known beforehand, experimental readings obtained from a single auger hole test being performed on the aquifer will be sufficient to get the required data for our models to be applied; if, however, the anisotropy ratio of the aquifer is not known *a priori*, auger hole experiments on two auger holes of different geometries may be designed in the aquifer in order that the requisite data needed for estimating the desired parameters be generated. We will now show a few applications of our developed models demonstrating how our derived solutions can be used to translate the data obtained from an auger hole test in an unconfined aquifer to the directional conductivities of the aquifer and also how the extent of horizontal spread of the perturbed zone associated with the test can be determined.

Example 1

Let us consider the auger hole experiment data obtained from Example 1 of Barua and Tiwari (1995) for a fully penetrating auger hole; in our notations, these data can be expressed as: soil isotropic, i.e., $K^a = 1$, thus, $K = K_r = K_z$, $h = 126.5$ cm, $H_1 = 126.5$ cm, $a = 5$ cm and the rate of rise of water in the auger hole $= 0.112$ cm/s, therefore, $Q_f = \pi(5)^2 0.112 = 8.7965$ cm^3/s. Applying Eq. (2.26) to these data, we get

$$K = \frac{8.7965}{-2\times\pi\times 5\sum_{m=1}^{M} C_m \left[\frac{K_0\left(\frac{-N_m b}{1}\right) I_1\left(\frac{-N_m\times 5}{1}\right) + K_1\left(\frac{-N_m\times 5}{1}\right) I_0\left(\frac{-N_m b}{1}\right)}{K_0\left(\frac{-N_m b}{1}\right) I_0\left(\frac{-N_m\times 5}{1}\right) - K_0\left(\frac{-N_m\times 5}{1}\right) I_0\left(\frac{-N_m b}{1}\right)} \right]}, \quad (2.58)$$

where

$$N_m = \left[\frac{(1-2m)\pi}{2\times 126.5} \right]$$

But, as can be seen in Eq. (2.58), for the calculation to proceed, we must need the value of *b*, which is an unknown. Assuming different values of *b* and calculating the corresponding conductivity values by summing up to ten terms of the infinite series appearing in Eq. (2.58) (i.e., *M* = 10), a graph like the one shown in Fig. 2. 13(a) can be drawn for the isotropic soil. It is clear that with the increase of *b* beyond 239 cm, the estimated *K* values become more or less constant thereby showing that the horizontal extent of the perturbed zone for the given flow situation is extending about 239 cm from the centre of the auger with the corresponding conductivity equaling 5.20×10^{-4} cm/s = 0.45 m/day. This conductivity figure is matching very well with the conductivity values of 0.43 m/day and 0.41 m/day obtained by applying the nomograph of Van Bavel and Kirkham (1948) and the modified Ernst's curve of Van Beers (1958; also reproduced by Bouwer and Jackson, 1974), respectively, to the given data.

If we carry out our calculation by summing up to only five terms of the infinite series (i.e., *M* = 5), we virtually land with the same value of *K* equaling to 5.173×10^{-4} cm/s $= 0.45$ m/day and *b* equal to about 240 cm. Thus, the matching of this conductivity value can also be taken as a check about the correctness of our developed solution for the fully penetrating auger hole problem Fig. 2.1.

If the entire computation is repeated (taking *M* = 10) by assuming the soil to be anisotropic with anisotropy ratios of 10:1 and 1:10, respectively, and at the same time keeping the other variables same as before, the resulting $K_r - b$ curves have been found [(Fig. 2.13(a)] to differ considerably from the one obtained for the isotropic case. For $K_r : K_z = 10:1$, the horizontal and the vertical conductivities now turn out to be 0.62 m/day and 0.062 m/day, respectively, with the radial perturbed zone extending up to about 481 cm from the centre of the hole and for $K_r : K_z = 1:10$, the corresponding values work out to be 0.29 m/day and 2.9

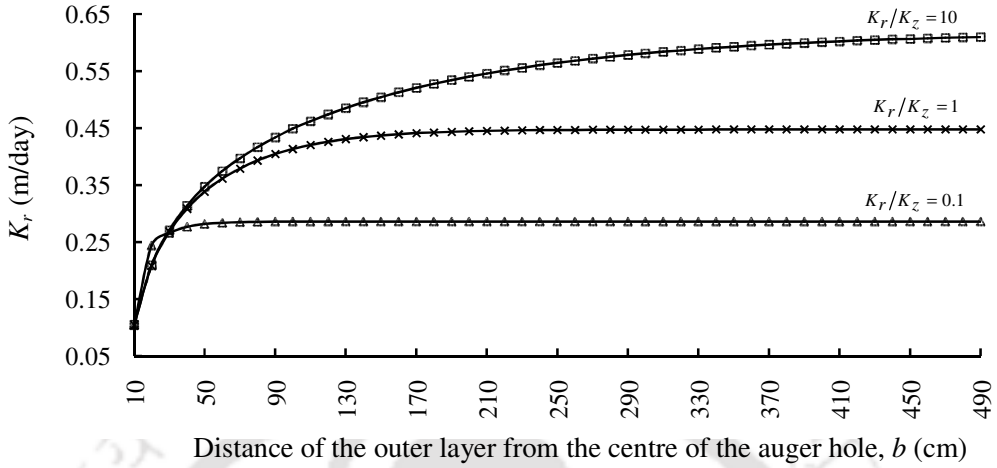

Fig. 2.13(a). Variation of horizontal hydraulic conductivity with the distance of the outer layer for the flow situation of Example 1 for various fixed values of the ratio K_r / K_z

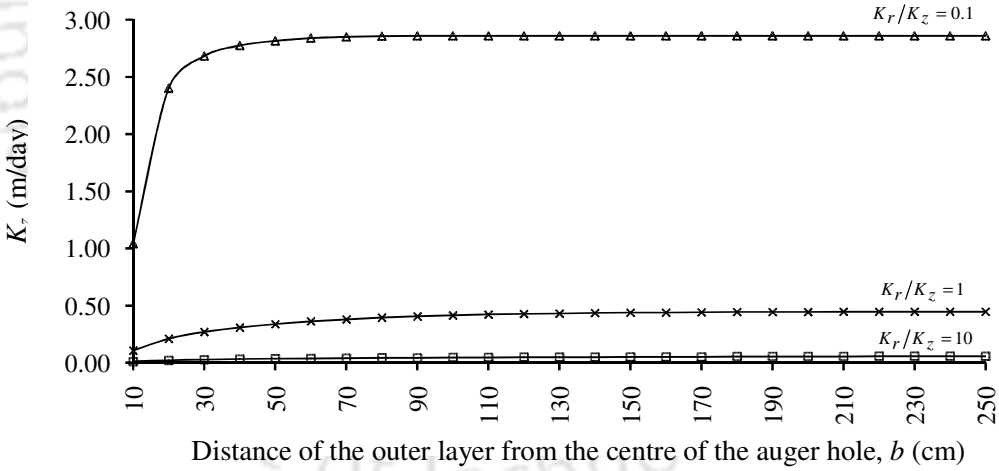

Fig. 2.13(b). Variation of vertical hydraulic conductivity with the distance of the outer layer for the flow situation of Example 1 for various fixed values of the ratio K_r / K_z

m/day, respectively, with the horizontal domain of influence now extending up to about 71 cm only from the centre of the hole. If $K_z - b$ curves [Fig. 2.13(b)] are now being plotted for the flow situation with the considered anisotropy ratios, we find that the influence of the vertical conductivity is confined to a much narrower domain from the centre of the auger hole as compared to the radial conductivity, both for situations when the soil is isotropic and when the anisotropy ratio of the soil is $10:1$. For $K_r : K_z = 1:10$, however, the influence of the vertical conductivity has been found to be about 77 cm for the considered flow geometry. Thus, among other factors remaining constant, the change in anisotropy ratio alone seems to make a lot of difference on the overall hydraulics of an auger hole – a higher anisotropy ratio may lead to the development of a large radially spread perturb zone whereas a low anisotropy may result in a radially shrunken active zone.

Example 2

Let us now consider the data considered by Kessler and Oosterbaan (see their Example 5, p.276, 1980) obtained from an auger hole test in a water table aquifer. The same set of data was also considered by Barua and Tiwari (see their Example 3, 1995) for estimating hydraulic conductivity using their series solution developed for an aquifer of infinite horizontal extent. In notations adopted in this paper, these data can be expressed as: soil isotropic, i.e., $K^a = 1$ and hence $K = K_r = K_z$, $h = 303$ cm, $H_1 = 28.4$ cm; $H_3 = 126$ cm, $a = 4$ cm and the average rate of rise of water in the pumped auger hole $= 0.112$ cm/s, therefore, $Q_p = \pi(4)^2(0.112) = 5.6297$ cm^3/s. Applying these figures to Eq. (2.55), we obtain

$$5.6297 = 2\times\pi\times 4\times K\times\sum_{n=1}^{N} B_n \left[\frac{K_0\left(\frac{-N_n b}{1}\right)I_1\left(\frac{-N_n\times 4}{1}\right)+K_1\left(\frac{-N_n\times 4}{1}\right)I_0\left(\frac{-N_n b}{1}\right)}{K_0\left(\frac{-N_n b}{1}\right)I_0\left(\frac{-N_n\times 4}{1}\right)-K_0\left(\frac{-N_n\times 4}{1}\right)I_0\left(\frac{-N_n b}{1}\right)}\right]$$

$$\times\left[\cos(N_n\times 126)-1\right]-2\times\pi\times 4\times K\times\sum_{m=1}^{M} A_m\left[\frac{I_1\left(\frac{-N_m\times 4}{1}\right)}{I_0\left(\frac{-N_m\times 4}{1}\right)}\right], \qquad (2.59)$$

where

$$N_n = \left[\frac{(1-2n)\pi}{2\times 303} \right] \tag{2.60}$$

and

$$N_m = \left[\frac{(1-2m)\pi}{2\times(303-28.4)} \right]. \tag{2.61}$$

Here again we need *b* for our calculation to proceed. Moving as we have done in Example 1 and summing up to ten terms (i.e., $N = M = 10$) of the series occurring in Eq. (2.59), the estimated isotropic conductivity of the aquifer and the horizontal extent of the perturbed zone are now coming out to be 7.60×10^{-4} cm/s = 0.66 m/day and about 271 cm, respectively. It is to be noted that this conductivity value is found to be matching exactly with the conductivity value of 0.66 m/day calculated by Kessler and Oosterbaan (see their Example 5, p.276, 1980) for the tested data using the Ernst's chart. If the computation is repeated by summing only five terms (i.e., $N = M = 5$) of the series solution, the estimated conductivity now comes out to be about 8.20×10^{-4} cm/s $= 0.71$ m/day and the extent of radial spread of the perturbed zone as about 271 cm – values which agree very well with those obtained from a ten term expansion of the series occurring in Eq. (2.59).

As in the previous example, if we repeat the calculations (considering $N = M = 10$) by assuming the aquifer to be a homogeneous and anisotropic one with an anisotropy ratio of first 10:1 and then a ratio of 1:10, the resulting $K_r - b$ and $K_z - b$ curves for the flow situations are now turning out to be as shown in Figs. 2.14(a) and 2.14(b), respectively. For $K_r : K_z = 10:1$, K_r and K_z are calculated to be 0.94 m/day and 0.09 m/day, respectively, with the influence of the horizontal and vertical hydraulic conductivities extending up to about 440 cm and 56 cm, respectively, from the centre of the hole; the corresponding values for the case when $K_r : K_z = 1:10$ are estimated to be 0.39 m/day and 3.93 m/day, respectively, with the domain of influence of the horizontal and vertical conductivities as about 70 cm and 85 cm, respectively.

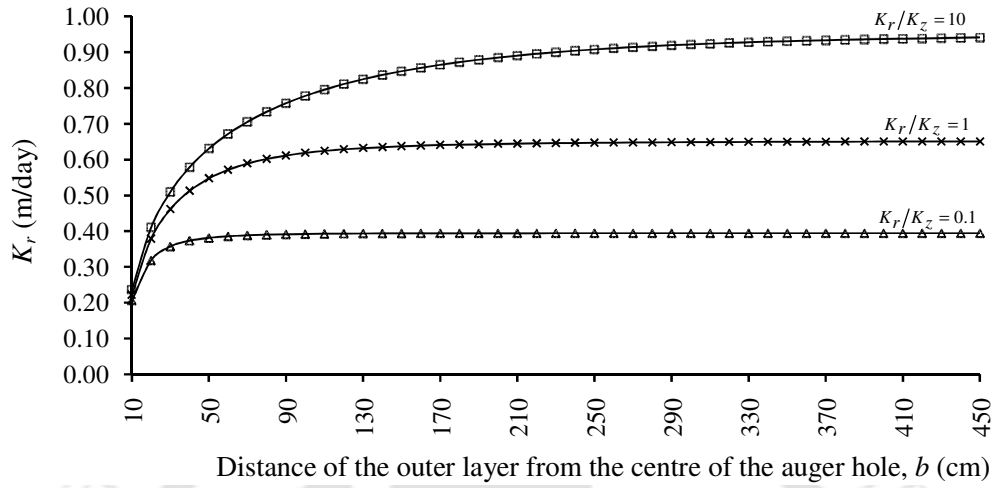

Fig. 2.14(a). Variation of horizontal hydraulic conductivity with the distance of the outer layer for the flow situation of Example 2 for various fixed values of the ratio K_r / K_z

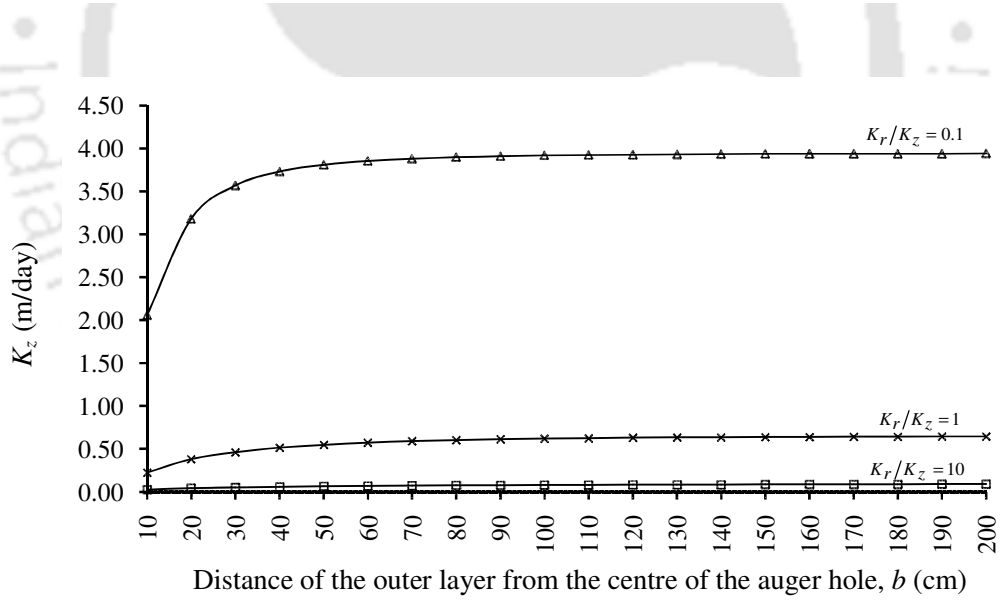

Fig. 2.14(b). Variation of vertical hydraulic conductivity with the distance of the outer layer for the flow situation of Example 2 for various fixed values of the ratio K_r / K_z

Example 3

This example shows how to compute the hydraulic conductivity of a homogeneous and isotropic unconfined aquifer utilizing data of an auger hole test performed on the aquifer by making a direct use of the shape factors given in Table A.1 (Appendix-A). Suppose an auger hole test performed in an isotropic phreatic aquifer yields the following data: $h = 60$ cm, $H_1 = 20$ cm, $H_3 = 40$ cm, $a = 4$ cm and the rate of rise of water in the auger hole $= 0.15$ cm/s, therefore, $Q_p = \pi(4)^2(0.15) =$ 7.5398 cm^3/s. Thus, for the considered flow situation, we have $H_3/a = 10$, $(h - H_3)/H_3 = 0.5$, and $H_1/H_3 = 0.5$. From Table A.1 (Appendix-A), we see that the shape factor corresponding to these data for $b = 4H_3$ is 19.62 and hence we have the corresponding hydraulic conductivity as 2.94 m/day. If we consider $b = 6H_3$, the shape factor now turns out to be 19.63 and the corresponding conductivity as 2.94 m/day, exactly same up to the second places of decimal as that obtained using the shape factor corresponding to the situation $b = 4H_3$. The $K - b$ distribution curve for the flow situation is as given in Fig. 2.15 showing that the domain of the perturbed zone for the test is getting extended up to about 173 cm from the auger hole axis.

If we now make use of the shape factor table of Boast and Kirkham (1971, see their Table 1) for the considered auger hole flow situation, we find the relevant shape factor to be 19.5 and the corresponding hydraulic conductivity to be $19.5 \times 0.15 = 2.93$ m/day, a conductivity figure very close to our figure of 2.94 m/day obtained using our shape factor table (Table A.1, Appendix) for situations where *b* is given a large value. This is the way it should be, as the solution presented here for the partially penetrating auger problem, for identical auger hole situations, should yield similar results with those obtained from the corresponding Boast and Kirkham's (1971) solution to the problem when *b* is given a very large value (theoretically infinite). That this has actually happened can also be treated as an additional proof about the accuracy of our developed solution for the partially penetrating auger hole problem.

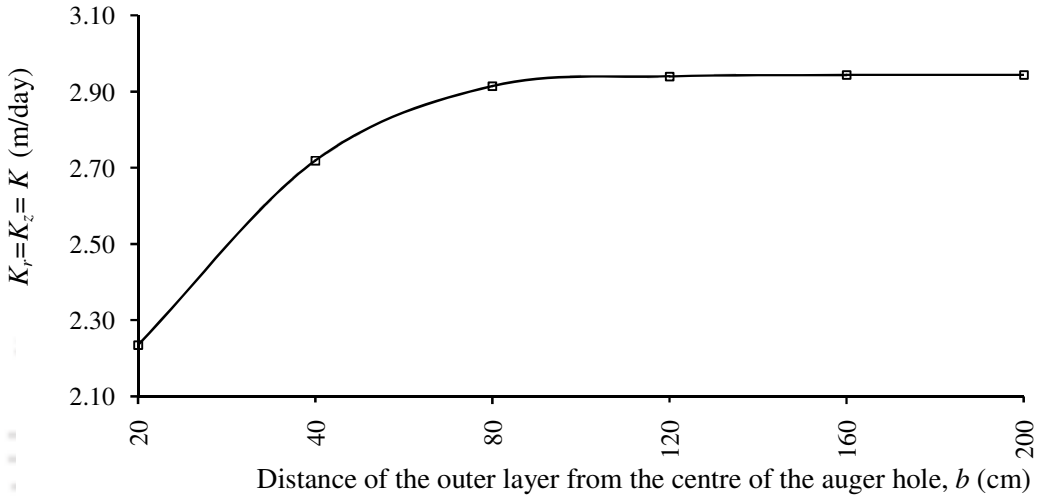

Fig. 2.15. Variation of hydraulic conductivity with the distance of the outer layer for the flow situation of Example 3

Example 4

We now consider an example where the anisotropy ratio of the tested aquifer is not known *a priori*. As mentioned before, we can then go for our simulation utilizing the data obtained from auger hole tests conducted on two auger holes of different geometries. Suppose the test data obtained from two fictitious auger holes in an unconfined aquifer be as follows:

Auger hole (1)	Auger hole (2)
$a(1) = 5$ cm	$a(2) = 15$ cm
$h(1) = 200$ cm	$h(2) = 200$ cm
$H_1(1) = 50$ cm	$H_1(2) = 50$ cm
$H_3(1) = 100$ cm	$H_3(2) = 100$ cm
$Q_p(1) = 33.8507$ cm^3/s	$Q_p(2) = 47.8751$ cm^3/s

Now, from Eq. (2.55), we have

$$\frac{Q_p(1)}{Q_p(2)} = \frac{33.8507}{47.8751} = \frac{[Q_s(1) + Q_b(1)]}{[Q_s(2) + Q_b(2)]}, \tag{2.62}$$

where Q_s and Q_b are discharge expressions related to the sides and bottom of a partially penetrating auger hole and given by Eqs. (2.51) and (2.54), respectively. Thus, for the flow situations, we have

$$Q_s(1) = 2\times\pi\times5\times\left(\frac{K_r}{K^a}\right)\sum_{n=1}^{N} B_n \left[\frac{K_0\left(\frac{-N_n b}{K^a}\right) I_1\left(\frac{-N_n\times5}{K^a}\right) + K_1\left(\frac{-N_n\times5}{K^a}\right) I_0\left(\frac{-N_n b}{K^a}\right)}{K_0\left(\frac{-N_n b}{K^a}\right) I_0\left(\frac{-N_n\times5}{K^a}\right) - K_0\left(\frac{-N_n\times5}{K^a}\right) I_0\left(\frac{-N_n b}{K^a}\right)}\right] [\cos(N_n\times100) - 1], \tag{2.63}$$

$$Q_b(1) = -2\times\pi\times5\times\left(\frac{K_r}{K^a}\right)\sum_{m=1}^{M} A_m \frac{I_1\left(\frac{-N_m\times5}{K^a}\right)}{I_0\left(\frac{-N_m\times5}{K^a}\right)}, \tag{2.64}$$

$$Q_s(2) = 2\times\pi\times15\times\left(\frac{K_r}{K^a}\right)\sum_{n=1}^{N} B_n \left[\frac{K_0\left(\frac{-N_n b}{K^a}\right) I_1\left(\frac{-N_n\times15}{K^a}\right) + K_1\left(\frac{-N_n\times15}{K^a}\right) I_0\left(\frac{-N_n b}{K^a}\right)}{K_0\left(\frac{-N_n b}{K^a}\right) I_0\left(\frac{-N_n\times15}{K^a}\right) - K_0\left(\frac{-N_n\times15}{K^a}\right) I_0\left(\frac{-N_n b}{K^a}\right)}\right]$$
$$\times[\cos(N_n\times100) - 1] \tag{2.65}$$

and

$$Q_b(2) = -2\times\pi\times 15\times\left(\frac{K_r}{K^a}\right)\sum_{m=1}^{M} A_m \frac{I_1\left(\frac{-N_m\times 15}{K^a}\right)}{I_0\left(\frac{-N_m\times 15}{K^a}\right)}, \tag{2.66}$$

where

$$N_n(1) = N_n(2) = \left[\frac{(1-2n)\pi}{2\times 200}\right] \tag{2.67}$$

and

$$N_m(1) = N_m(2) = \left[\frac{(1-2m)\pi}{2(200-100)}\right]. \tag{2.68}$$

It should be noted that Eq. (2.62) contains two unknowns K^a and b and hence to get the K^a value, a suitable b applicable to both the flow configurations must be assumed to start with the simulation. We have, however, observed that for any auger hole flow configuration, the effect of b on the overall hydraulics of flow to the hole becomes negligible with the increase of b beyond a threshold point; this point, of course, in general varies from one test situation to the other. Thus, we can always choose a b falling outside the radial extent of the perturb zones of both the stressed auger hole situations by simply assigning a very large value to it as this b then should be adaptable to both the tested situations. Assigning a b equal to 2500 cm in Eq. (2.62) and summing up to 10 terms (i.e., $N = M = 10$) of our series solution, we find K^a, by trial and error, to be $K^a = 4.295$, i.e., $(K^a)^2 = K_r / K_z = 18.447$.

If we consider b as 2000 cm in Eq. (2.62), K^a then works out to be 4.298, a value very nearly same as that obtained using b as 2500 cm in Eq. (2.62). Thus, it is clear that for the auger hole flow situations considered, the horizontal extent of the perturbed zone is not getting extended beyond 2000 cm from the centre of the hole. Once we have K^a, individual values of K_r and K_z can now be easily calculated by considering the experimental readings of either of the holes. Considering the second hole test data, we find K_r and K_z to be 4.61 m/day and 0.25 m/day, respectively. It should, however, be noted that the domain of radial influence of both the tests will not be same; proceeding as we have done in the previous examples, the domain of influence of the horizontal and vertical conductivities for the first

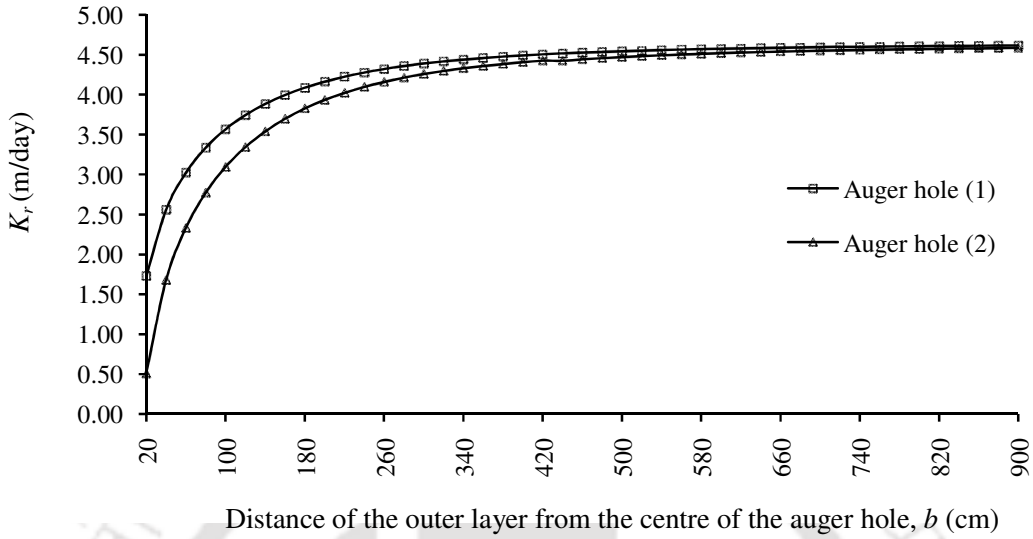

Fig. 2.16(a). Variation of horizontal hydraulic conductivity with the distance of the outer layer for the flow situation of Example 4 for auger hole (1) and auger hole (2), respectively

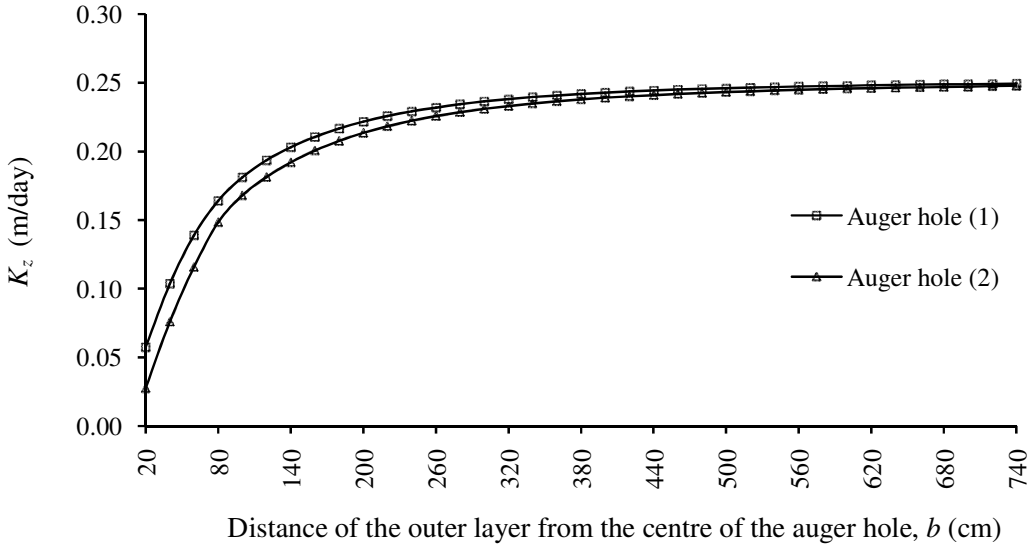

Fig. 2.16(b). Variation of vertical hydraulic conductivity with the distance of the outer layer for the flow situation of Example 4 for auger hole (1) and auger hole (2), respectively

test data are turning out to be about 536 cm and 332 cm [Fig. 2.13(a)], respectively, and for the second test data as about 869 cm and 604 cm [Fig. 2.13(b)], respectively, from the centre of the holes.

2.7 Conclusions

Equation of the hydraulic head function and from it the stream function and the expression of discharge have been derived for groundwater seeping into a stressed auger hole in an unconfined aquifer of finite horizontal and vertical extents and underlain by an impervious layer. The problem has been solved both for the cases when the auger hole fully penetrates the aquifer and rests on the impervious base and when the hole suspends above it. The theories proposed here may be considered as an extension of the works of Kirkham and Van Bavel (1948), Kirkham (1958), Boast and Kirkham (1971) and Barua and Tiwari (1995) on the auger hole seepage theory for a phreatic aquifer of infinite horizontal extent to that of a finite one, the aquifer being underlain by an impervious barrier. The study shows that the domain of influence of an auger hole test in a phreatic aquifer does not extend to an infinitely large distance in the horizontal plane, as has been commonly assumed in the derivation of the existing auger hole seepage theories (Kirkham and Van Bavel, 1948; Boast and Kirkham, 1971; Dagan, recovery test, 1978; Barua and Tiwari, 1995), but still can be of several metres in the lateral direction, particularly if the test is being conducted in an aquifer having a high anisotropy ratio. However, for a test carried in a low anisotropic aquifer, the situation may be reversed – the extent of the active zone in the horizontal plane may now be considerably small but the domain of influence of the test in the vertical plane may, at the same time, be relatively high. The study also reveals that the fraction of the total flow entering through the bottom of a partially penetrating auger hole may be considerably high, particularly if the diameter of the hole is large and/or the hole is being dug in a soil having a low anisotropy ratio. The study also shows that the distance of the outer layer and depth of the underlying impervious layer, influence flow into a stressed auger hole, mainly in situations where these layers lie at a close proximity to the centre of the hole. However, the effect of these layers on flow to an auger hole diminishes with the increase of their distance from the hole. It is also observed that the level of water in an auger hole also plays an important part in deciding flow around a pumped auger hole.

The validity of the developed solutions for both the fully and partially penetrating auger problems have been checked by first reducing these solutions from an aquifer of finite horizontal spread to that of an infinite one by adopting a high value of the distance of the outer layer in these solutions, and then comparing the analytical results obtained from them for a few auger hole situations with identical results obtained from the analytical works of others. A few MODFLOW checks on the partially penetrating auger hole solution have also been performed.

The proposed analytical models can be used to convert the experimental data obtained from an auger hole test in a phreatic aquifer into the directional conductivities of the tested aquifer and can also be utilized to estimate the horizontal extent of the perturbed zone resulting due to the test. It should be noted that this measure of horizontal extent of the perturbed zone associated with the test is important as it gives information about the radial extent of the soil space over which the directional conductivities of the soil are actually been measured in the test. We would like to point out here that, unlike the proposed solutions, the existing analytical models on the subject cannot be used to trace the zone of influence associated with an auger hole test, since these models were developed with the assumption of an aquifer extending to infinity in the radial direction and as such, so far as these models are concerned, the perturbed zones of all auger hole tests always extend up to infinity (Van Bavel and Kirkham, 1948). In order that the computational effort on the part of a user applying these solutions is minimized, a shape factor table (Table A.1, Appendix) corresponding to a few auger flow situations is also presented. It is hoped that the analytical models proposed herein along with these tabulated shape factors will be of use in estimating the directional conductivities of an unconfined aquifer as well as in working out the domain of influence of an auger hole test, utilizing data obtained from a standard auger hole test being performed on the aquifer.

2.8 List of Notations

The following notations are used in this chapter

A_m, B_n, C_m = constants with m = 1, 2, 3, …∝ and n = 1, 2, 3, …∝

a = radius of the auger holes of Figs. 2.1 and 2.2 [L];

b = horizontal extent of the aquifers of Figs. 2.1 and 2.2 as measured from the centre of the auger hole [L];

C = shape factor (dimensionless);

h = depth to the impervious layers of Figs. 2.1 and 2.2 as measured from the water table;

H_1 = depth of water in the auger holes of Figs. 2.1 and 2.2 as measured from the water table [L];

H_3 = depth of penetration of the partially penetrating auger hole of Fig. 2.2 as measured from the water table [L];

$I_0(.)$ = zero order modified Bessel function of first kind;

$I_1(.)$ = first order modified Bessel function of first kind;

K = hydraulic conductivity of homogeneous and isotropic aquifer [LT^{-1}];

$K_0(.)$ = zero order modified Bessel function of second kind;

$K_1(.)$ = first order modified Bessel function of second kind;

K_r = horizontal hydraulic conductivity of homogeneous and isotropic aquifers of Figs. 2.1 and 2.2 [LT^{-1}];

K_z = vertical hydraulic conductivity of homogeneous and isotropic aquifers of Figs. 2.1 and 2.2 [LT^{-1}];

$\left(K^a\right)^2$ = (K_r/K_z) anisotropy ratio (dimensionless);

M, N = number of terms to be summed in the infinite series solutions, 1, 2, 3, …

Q_b = discharge through the bottom of the partially penetrating auger hole of Fig. 2.2 [L^3T^{-1}];

Q_f = discharge of the fully penetrating auger hole of Fig. 2.1 [L^3T^{-1}];

Q_p = total discharge of the partially penetrating auger hole of Fig. 2.2 [L^3T^{-1}];

Q_s = discharge through the sides of the partially penetrating auger hole of Fig. 2.2 [L^3T^{-1}];

r = radial coordinate as measured from the centre of the auger holes of Figs. 2.1 and 2.2, [L];

z = vertical coordinate as measured from the centre of the auger holes of Figs. 2.1 and 2.2 [L];

ϕ = hydraulic head distribution for the fully penetrating auger hole problem of Fig. 2.1 [L];

ϕ_1 = hydraulic head distribution for the sub-domain R-I of Fig. 2.2 [L];

ϕ_2 = hydraulic head distribution for the sub-domain R-II of Fig. 2.2 [L];

ψ = stream function for the fully penetrating auger hole problem of Fig. 2.1 [L^2T^{-1}];

ψ_1 = stream function for the sub-domain R-I of Fig. 2.2 [L^2T^{-1}];

ψ_2 = stream function for the sub-domain R-II of Fig. 2.2 [L^2T^{-1}];

ψ^n = normalized stream function for the fully penetrating auger hole problem of Fig. 2.1 (dimensionless);

ψ_1^n = normalized stream function for the sub-domain R-I of Fig. 2.2 (dimensionless);

ψ_2^n = normalized stream function for the sub-domain R-II of Fig. 2.2 (dimensionless).

CHAPTER 3

ANALYTICAL SOLUTIONS FOR PREDICTING TRANSIENT SEEPAGE INTO DITCH DRAINS FROM A PONDED FIELD

This chapter deals with the development of a few transient analytical models for predicting flow into equally spaced ditch drains receiving water from a ponded field. The solution to the ditch drainage problem is first obtained by considering the water levels in the adjacent ditches to be as equal and the ponding depth as uniform, it is next solved by assuming the water levels of the adjacent ditches to be as unequal and the ponding depth as uniform and finally, a general solution to the problem is achieved by assuming the levels of water in the adjacent ditches to be as unequal and taking the ponding field over the surface of the soil as a variable one, instead of the uniform ponding depth assumption made while deriving solutions to the earlier two variants of the problem. The accuracy of the developed models is checked, in several instances, by comparing them with other simplified models. A MODLFOW test on the general analytical model for the variably ponded drainage situation is also carried out. The effects of depth and spacing of ditch drains, directional conductivities and specific storage of soil, levels of water in the adjacent ditches, nature of ponding field distribution on the surface of the soil, on drain discharge are also studied. Further, the times taken by a transient ditch drainage system to go to steady state for different flow situations are also analyzed. It is also shown with a few examples how the streamline and surface discharge distribution in a ponded soil profile can be modulated by adjusting the water level heights in between the adjacent drains and/or changing the ponding field distribution over the surface of the soil.

3.1 Introduction and Review of Related Work

Drainage is essential in many irrigated areas of the world for increasing agricultural productivity. The introduction of irrigation in arid and semi-arid regions generally brings in its wake the problems of water logging and salinity which must be tackled in order to achieve full potential of the irrigated lands. Irrigated agriculture has been reported to cause considerable increase in areas pertaining to water logging and salinity in India (Manjunath, et al., 2004; Chahar and Vadodaria, 2008a; 2008b). Drainage helps in controlling water logging by removing excess water from the soil surface and the root zones of crops and also

assists in preventing salinity build up of irrigated soils. Drainage is also required for reinstatement of flooded areas within a desired time frame, to maintain appropriate water balance in rice fields (Van Hoorn et al., 1994; Jia et al., 2006) and also to provide controlled groundwater environments for wildlife habitats (Youngs, 1994). Subsurface drainage is also provided to keep the water table at a desired level in playgrounds and race courses (Chahar and Vadodaria, 2008b) on an all season basis so that these facilities are in good order throughout the year.

One of the commonly used methods of leaching harmful salts from a soil profile is to artificially flood the soil surface with good quality irrigation water [electrical conductivity < 0.7 deci-Siemens per metre (Rhodes et al., 1992)] and then discharging the leached water through subsurface drains (Dielman, 1973; Martinez Beltran, 1978). Open ditches can be conveniently used for removing subsurface water, particularly in heavy clay soils and in areas where the topography is almost flat (Abrol et al., 1988). The procedure of reclamation of a salt affected soil mostly involves impounding the surface of the salt affected soil with water up to a desirable thickness so as to build the necessary head for forcing its movement though the soil with the intention that the seeping water takes a part of the salt present in the soil profile, this salt laden water is then collected and disposed of by a network of parallely placed ditch drains installed for the purpose. In order to understand the underlying hydraulics of flow to drainage ditches from a ponded field, several mathematical models have been worked out in the past for various flow situations. By providing appropriate limits to the solution of the fully penetrating auger hole problem of Kirkham and Van Bavel (1948) for a homogeneous and isotropic soil, Kirkham (1950) obtained a steady state solution to the ponded ditch drainage problem for the case when the ponded depth is zero and when the ditch drains are dug all the way down to the impervious base. For ditch drains partially penetrating a soil profile and resting above an impervious barrier, Fukuda (1957) provided an analytical solution to the steady ponded ditch drainage problem for the case when the ditches are running empty and when the depth of ponding over the soil surface is zero every time. He utilized conformal transformation to arrive at his results. It should, however, be noted that Fukuda's (1957) solution is strictly valid only for partially penetrating ditches drains of negligible width; for finite width of the ditch drains, this solution is only

approximately correct. Kirkham (1945) provided a steady state solution to the fully penetrating ditch drainage problem for the instance when the ditch drains rest on a gravel substratum, the gravel substratum in turn overlies an impervious layer. This solution can handle both zero depth as well as a uniform depth of ponding at the surface of the soil. Kirkham (1965) (see also Kirkham et al., 1974) provided a more generalized steady state seepage theory for predicting flow from a ponded field into an array of equally spaced drains in a homogeneous soil. This solution is relatively of a more general nature as compared to his 1950's (Kirkham, 1950) ponded drainage solution in the sense that, unlike his previous solution, it can account for both unequal water level heights in between adjacent drains and non-zero depth of ponding at the soil surface. For ditches running full upto the soil surface or higher all the time and fully or partially penetrating a homogeneous soil overlying an impervious layer, Warrick and Kirkham (1969) presented conformal mapping solutions for different variants of the steady state ponded ditch drainage problem by suitably representing the surfaces of the ditch drains with appropriate equipotentials. Using the same method, Youngs (1994) provided analytical expressions for predicting seepage from an infinite horizontal soil surface into a ditch in a homogeneous soil, both for the extreme cases when the ditch rests on an impervious barrier and also when there exists an infinitely deep soil layer below the bottom of the ditch. The solution assumes the width of the ditch to be negligible and the ponding depth on the surface of the soil to be nonexistent. Barua and Tiwari (1995) provided a comprehensive series solution to the partially ponded ditch drainage problem by suitably splitting the flow domain into two sub-domains and then solving the governing equations of flow in each of these sub-domains, seeing at the same time that the boundary and the interfacial conditions are satisfied concurrently. Their solution can account for finite width and partial penetration of the ditch drains, soil anisotropy and both zero and uniform depth of ponding on the surface of the soil. However, this solution is also based on the assumption of steady state flow and here also the solution fails to entertain the non-uniform depth of ponding at the soil surface. The ponded ditch drainage problem was revisited by Chahar and Vadodaria (2008a, 2008b, 2011) using conformal mapping and provided analytical solutions to the problem for the cases when (i) the ditches end in an impervious barrier, (ii) the impervious barrier lies at an infinite

distance from the base of the ditches and (iii) the ditch bottoms are kept suspended at a finite distance from the impervious barrier. For the first two cases of the problem, Chahar and Vadodaria (2008a, 2008b) obtained their solution by assuming the depth of ponded water over the surface of the soil as negligible; however, for the third case, they (Chahar and Vadodaria, 2011) could successfully incorporate a non-zero uniform depth of ponding in their hodograph solution. It should be noted that all these variants of the ponded ditch problem considered by Chahar and Vadodaria (2008a, 2008b, 2011), for the situation when the levels of water in the adjacent ditch drains are equal, can be treated as special cases of the general ditch drainage problem considered by Barua and Tiwari (1995) and hence solutions to these special cases of the problem can very well be obtained from their series solution as well. However, Barua and Tiwari's (1995) solution is inadequate to handle ponded ditch drainage flow situations when the levels of water in the neighboring ditches are not equal as this analytical model is based on the assumption of equal water level heights in the ditch drains.

Numerous studies on the ponded drainage problem (Chahar and Vadodaria, 2008a, 2008b, 2011; Kirkham, 1949, 1950; Fukuda, 1957; Warrick and Kirkham, 1969; Barua and Tiwari, 1995; Rao and Leeds-Harrison, 1991; Youngs and Leeds-Harrison, 2000) – to name a few) for both ditch and tile drains show that the streamlines at the soil surface are more concentrated within the immediate vicinity of the drains and there is a rapid fall in the steady surface flux as one moves away from the centre of the drains. This has been observed to be true both for the cases when the surface of the soil is being subjected to a negligible depth or a uniform depth of ponding. Thus, if a salt affected field is uniformly ponded with the intention of leaching down harmful salts from its profile by installing subsurface drains to collect the leached water, regions close to the drains will be over washed whereas regions away from the drains will be under washed. Apart from uneven cleaning of the soil profile, this way of leaching is also causing unnecessary wastage of a large quantity of water. A better way of leaching can be achieved by draining the soil profile in stages; complete ponding followed by progressively decreasing fractional areas of ponding or starting from a small fractional area of leaching and progressively increasing it to cover the whole area, may be attempted to achieve the purpose (Rao and Leeds-Harrison, 1991; Youngs and Leeds-

Harrison, 2000). Zaslavsky (1979) used electric analog to study seepage of water to subsurface drains receiving water from both fully and partially ponded field situations and Rao and Leeds-Harrison (1991) used the over-relaxation method (Luthin and Gaskell, 1950) to study the same. Rao and Leeds-Harrison (1991) reported that desalinization away from the drains get markedly improved if the partial ponding of the soil surface is done in steps and in a judicious way. Youngs and Leeds-Harrison (2000) presented a conformal mapping solution to the steady partially ponded tube drainage problem for the situation when the soil profile is being underlain by an impervious barrier. From their study, they observed that better uniformity in leaching with less water may be achieved by adopting a progressive leaching procedure compared to the traditional method of fully flooding the soil at one go.

From the above review, it is clear that there does not exist currently any analytical solution to the ponded ditch drainage problem for the transient situation. In fact, even for the steady state case, there does not appear to be any analytical model which can take into account a variable ponding field at the surface of the soil. In view of the same, an effort is being made in this study to achieve the following objectives.

3.2 Objectives

To work out analytical expressions for the hydraulic head function, the stream function and the discharge rate, for groundwater seeping into an array of equally spaced ditch drains in a homogeneous and anisotropic soil receiving water from a ponded field when

(i) the levels of water in the adjacent ditches are equal and the ponding field over the soil surface is uniform,

(ii) the levels of water in the adjacent ditches are unequal and the ponding field over the soil surface is uniform and

(iii) the levels of water in the adjacent ditches are unequal and the ponding field over the soil surface is a variable one.

3.3 A General Solution of the Two-Dimensional Continuity Equation of Transient Groundwater Flow in a Homogeneous and Anisotropic Soil

In this section, we provide a general solution to the two-dimensional continuity equation of transient groundwater flow in a compressible, homogeneous and anisotropic soil medium using the separation of variable method (Kirkham and Powers, 1972). For such a situation, the concerned equation can be expressed as

$$K_x \frac{\partial^2 \phi}{\partial x^2} + K_y \frac{\partial^2 \phi}{\partial y^2} = S_s \left(\frac{\partial \phi}{\partial t} \right), \tag{3.1}$$

where φ is the hydraulic head, S_s is the specific storage, K_x and K_y and x and y are the hydraulic conductivities and spatial dimensions in the horizontal and vertical directions, respectively, and t is the time variable.

Dividing both sides of Eq. (3.1) by K_y, we get

$$\left(\frac{K_x}{K_y} \right) \frac{\partial^2 \phi}{\partial x^2} + \frac{\partial^2 \phi}{\partial y^2} = \left(\frac{S_s}{K_y} \right) \left(\frac{\partial \phi}{\partial t} \right). \tag{3.2}$$

Before proceeding to obtain a general solution to Eq. (3.1), for mathematical convenience, we first perform a transformation on the horizontal axis as

$$X = \left(\sqrt{\frac{K_y}{K_x}} \right) x = \frac{x}{K^a}, \tag{3.3}$$

where X is the transformed variable in the horizontal space and

$$(K^a)^2 = \frac{K_x}{K_y}, \tag{3.4}$$

is the anisotropy ratio of the soil.

Applying Eq. (3.3) to Eq. (3.2), the governing equation in the computational domain now turns out to be

$$\frac{\partial^2 \phi}{\partial X^2} + \frac{\partial^2 \phi}{\partial y^2} = (K_1)^2 \left(\frac{\partial \phi}{\partial t} \right), \tag{3.5}$$

where

$$(K_1)^2 = \left(\frac{S_s}{K_Y} \right) \tag{3.6}$$

and the equivalent isotropic hydraulic conductivity (Maasland, 1957), K, of the computational domain is

$$K = \sqrt{K_x K_y}. \tag{3.7}$$

It should be noted at this stage that in Eq. (3.5), only the horizontal dimension X in the computational domain is different from that of x in the real domain, the vertical variable y and the time variable t are the same in both the real and the computational domains.

Let $u_p(X, y, t)$ be a solution of Eq. (3.5) and $u_c(X, y)$ be a solution of the differential equation

$$\frac{\partial^2 \phi}{\partial X^2} + \frac{\partial^2 \phi}{\partial y^2} = 0. \tag{3.8}$$

Naturally then, $\phi = u_p + u_c$ will be a solution of Eq. (3.5). This is because

$$\frac{\partial^2 \phi}{\partial X^2} + \frac{\partial^2 \phi}{\partial y^2} = \frac{\partial^2 u_p}{\partial X^2} + \frac{\partial^2 u_p}{\partial y^2} + \frac{\partial^2 u_c}{\partial X^2} + \frac{\partial^2 u_c}{\partial y^2} = \frac{\partial^2 u_p}{\partial X^2} + \frac{\partial^2 u_p}{\partial y^2} + 0 = (K_1)^2 \left(\frac{\partial \phi}{\partial t} \right). \tag{3.9}$$

We first obtain a solution of Eq. (3.5). Let

$$u_p(X, y, t) = Z(X)Y(y)T(t), \tag{3.10}$$

be a solution of Eq. (3.5), where $Z(X)$, $Y(y)$ and $T(t)$ are taken as functions of only X, y and t, respectively.

Applying Eq. (3.10) to Eq. (3.5) and simplifying, we get

$$\frac{Z''(X)}{Z(X)} + \frac{Y''(y)}{Y(y)} = (K_1)^2 \frac{T'(t)}{T(t)}. \tag{3.11}$$

Equating $Z''(X)/Z(X) = -\alpha^2$ and $Y''(y)/Y(y) = -\beta^2$, where α and β are any constants, we get the ensuing solutions of these equations as

$$Z(X) = C_1 \sin(\alpha X) \tag{3.12}$$

and

$$Y(y) = C_2 \sin(\beta y), \tag{3.13}$$

respectively, where C_1 and C_2 are any arbitrary constants. Also, we will then have the equation

$$\frac{T'(t)}{T(t)} = \frac{-(\alpha^2 + \beta^2)}{(K_1)^2} = -\frac{\lambda^2}{(K_1)^2}, \tag{3.14}$$

where $\lambda^2 = (\alpha^2 + \beta^2)$. A solution of Eq. (3.14) can be expressed as

$$T(t) = C_3 \exp\left\{-\left[\frac{(\alpha)^2 + (\beta)^2}{(K_1)^2}\right]t\right\}, \tag{3.15}$$

where C_3 is any arbitrary constant. Substituting Eqs. (3.12), (3.13) and (3.15) in Eq. (3.10), we thus obtain a solution of Eq. (3.5) as

$$u_p(X, y, t) = A[\sin(\alpha X)\sin(\beta y)]\exp\left\{-\left[\frac{(\alpha)^2 + (\beta)^2}{(K_1)^2}\right]t\right\}, \tag{3.16}$$

where A is any constant. As adding solutions of a differential equation will also result in an another solution of the differential equation, a solution of Eq. (3.5) can also be expressed as

$$u_p(X, y, t) = \sum_{m=1}^{M}\sum_{n=1}^{N} A_{mn}[\sin(\alpha_m X)\sin(\beta_n y)]\exp\left\{-\left[\frac{(\alpha_m)^2 + (\beta_n)^2}{(K_1)^2}\right]t\right\}, \tag{3.17}$$

where, A_{mn} are any constants, m and n are summation indices and M and N are any positive integers. We adopt a similar procedure to obtain a solution of Eq. (3.8). Let us now take

$$u_c(X, y) = E(X)F(y), \tag{3.18}$$

as a solution of Eq. (3.8). Applying Eq. (3.18) to Eq. (3.8), we get, after some rearrangement of the terms of the resultant equation

$$\frac{E''(X)}{E(X)} = -\frac{F''(y)}{F(y)}. \tag{3.19}$$

As the left hand side of the above equation is a function of X only and the right hand side a function of y only, here also we can equate both of these functions to some common constant, say, γ^2, where γ is any constant. Solving the resultant equations, we get

$$E(X) = C_4 \sinh(\gamma X) \tag{3.20}$$

and

$$E(X) = C_5 \cosh(\gamma X), \tag{3.21}$$

as solutions of $E''(X)/E(X) = \gamma^2$ and

$$F(y) = C_6 \sin(\gamma y), \tag{3.22}$$

as a solution of $-F''(y)/F(y)=\gamma^2$, where C_4, C_5 and C_6 are any arbitrary constants. Remembering again that sum of solutions of a differential equation is also its solution, a solution of Eq. (3.8) can thus be represented using Eq. (3.18) as

$$u_c(X,y)=\sum_{p=1}^{P}B_p\sinh(\gamma_p X)\sin(\gamma_p y)+\sum_{q=1}^{Q}C_q\cosh(\gamma_q X)\sin(\gamma_q y), \tag{3.23}$$

where B_p and C_q are any constants, p and q are summation indices and P and Q are any positive integers.

Similarly, equating the right and left hand sides of Eq. (3.19) with $-\gamma^2$, an another solution of Eq. (3.8) can be expressed as

$$u_c(X,y)=\sum_{r=1}^{R}E_r\cosh(\gamma_r y)\sin(\gamma_r X), \tag{3.24}$$

where E_r are any constants, r is a summation index and R is any positive integer.

From the above and noting that a constant is also a solution of Eq. (3.5), we see that a general solution of Eq. (3.5) can be expressed as

$$\begin{aligned}\phi(X,y,t)=u_p+u_c=&\sum_{m=1}^{M}\sum_{n=1}^{N}A_{mn}\sin(\alpha_m X)\sin(\beta_n y)\exp\left\{-\left[\frac{(\lambda_{mn})^2 t}{(K_1)^2}\right]\right\}\\&+\sum_{p=1}^{P}B_p\sinh(\gamma_p X)\sin(\gamma_p y)+\sum_{q=1}^{Q}C_q\cosh(\gamma_q X)\sin(\gamma_q y)\\&+\sum_{r=1}^{R}D_r\cosh(\gamma_r y)\sin(\gamma_r X)+T,\end{aligned} \tag{3.25}$$

where

$$(\lambda_{mn})^2=(\alpha_m)^2+(\beta_n)^2 \tag{3.26}$$

and T is any constant. As mentioned before, since sum of solutions of a differential equation is also its solution, the first term of Eq. (3.25) plus any other term(s) of Eq. (3.25) will also yield an another solution of Eq. (3.5). Thus,

$$\begin{aligned}\phi(X,y,t)=&\sum_{m=1}^{M}\sum_{n=1}^{N}A_{mn}\sin(\alpha_m X)\sin(\beta_n y)\exp\left\{-\left[\frac{(\lambda_{mn})^2 t}{(K_1)^2}\right]\right\}\\&+\sum_{r=1}^{R}D_r\cosh(\gamma_r y)\sin(\gamma_r X)+T,\end{aligned} \tag{3.27}$$

$$\phi(X,y,t)=\sum_{m=1}^{M}\sum_{n=1}^{N}A_{mn}\sin(\alpha_m X)\sin(\beta_n y)\exp\left\{-\left[\frac{(\lambda_{mn})^2 t}{(K_1)^2}\right]\right\}$$

$$+\sum_{p=1}^{P}B_p\sinh(\gamma_p X)\sin(\gamma_p y)+T \qquad (3.28)$$

and

$$\phi(X,y,t)=\sum_{m=1}^{M}\sum_{n=1}^{N}A_{mn}\sin(\alpha_m X)\sin(\beta_n y)\exp\left\{-\left[\frac{(\lambda_{mn})^2 t}{(K_1)^2}\right]\right\}$$

$$+\sum_{p=1}^{P}B_p\sinh(\gamma_p X)\sin(\gamma_p y)+\sum_{r=1}^{R}D_r\cosh(\gamma_r y)\sin(\gamma_r X) \qquad (3.29)$$

are also solutions of the differential Eq. (3.5). We will make use of these solutions to obtain solutions to the flow problems considered in this chapter.

3.4 Mathematical Formulation and Solution

3.4.1 Case 1: An analytical model for predicting flow into an array of equally spaced ditch drains with equal water level heights in between adjacent drains and receiving water from a ponded field subjected to uniform depth of ponding

The geometry of the ditch drainage problem considered for study is as shown in Fig. 3.1. A series (only two are shown here) of parallel equally spaced ditch drains dug in a homogeneous and anisotropic water saturated soil of infinite areal extent, the soil column being underlain by an impervious barrier. The thickness of the soil up to the impervious layer is taken as h and the directional conductivities of the soil in the horizontal and vertical directions are taken as K_x and K_y, respectively. The ditches are assumed to have the same water level depth of H_1, as measured from the origin O, and the spacing and semi-spacing distances between the adjacent ditches are taken as $S_{a(1)}$ and $S_{h(1)}$, respectively. Also, we assume the ditches to penetrate all the way up to the impervious base in our analysis. These heights of water in the ditches are as a result of an instantaneous lowering of water in the ditches, the water being previously assumed to be standing in the ditches up to the soil surface. Further, it is also assumed that a constant (this constant can also be zero) depth of ponding δ_0 is imposed instantaneously over the surface of the soil with the help of side bunds of width ε_a each running parallely to the drains (Rao et al., 1991; Youngs and Leeds-

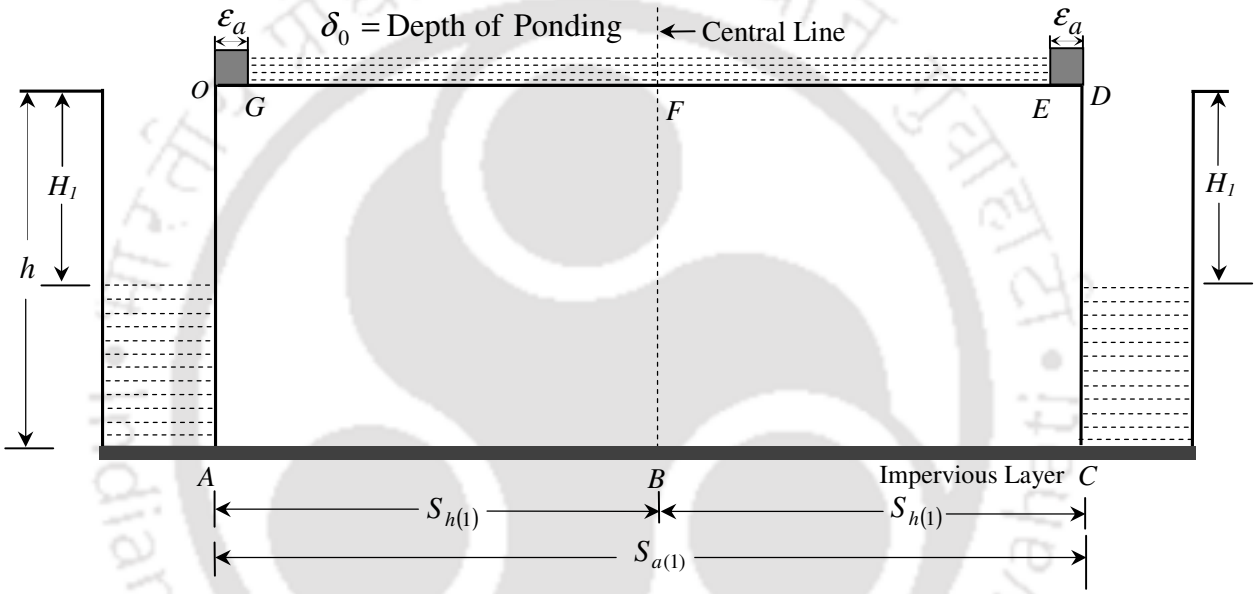

Fig. 3.1. Geometry of a fully penetrating ditch drainage system with equal water level heights in between adjacent drains and subjected to a uniform depth of ponding at the surface of the soil

Harrison, 2000), the soil system, as mentioned before, been previously water saturated flush up to the surface of the soil. The ponded water inside the bunds at the surface of the soil can be maintained constant by being continuously fed with irrigation water as otherwise the depth of ponding will go on decreasing with time and eventually, after the exhaustion of the surface water, unsaturated flow conditions will start developing from the surface of the soil profile – conditions which have not been considered in the present study. Because of symmetry, we consider only half of the flow domain of *OABFGO* of Fig. 3.1 for analysis. The hydraulic head function in the flow domain is designated as $\phi_{(1)}$, the head function being measured with respect to the origin *O*. Further, for ease of solving the problem, we take the *x*-axis to be positive towards the right and the *y*-axis to be positively vertically down, as traced from the origin *O*. With the above nomenclature and also naming the time variable as t, the initial and boundary conditions for the two-dimensional transient seepage ditch drainage problem considered in Fig. 3.1 can be expressed for the sub-domain *OABFGO* as

$$\phi_{(1)}(x, y, t = 0) = 0, \qquad 0 < x < S_{h(1)}, \qquad 0 < y < h, \tag{I}$$

$$\phi_{(1)}(x, y, t > 0) = -y, \qquad x = 0, \qquad 0 < y < H_1, \tag{IIa}$$

$$\phi_{(1)}(x, y, t > 0) = -H_1, \qquad x = 0, \qquad H_1 \le y < h, \tag{IIb}$$

$$\frac{\partial \phi_{(1)}(x, y, t > 0)}{\partial y} = 0, \qquad y = h, \qquad 0 < x < S_{h(1)}, \tag{III}$$

$$\frac{\partial \phi_{(1)}(x, y, t > 0)}{\partial x} = 0, \qquad x = S_{h(1)}, \qquad 0 < y < h, \tag{IV}$$

$$\phi_{(1)}(x, y, t > 0) = \delta_0, \qquad y = 0, \qquad 0 < x < S_{h(1)}. \tag{V}$$

The solution of the problem requires that the governing Eq. (3.1) [which is the same as Eq. (3.5) in the computational domain] be solved together with the conditions as listed above. Taking into cognizance the nature of the initial and boundary conditions, a solution of the differential equation Eq. (3.1) in the horizontally transformed space [i.e., see Eq. (3.5)] can be expressed, in view of Eq. (3.27), as

$$\phi_{(1)}(X, y, t) = \sum_{p=1}^{P} C_{p(1)} \frac{\cosh[N_{p(1)}(S_h - X)]}{\cosh(N_{p(1)} S_h)} \sin(N_{p(1)} y)$$

$$+\sum_{m=1}^{M}\sum_{n=1}^{N} A_{mn(1)} \sin(N_{m(1)}X)\sin(N_{n(1)}y)\exp\left[\frac{-(\lambda_{mn(1)})^2 t}{(K_1)^2}\right]+\delta_0, \tag{3.30}$$

where

$$S_h = \left(\sqrt{\frac{K_y}{K_x}}\right) S_{h(1)}, \tag{3.31}$$

$$N_{m(1)} = \left[\left(\frac{1-2m}{2}\right)\frac{\pi}{S_h}\right], \tag{3.32}$$

$$N_{n(1)} = \left[\left(\frac{1-2n}{2}\right)\frac{\pi}{h}\right], \tag{3.33}$$

$$N_{p(1)} = \left[\left(\frac{1-2p}{2}\right)\frac{\pi}{h}\right] \tag{3.34}$$

and

$$(\lambda_{mn(1)})^2 = (N_{m(1)})^2 + (N_{n(1)})^2. \tag{3.35}$$

As may be observed, Eq. (3.30) inherently satisfies boundary conditions III, IV and V by its very definition. We will now evaluate the constants $C_{p(1)}$ of Eq. (3.30) by making use of boundary conditions IIa and IIb and the constants $A_{mn(1)}$ utilizing the initial condition I. Transforming first boundary conditions IIa and IIb from the real plane to the computational plane and then applying them to Eq. (3.30), respectively, we get, at $X = 0$

$$\sum_{p=1}^{P} C_{p(1)} \sin(N_{p(1)}y) = -\delta_0 - y, \qquad 0 < y \le H_1,$$

$$\sum_{p=1}^{P} C_{p(1)} \sin(N_{p(1)}y) = -\delta_0 - H_1, \qquad 0 \le y < h.$$

By running a Fourier series in the interval $0 < y < h$ after letting $P \to \infty$ in the above equations, we get an expression for the constant $C_{p(1)}$ as

$$C_{p(1)} = \frac{2}{h}\left[\int_0^{H_1}(-\delta_0 - y)\sin(N_{p(1)}y)dy + \int_{H_1}^{h}(-\delta_0 - H_1)\sin(N_{p(1)}y)dy\right]. \tag{3.36}$$

Eq (3.36), upon simplification, gives

$$C_{p(1)} = \left(\frac{-2\delta_0}{hN_{p(1)}}\right) - \left(\frac{2}{h}\right)\left[\frac{\sin(N_{p(1)}H_1)}{(N_{p(1)})^2}\right]. \tag{3.37}$$

Now to get the constants $A_{mn(1)}$ of Eq. (3.30), we apply the initial condition I to it; the resultant expression at $t = 0$ works out to be

$$\sum_{m=1}^{M}\sum_{n=1}^{N} A_{mn(1)} \sin(N_{m(1)}X)\sin(N_{n(1)}y) = -\delta_0 - \sum_{p=1}^{Q} C_{p(1)} \frac{\cosh[N_{p(1)}(S_h - X)]}{\cosh(N_{p(1)}S_h)} \sin(N_{p(1)}y). \tag{3.38}$$

In the above equation, if we let M and N to go to infinity, constants $A_{mn(1)}$ can then be evaluated by running a double Fourier series on the defined computational domain, i.e. on the area encompassed by $0 < X < S_h$ and $0 < y < h$; thus, $A_{mn(1)}$ can then be determined as

$$A_{mn(1)} = \left(\frac{2}{h}\right)\left(\frac{2}{S_h}\right)\left[\int_{y=0}^{y=h}\int_{X=0}^{X=S_h}(-\delta_0)\sin(N_{m(1)}X)\sin(N_{n(1)}y)dXdy\right]$$

$$-\left(\frac{2}{h}\right)\left(\frac{2}{S_h}\right)\left\{\int_{y=0}^{y=h}\int_{X=0}^{X=S_h}\sum_{p=1}^{P} C_{p(1)} \frac{\cosh[N_{p(1)}(S_h - X)]}{\cosh(N_{p(1)}S_h)} \sin(N_{p(1)}y)\sin(N_{m(1)}X)\sin(N_{n(1)}y)dXdy\right\}. \tag{3.39}$$

Naming the first integral on the right of the above equation as $I^1_{(1)}$ and the second integral as $I^2_{(1)}$, Eq. (3.39) can then be written in a condensed form as

$$A_{mn(1)} = I^1_{(1)} + I^2_{(1)}. \tag{3.40}$$

Simplifying the above integrals, we get

$$I^1_{(1)} = \frac{-4\delta_0}{hS_h}\left[\left(\frac{1}{N_{m(1)}}\right)\left(\frac{1}{N_{n(1)}}\right)\right] \tag{3.41}$$

and for $p = n$

$$I^2_{(1)} = \left(\frac{-2}{S_h}\right)\sum_{p=1}^{P} C_{p(1)}\left\{\frac{N_{m(1)}[\cos(N_{p(1)}S_h) - \cos(N_{m(1)}S_h)]}{[(N_{m(1)})^2 + (N_{p(1)})^2]\cosh(N_{p(1)}S_h)}\right\} \tag{3.42}$$

and for $p \neq n$

$$I^2_{(1)} = \left(\frac{-4}{hS_h}\right)\sum_{p=1}^{P} C_{p(1)}\left\{\frac{N_{m(1)}}{[(N_{m(1)})^2 + (N_{p(1)})^2]}\right\}\left\{\frac{\sin[(N_{p(1)} - N_{n(1)})h]}{2(N_{p(1)} - N_{n(1)})} - \frac{\sin[(N_{p(1)} + N_{n(1)})h]}{2(N_{p(1)} + N_{n(1)})}\right\}$$

$$\times\left[\frac{\cosh(N_{p(1)}S_h)-\cos(N_{m(1)}S_h)}{\cosh(N_{p(1)}S_h)}\right]. \tag{3.43}$$

All the constants of Eq. (3.30) are thus determined and our boundary value problem stands solved.

The time dependent discharge expression to one side per unit length of a ditch, Q_{shalf}, can be estimated as

$$Q_{shalf}(t)=(\sqrt{K_xK_y})\int_0^h\left(\frac{\partial\phi_{(1)}}{\partial X}\right)_{X=0}dy. \tag{3.44}$$

Substituting $\phi_{(1)}$ of Eq. (3.30) in Eq. (3.44) and then integrating the resultant expression, we get

$$Q_{shalf}(t)=-(\sqrt{K_xK_y})\sum_{p=1}^{P}C_{p(1)}\frac{\sinh(N_{p(1)}S_h)}{\cosh(N_{p(1)}S_h)}$$
$$+(\sqrt{K_xK_y})\sum_{m=1}^{M}\sum_{n=1}^{N}A_{mn(1)}\left(\frac{N_{m(1)}}{N_{n(1)}}\right)\exp\left[\frac{-(\lambda_{mn(1)})^2t}{(K_1)^2}\right]. \tag{3.45}$$

Hence, the total discharge through both the sides of the ditch per unit length, Q_{side}, can be calculated as

$$Q_{side}(t)=2\times Q_{shalf}(t). \tag{3.46}$$

Now, the total discharge per unit length of the ditches, $Q_{top}(t)$, coming from the surface of the soil can be obtained as

$$Q_{top(1)}(t)=-2\times(\sqrt{K_xK_y})\int_{X=\varepsilon}^{X=S_h}\left(\frac{\partial\phi_{(1)}}{\partial y}\right)_{y=0}dX. \tag{3.47}$$

Carrying out the above integral using Eq. (3.30), we get

$$Q_{top(1)}(t)=-(\sqrt{K_xK_y})\sum_{p=1}^{P}C_{p(1)}\frac{\sinh[N_{p(1)}(S_h-\varepsilon)]}{\cosh(N_{p(1)}S_h)}\times 2$$
$$-(\sqrt{K_xK_y})\sum_{m=1}^{M}\sum_{n=1}^{N}A_{mn(1)}\left[\frac{N_{n(1)}}{N_{m(1)}}\right]\cos(N_{m(1)}\varepsilon)\exp\left[\frac{-(\lambda_{mn(1)})^2t}{(K_1)^2}\right]\times 2 \tag{3.48}$$

where ε is the width of the ditch banks in the computational domain, i.e.,

$$\varepsilon = \left(\sqrt{\frac{K_y}{K_x}} \right) \varepsilon_a . \tag{3.49}$$

The volume of water entering through the sides of a ditch per unit length, V_{stot}, can now be easily calculated by performing a time integral on the total side discharge expression, namely

$$V_{stot} = 2 \times \int_0^t Q_{side} dt. \tag{3.50}$$

By solving the above integral using Eq. (3.45), we get

$$V_{stot} = -2(\sqrt{K_x K_y}) \sum_{p=1}^{P} C_{p(1)} \left[\frac{\sinh(N_{p(1)} S_h)}{\cosh(N_{p(1)} S_h)} \right] t$$

$$-2(\sqrt{K_x K_y}) \sum_{m=1}^{M} \sum_{n=1}^{N} A_{mn(1)} \left[\frac{(K_1)^2}{(\lambda_{mn(1)})^2} \right] \left[\frac{N_{m(1)}}{N_{n(1)}} \right] \left\{ \exp\left[\frac{-(\lambda_{mn(1)})^2 t}{(K_1)^2} \right] - 1 \right\}. \tag{3.51}$$

Similarly, the volume of water seeping per unit length of the drains from the surface of the soil, $V_{top(1)}$, in the time interval t in between two adjacent drains can also be evaluated by integrating Eq. (3.48) within the time t; the relevant expression works out as

$$V_{top(1)} = -2(\sqrt{K_x K_y}) \sum_{p=1}^{P} C_{p(1)} \left\{ \frac{\sinh[N_{p(1)}(S_h - \varepsilon)]}{\cosh(N_{p(1)} S_h)} \right\} t$$

$$+2(\sqrt{K_x K_y}) \sum_{m=1}^{M} \sum_{n=1}^{N} A_{mn(1)} \left[\frac{(K_1)^2}{(\lambda_{mn(1)})^2} \right] \left[\frac{N_{n(1)}}{N_{m(1)}} \right] \cos(N_{m(1)} \varepsilon) \left\{ \exp\left[\frac{-(\lambda_{mn(1)})^2 t}{(K_1)^2} \right] - 1 \right\}. \tag{3.52}$$

To obtain expressions for the hydraulic head function and side and top discharges corresponding to the steady state situation, we need to simply allow the time variable appearing in these expressions to go to infinity; as can be seen this will make the exponential terms of these equations to go to zero and the relevant expressions for the steady state will then turn out to be

$$\phi_{(1)}^{(st)}(X, y) = \sum_{p=1}^{P} C_{p(1)} \frac{\cosh[N_{p(1)}(S_h - X)]}{\cosh(N_{p(1)} S_h)} \sin(N_{p(1)} y) + \delta_0, \tag{3.53}$$

$$Q_{side}^{(st)} = -2(\sqrt{K_x K_y}) \sum_{p=1}^{P} C_{p(1)} \frac{\sinh(N_{p(1)} S_h)}{\cosh(N_{p(1)} S_h)} \tag{3.54}$$

and

$$Q_{top(1)}^{(st)} = -(\sqrt{K_x K_y})\sum_{p=1}^{P} C_{p(1)} \frac{\sinh[N_{p(1)}(S_h - \varepsilon)]}{\cosh(N_{p(1)} S_h)}, \tag{3.55}$$

respectively, where the superscript '*st*' under the parenthesis sign in these expressions show that they are applicable to the steady state only.

Now, to obtain the steady state stream function, $\psi_{(1)}$, from the hydraulic head function given by Eq. (3.53), we apply the following relations (Bear, 1972) linking them in the computational plane, namely

$$K\frac{\partial \phi_{(1)}}{\partial X} = \frac{\partial \psi_{(1)}}{\partial y} \tag{3.56}$$

and

$$K\frac{\partial \phi_{(1)}}{\partial y} = -\frac{\partial \psi_{(1)}}{\partial X}. \tag{3.57}$$

Applying Eqs (3.56) and (3.57) to Eq. (3.53) and simplifying, we get

$$\psi_{(1)}(X, y) = (\sqrt{K_x K_y})\sum_{p=1}^{P} C_{p(1)} \frac{\sinh[N_{p(1)}(S_h - X)]}{\cosh(N_{p(1)} S_h)} \cos(N_{p(1)} y) + C \tag{3.58}$$

where C is the constant of integration. In order that the value of the stream function remains finite in the entire flow domain, we take the zero streamline to pass though the point $(\varepsilon, 0)$ in the computational domain, i.e., by taking $\varphi_{(1)}(\varepsilon, 0) = 0$; applying the same in Eq. (3.58), we get the constant of integration C of the above equation as

$$C = -(\sqrt{K_x K_y})\sum_{p=1}^{P} C_{p(1)} \frac{\sinh[N_{p(1)}(S_h - \varepsilon)]}{\cosh(N_{p(1)} S_h)}. \tag{3.59}$$

Substituting Eq. (3.59) in Eq. (3.58), the expression for the stream function finally turns out to be

$$\psi_{(1)}(X, y) = (\sqrt{K_x K_y})\sum_{p=1}^{P} C_{p(1)} \frac{\sinh[N_{p(1)}(S_h - X)]}{\cosh(N_{p(1)} S_h)} \cos(N_{p(1)} y)$$

$$-(\sqrt{K_x K_y})\sum_{p=1}^{P} C_{p(1)} \frac{\sinh[N_{p(1)}(S_h - \varepsilon)]}{\cosh(N_{p(1)} S_h)}. \tag{3.60}$$

To have the values of the stream function within zero and one, the expression above can be normalized by dividing it by the maximum value of the stream function within the flow domain – naming such a function as $\psi^n_{(1)}$, an expression for the same can be represented as

$$\psi^n_{(1)}(X,y)=\frac{\psi_{(1)}(X,y)}{\psi_{(1)}(S_h,0)}. \tag{3.61}$$

3.4.2 Case 2: An analytical model for predicting flow into an array of equally spaced ditch drains with unequal water level heights in between adjacent drains and receiving water from a ponded field subjected to uniform depth of ponding

The ponded ditch drainage considered for study in this section is as shown in Fig. 3.2. As may be observed, unlike the problem considered earlier, the water level heights in between the adjacent drains are now not equal. Thus, in this case, the flow is not symmetrical and as such, the whole flow domain *OABCDEFGO* need be considered for analyzing the problem. Denoting the spacing between the adjacent drains as $S_{a(2)}$ and the depth of water level (as measured from the origin *O*) of the right ditch as H_3, the initial and boundary conditions for the flow problem can now be expressed as

$$\phi_{(2)}(x,y,t=0)=0, \qquad 0<x<S_{a(2)}, \qquad 0<y<h, \tag{I}$$

$$\phi_{(2)}(x,y,t>0)=-y, \qquad x=0, \qquad 0<y<H_1, \tag{IIa}$$

$$\phi_{(2)}(x,y,t>0)=-H_1, \qquad x=0, \qquad H_1\le y<h, \tag{IIb}$$

$$\frac{\partial\phi_{(2)}(x,y,t>0)}{\partial y}=0, \qquad y=h, \qquad 0<x<S_{a(2)}, \tag{III}$$

$$\phi_{(2)}(x,y,t>0)=-y, \qquad x=S_{a(2)}, \qquad 0<y<H_3, \tag{IVa}$$

$$\phi_{(2)}(x,y,t>0)=-H_3, \qquad x=S_{a(2)}, \qquad H_3\le y<h, \tag{IVb}$$

$$\phi_{(2)}(x,y,t>0)=\delta_0, \qquad y=0, \qquad 0<x<S_{a(2)}, \tag{V}$$

where subscript 2 is attached to the hydraulic head and spacing symbols for the current problem in order to distinguish them from the corresponding values in the previous problem and the symbols for the common parameters for both the problems are kept the same as before, as can be seen in Figs. 3.1 and 3.2, respectively. The solution to the problem now

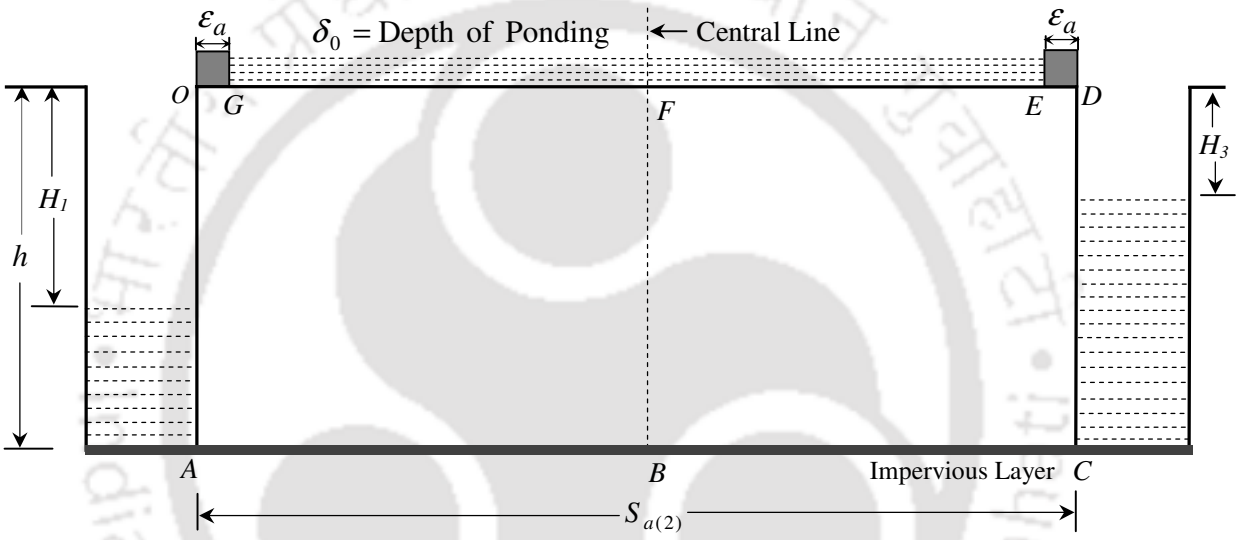

Fig. 3.2. Geometry of a fully penetrating ditch drainage system with unequal water level heights in between adjacent drains and subjected to a uniform depth of ponding at the surface of the soil

demands that Eq. (3.5) be satisfied along with the initial and boundary conditions as mentioned above. Keeping an eye on the initial and boundary conditions, an expression for the hydraulic head function for the flow problem in the computational space can be defined, in view of Eq. (3.28), as

$$\phi_{(2)}(X,y,t) = \sum_{q=1}^{Q} B_{q(2)} \frac{\sinh(N_{q(2)}X)}{\sinh(N_{q(2)}S_2)} \sin(N_{q(2)}y) + \sum_{p=1}^{P} C_{p(2)} \frac{\sinh[N_{p(2)}(S_2 - X)]}{\sinh(N_{p(2)}S_2)} \sin(N_{p(2)}y) + \sum_{m=1}^{M}\sum_{n=1}^{N} A_{mn(2)} \sin(N_{m(2)}X) \sin(N_{n(2)}y) \exp\left[\frac{-(\lambda_{mn(2)})^2 t}{(K_1)^2}\right] + \delta_0, \quad (3.62)$$

where

$$S_2 = \left(\sqrt{\frac{K_y}{K_x}}\right) S_{a(2)}, \quad (3.63)$$

$$N_{m(2)} = \left(\frac{m\pi}{S_2}\right), \quad (3.64)$$

$$N_{n(2)} = \left[\left(\frac{1-2n}{2}\right)\frac{\pi}{h}\right], \quad (3.65)$$

$$N_{p(2)} = \left[\left(\frac{1-2p}{2}\right)\frac{\pi}{h}\right], \quad (3.66)$$

$$N_{q(2)} = \left[\left(\frac{1-2q}{2}\right)\frac{\pi}{h}\right], \quad (3.67)$$

and

$$(\lambda_{mn(2)})^2 = (N_{m(2)})^2 + (N_{n(2)})^2. \quad (3.68)$$

We see from Eq. (3.62) that it already satisfies boundary conditions III and V; we now seek to evaluate the constants of Eq. (3.62) using the remaining boundary conditions IIa, IIb, IVa, IVb and the initial condition I.

Applying IIa and IIb to Eq. (3.62) (after first converting them from the real to the computational domain) and then running a Fourier series in the interval $0 < y < h$, we get, like in the previous case, an expression for the constants $C_{p(2)}$ as

$$C_{p(2)} = \left(\frac{-2\delta_0}{hN_{p(2)}}\right) - \left(\frac{2}{h}\right)\left[\frac{\sin(N_{p(2)}H_1)}{(N_{p(2)})^2}\right]. \tag{3.69}$$

Similarly, an application of the transformed boundaries IVa and IVb to Eq. (3.62) yields

$$B_{q(2)} = \left(\frac{-2\delta_0}{hN_{q(2)}}\right) - \left(\frac{2}{h}\right)\left[\frac{\sin(N_{q(2)}H_3)}{(N_{q(2)})^2}\right]. \tag{3.70}$$

There still remain the constants $A_{mn(2)}$ of Eq. (3.62) to be evaluated; towards this end, we apply the initial condition I in the transformed space to Eq. (3.62) – the resultant expression turns out to be

$$\sum_{m=1}^{M}\sum_{n=1}^{N} A_{mn(2)} \sin(N_{m(2)}X)\sin(N_{n(2)}y) = -\delta_0 - \sum_{q=1}^{Q} B_{q(2)} \frac{\sinh(N_{q(2)}X)}{\sinh(N_{q(2)}S_2)} \sin(N_{q(2)}y)$$
$$- \sum_{p=1}^{P} C_{p(2)} \frac{\sinh[N_{p(2)}(S_2 - X)]}{\sinh(N_{p(2)}S_2)} \sin(N_{p(2)}y). \tag{3.71}$$

In the above equation, if we let M and N to go to infinity, the constants $A_{mn(2)}$ can then be evaluated by running a double Fourier series on the domain encompasses by $0 < X < S_2$ and $0 < y < h$; the expression for the constants $A_{mn(2)}$, thus, can be represented as

$$A_{mn(2)} = -\left(\frac{2}{h}\right)\left(\frac{2}{S_2}\right)\left[\int_{y=0}^{y=h}\int_{X=0}^{X=S_2} (-\delta_0)\sin(N_{m(2)}X)\sin(N_{n(2)}y)\,dXdy\right]$$
$$-\left(\frac{2}{h}\right)\left(\frac{2}{S_2}\right)\left\{\int_0^h\int_0^{S_2}\sum_{q=1}^{Q} B_{q(2)} \frac{\sinh(N_{q(2)}X)}{\sinh(N_{p(2)}S_2)} \sin(N_{q(2)}y)\sin(N_{m(2)}X)\sin(N_{n(2)}y)\,dXdy\right\}$$
$$-\left(\frac{2}{h}\right)\left(\frac{2}{S_2}\right)\left\{\int_0^h\int_0^{S_2}\sum_{p=1}^{P} C_{p(2)} \frac{\sinh[N_{p(2)}(S_2 - X)]}{\sinh(N_{p(2)}S_2)} \sin(N_{p(2)}y)\sin(N_{m(2)}X)\sin(N_{n(2)}y)\,dXdy\right\}. \tag{3.72}$$

Calling the first, second and third integrals on the right-hand-side of Eq. (3.72) as $I^1_{(2)}$, $I^2_{(2)}$ and $I^3_{(2)}$, respectively, the above equation then can be written in a concise form as

$$A_{mn(2)} = I^1_{(2)} + I^2_{(2)} + I^3_{(2)}. \tag{3.73}$$

After carrying out the above integrals, we get

$$I^1_{(2)} = \left[\frac{4\delta_0}{hS_2 N_{m(2)} N_{n(2)}}\right][\cos(N_{m(2)} S_2) - 1] \tag{3.74}$$

and for $q = n$

$$I^2_{(2)} = \left(\frac{2}{S_2}\right)\sum_{q=1}^{Q} B_{q(2)}\left[\frac{N_{m(2)}}{(N_{m(2)})^2 + (N_{q(2)})^2}\right]\cos(N_{m(2)} S_2) \tag{3.75}$$

and for $q \neq n$

$$I^2_{(2)} = \left(\frac{4}{hS_2}\right)\sum_{q=1}^{Q} B_{q(2)}\left[\frac{N_{m(2)}\cos(N_{m(2)} S_2)}{(N_{m(2)})^2 + (N_{q(2)})^2}\right]\left\{\frac{1}{2(N_{q(2)} - N_{n(2)})}\sin[(N_{q(2)} - N_{n(2)})h]\right.$$
$$\left. - \frac{1}{2(N_{q(2)} + N_{n(2)})}\sin[(N_{q(2)} + N_{n(2)})h]\right\}; \tag{3.76}$$

for $p = n$

$$I^3_{(2)} = -\left(\frac{2}{hS_2}\right)\sum_{p}^{P} C_{p(2)}\left[\frac{N_{m(2)}}{(N_{m(2)})^2 + (N_{p(2)})^2}\right] \tag{3.77}$$

and for $p \neq n$

$$I^3_{(2)} = -\left(\frac{4}{hS_2}\right)\sum_{p=1}^{P} C_{p(2)}\left[\frac{N_{m(2)}}{(N_{m(2)})^2 + (N_{p(2)})^2}\right]\left\{\frac{1}{2(N_{p(2)} - N_{n(2)})}\sin[(N_{p(2)} - N_{n(2)})h]\right.$$
$$\left. - \frac{1}{2(N_{p(2)} + N_{n(2)})}\sin[(N_{p(2)} + N_{n(2)})h]\right\}. \tag{3.78}$$

Thus, all the constants of Eq. (3.59) are now being evaluated the flow problem of Fig. 3.2 stands solved.

Now, an expression of discharge per unit length into one side (i.e., through face *OA* of Fig. 3.2) of the left ditch, $Q_{l(2)}$, can be calculated by applying the Darcy's law on the concerned face, namely,

$$Q_{l(2)}(t) = (\sqrt{K_x K_y}) \int_0^h \left(\frac{\partial \phi_{(2)}}{\partial X} \right)_{X=0} dy. \tag{3.79}$$

Solving the above integral using Eq. (3.62), we obtain

$$Q_{l(2)} = (\sqrt{K_x K_y}) \sum_{q=1}^{Q} B_{q(2)} \frac{1}{\sinh(N_{q(2)} S_2)} - (\sqrt{K_x K_y}) \sum_{p=1}^{P} C_{p(2)} \frac{\cosh(N_{p(2)} S_2)}{\sinh(N_{p(2)} S_2)}$$

$$+ (\sqrt{K_x K_y}) \sum_{m=1}^{M} \sum_{n=1}^{N} A_{mn(2)} \left[\frac{N_{m(2)}}{N_{n(2)}} \right] \exp\left[\frac{-(\lambda_{mn(2)})^2 t}{(K_1)^2} \right]. \tag{3.80}$$

Similarly, an expression of discharge per unit length from one side (i.e., through face *CD* of Fig. 3.2) of the right ditch, $Q_{r(2)}$, can be represented as

$$Q_{r(2)}(t) = -(\sqrt{K_x K_y}) \int_0^h \left(\frac{\partial \phi_{(2)}}{\partial X} \right)_{X=S_2} dy. \tag{3.81}$$

Simplification of the above integral, using Eq. (3.62), yields

$$Q_{r(2)} = -(\sqrt{K_x K_y}) \sum_{q=1}^{Q} B_{q(2)} \frac{\cosh(N_{q(2)} S_2)}{\sinh(N_{q(2)} S_2)} + (\sqrt{K_x K_y}) \sum_{p=1}^{P} C_{p(2)} \frac{1}{\sinh(N_{p(2)} S_2)}$$

$$- (\sqrt{K_x K_y}) \sum_{m=1}^{M} \sum_{n=1}^{N} A_{mn(2)} \left[\frac{N_{m(2)}}{N_{n(2)}} \right] \cos(N_{m(2)} S_2) \exp\left[\frac{-(\lambda_{mn(2)})^2 t}{(K_1)^2} \right]. \tag{3.82}$$

The discharge coming from the surface of the soil in between the adjacent ditches per unit length of the ditches, $Q_{top(2)}$, can also be obtained by an application of Darcy's law at the surface of the soil; thus, we have

$$Q_{top(2)}(t) = -(\sqrt{K_x K_y}) \int_{X=\varepsilon}^{X=S_2-\varepsilon} \left(\frac{\partial \phi_{(2)}}{\partial y} \right)_{y=0} dX. \tag{3.83}$$

After carrying out the above integral utilizing Eq. (3.62), we get

$$Q_{top(2)}(t) = -(\sqrt{K_x K_y}) \sum_{q=1}^{Q} B_{q(2)} \frac{1}{\sinh(N_{q(2)} S_2)} \left\{ \cosh[N_{q(2)}(S_2 - \varepsilon)] - \cosh(N_{q(2)} \varepsilon) \right\}$$

$$+ (\sqrt{K_x K_y}) \sum_{p=1}^{P} C_{p(2)} \frac{1}{\sinh(N_{p(2)} S_2)} \left\{ \cosh(N_{p(2)} \varepsilon) - \cosh[N_{p(2)}(S_2 - \varepsilon)] \right\}$$

$$+ (\sqrt{K_x K_y}) \sum_{m=1}^{M} \sum_{n=1}^{N} A_{mn(2)} \left[\frac{N_{n(2)}}{N_{m(2)}} \right] \exp\left[\frac{-(\lambda_{mn(2)})^2 t}{(K_1)^2} \right] \left\{ \cos[N_{m(2)}(S_2 - \varepsilon)] - \cos(N_{m(2)} \varepsilon) \right\}. \tag{3.84}$$

Like before, the volume of water seeping per unit length of the ditches though the faces *OA* and *CD* of the right and the left ditches of Fig. 3.2 ($V_{l(2)}$ and $V_{r(2)}$, respectively) can be evaluated by performing time integrals on the left and right discharge expressions [Eqs. (3.80) and (3.82)] in the interval *t*; the relevant expressions turn out to be

$$V_{l(2)} = (\sqrt{K_x K_y}) \sum_{q=1}^{Q} B_{q(2)} \left[\frac{1}{\sinh(N_{q(2)} S_2)} \right] t - (\sqrt{K_x K_y}) \sum_{p=1}^{P} C_{p(2)} \left[\frac{\cosh(N_{p(2)} S_2)}{\sinh(N_{p(2)} S_2)} \right] t$$

$$- (\sqrt{K_x K_y}) \sum_{m=1}^{M} \sum_{n=1}^{N} A_{mn(2)} \left[\frac{(K_1)^2}{(\lambda_{mn(2)})^2} \right] \left[\frac{N_{m(2)}}{N_{n(2)}} \right] \left\{ \exp\left[\frac{-(\lambda_{mn(2)})^2 t}{(K_1)^2} \right] - 1 \right\} \tag{3.85}$$

and

$$V_{r(2)} = -(\sqrt{K_x K_y}) \sum_{q=1}^{Q} B_{q(2)} \left[\frac{\cosh(N_{q(2)} S_2)}{\sinh(N_{q(2)} S_2)} \right] t + (\sqrt{K_x K_y}) \sum_{p=1}^{P} C_{p(2)} \left[\frac{1}{\sinh(N_{p(2)} S_2)} \right] t$$

$$+ (\sqrt{K_x K_y}) \sum_{m=1}^{M} \sum_{n=1}^{N} A_{mn(2)} \left[\frac{(K_1)^2}{(\lambda_{mn(2)})^2} \right] \left[\frac{N_{m(2)}}{N_{n(2)}} \right] \cos(N_{m(2)} S_2) \left\{ \exp\left[\frac{-(\lambda_{mn(2)})^2 t}{(K_1)^2} \right] - 1 \right\}, \tag{3.86}$$

respectively. Similarly, the volume of water seeping through the surface of the soil per unit length of the drains in between two adjacent drains, $V_{top(2)}$, in the time interval *t* can be easily evaluated, like in the previous case, by performing a time integral on Eq. (3.84); the relevant expression now works out to be

$$V_{top(2)} = -(\sqrt{K_x K_y}) \sum_{q=1}^{Q} B_{q(2)} \frac{1}{\sinh(N_{q(2)} S_2)} \{\cosh[N_{q(2)}(S_2 - \varepsilon)] - \cosh(N_{q(2)} \varepsilon)\} t$$

$$+ (\sqrt{K_x K_y}) \sum_{p=1}^{P} C_{p(2)} \frac{1}{\sinh(N_{p(2)} S_2)} \{\cosh(N_{p(2)} \varepsilon) - \cosh[N_{p(2)}(S_2 - \varepsilon)\} t$$

$$- (\sqrt{K_x K_y}) \sum_{m=1}^{M} \sum_{n=1}^{N} A_{mn(2)} \left[\frac{N_{n(2)}}{N_{m(2)}} \right] \left[\frac{(K_1)^2}{(\lambda_{mn(1)})^2} \right] \{\cos[N_{m(2)}(S_2 - \varepsilon)] - \cos(N_{m(2)} \varepsilon)\}$$

$$\times \left\{ \exp\left[\frac{-(\lambda_{mn(1)})^2 t}{(K_1)^2} \right] - 1 \right\}. \tag{3.87}$$

Also, the steady state expressions for the hydraulic head function, the left, right and the top discharges for the flow problem can be obtained, like in the previous case, from their

respective transient equations by simply allowing time to extend to infinity in these equations; the pertinent expressions turn out to be

$$\phi_{(2)}^{(st)}(X,y)=\sum_{q=1}^{Q}B_{q(2)}\frac{\sinh(N_{q(2)}X)}{\sinh(N_{q(2)}S_2)}\sin(N_{q(2)}y)$$

$$+\sum_{p=1}^{P}C_{p(2)}\frac{\sinh[N_{p(2)}(S_2-X)]}{\sinh[N_{p(2)}S_2]}\sin(N_{q(2)}y)+\delta_0, \tag{3.88}$$

$$Q_{l(2)}^{(st)}=(\sqrt{K_xK_y})\sum_{q=1}^{Q}B_{q(2)}\frac{1}{\sinh(N_{q(2)}S_2)}-(\sqrt{K_xK_y})\sum_{p=1}^{P}C_{p(2)}\frac{\cosh(N_{p(2)}S_2)}{\sinh(N_{p(2)}S_2)} \tag{3.89}$$

and

$$Q_{r(2)}^{(st)}=-(\sqrt{K_xK_y})\sum_{q=1}^{Q}B_{q(2)}\frac{\cosh(N_{q(2)}S_2)}{\sinh(N_{q(2)}S_2)}+(\sqrt{K_xK_y})\sum_{p=1}^{P}C_{p(2)}\frac{1}{\sinh(N_{p(2)}S_2)}, \tag{3.90}$$

respectively, where, like in the previous case, the superscript '*st*' signifies that these expressions are related to the steady state only.

If we now apply Eqs. (3.56) and (3.57) to Eq. (3.88), we obtain the steady state stream function, $\psi_{(2)}$, for the flow problem of Fig. 3.2 as

$$\psi_2(X,y)=-(\sqrt{K_XK_Y})\sum_{q=1}^{Q}B_{q(2)}\frac{\cosh(N_{q(2)}X)}{\sinh(N_{q(2)}S_2)}\cos(N_{q(2)}y)$$

$$+(\sqrt{K_XK_Y})\sum_{p=1}^{P}C_{p(2)}\frac{\cosh[N_{p(2)}(S_2-X)]}{\sinh(N_{p(2)}S_2)}\cos(N_{p(2)}y)$$

$$+(\sqrt{K_XK_Y})\sum_{q=1}^{Q}B_{q(2)}\frac{\cosh(N_{q(2)}\varepsilon)}{\sinh(N_{q(2)}S_2)}-(\sqrt{K_XK_Y})\sum_{p=1}^{P}C_{p(2)}\frac{\cosh[N_{p(2)}(S_2-\varepsilon)]}{\sinh(N_{p(2)}S_2)} \tag{3.91}$$

where it is assumed that the zero stream line passes through the point $(\varepsilon,0)$ in the transformed domain. Further, the equation above can also be used to express the normalized form of the stream function, $\psi_{(2)}^{n}$, as

$$\psi_{(2)}^{n}=\frac{\psi_2(X,y)}{\psi_2(S_2-\varepsilon,0)}. \tag{3.92}$$

3.4.3 Case 3: An analytical model for predicting flow into an array of equally spaced ditch drains with unequal water level heights in between adjacent drains and receiving water from a ponded field subjected to variable depth of ponding

We now obtain a general solution to the ponded ditch drainage problem where both unequal water level heights between adjacent drains as well as variable depths of ponding over the surface of the soil is considered. Fig. 3.3 shows such a ponded flow configuration. As can be seen, this problem is an extension of the previous problem, where now a variable distribution of ponding depth is imposed instantaneously over the surface of the soil with the help of an array of inner bunds running parallely to the drains. The thickness of each of the inner bunds is assumed negligible. As can be seen in the figure, the surface of ponding is split into N_0 segments and a ponding depth δ_i $(1 \le i \le N_0)$ is assigned to the *i*-th segment. For creating N_0 ponding strips on the soil surface, naturally, $N_0 - 1$ inner bunds need be constructed; let us denote by S_{vai} $(1 \le i \le N_0 - 1)$, the distance of the *i*-th bund from the origin *O*. It should be noted that if δ_i are all taken as equal in Fig. 3.3, the flow problem of Fig. 3.3 will then be reduced to that of the problem of Fig. 3.2;

further, if both δ_i and the levels of water in ditches are taken as equal in Fig. 3.3, the problem will then be reduced to that of the one considered in the first case (Fig. 3.1). Naming the hydraulic head and the spacing between the adjacent drains now as $\phi_{(3)}$ and $S_{a(3)}$, respectively, to make them distinct from the corresponding values of the earlier two cases, the initial and boundary conditions for the flow domain *OABCDEFGO* of Fig. 3.3 can then be expressed as

$$\phi_{(3)}(x, y, t = 0) = 0, \qquad 0 < x < S_{a(3)}, \qquad 0 < y < h, \tag{I}$$

$$\phi_{(3)}(x, y, t > 0) = -y, \qquad x = 0, \qquad 0 < y < H_1, \tag{IIa}$$

$$\phi_{(3)}(x, y, t > 0) = -H_1, \qquad x = 0, \qquad H_1 \le y < h, \tag{IIb}$$

$$\frac{\partial \phi_{(3)}(x, y, t > 0)}{\partial y} = 0, \qquad y = h, \qquad 0 < x < S_{a(3)}, \tag{III}$$

$$\phi_{(3)}(x, y, t > 0) = -y, \qquad x = S_{a(3)}, \qquad 0 < y < H_3, \tag{IVa}$$

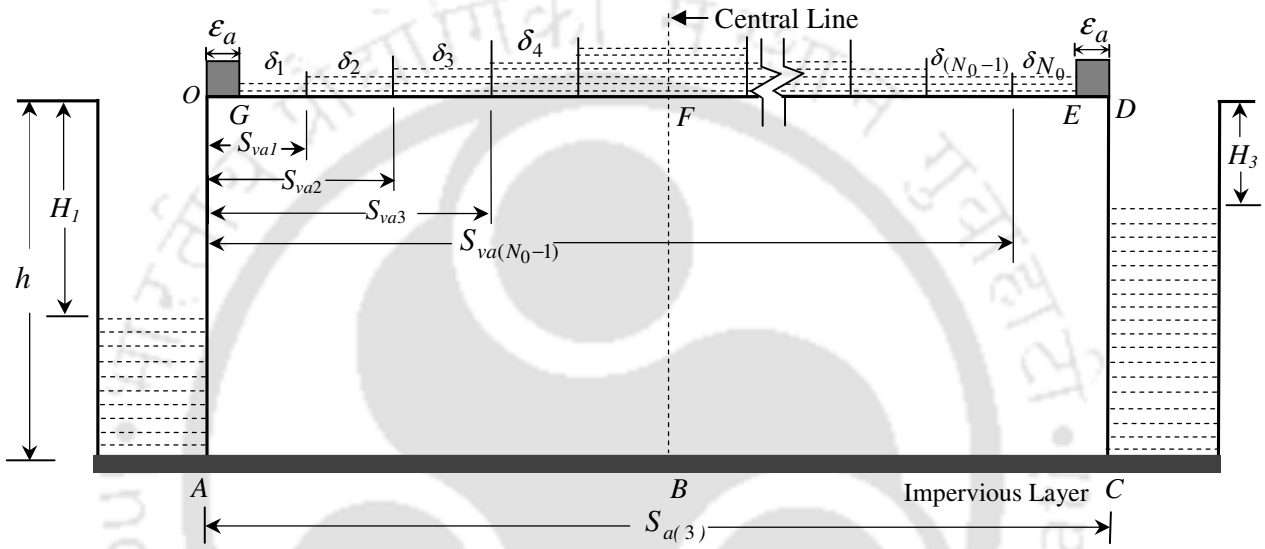

Fig. 3.3. Geometry of a fully penetrating ditch drainage system with unequal water level heights in between adjacent drains and subjected to a variable depth of ponding at the surface of the soil

$$\phi_{(3)}(x,y,t>0) = -H_3, \qquad x = S_{a(3)}, \qquad H_3 \le y < h, \tag{IVb}$$

$$\phi_{(3)}(x,y,t>0) = \delta_1, \qquad y = 0, \qquad 0 < x < S_{va1}, \tag{Va}$$

$$\phi_{(3)}(x,y,t>0) = \delta_i, \qquad y = 0, \qquad S_{va(i-1)} < x < S_{vai} \quad (2 \le i \le N_0 - 1), \tag{Vb}$$

$$\phi_{(3)}(x,y,t>0) = \delta_{N_0}, \qquad y = 0, \qquad S_{va(N_0-1)} < x < S_{a(3)}, \tag{Vc}$$

Taking into cognizance the nature of the initial and boundary conditions, the hydraulic head function for the flow problem of Fig. 3.3 can be represented, in view of Eq. (3.29) as

$$\begin{aligned}\phi_{(3)}(X,y,t) = {} & \sum_{q=1}^{Q} B_{q_{(3)}} \frac{\sinh(N_{q(3)}X)}{\sinh(N_{q(3)}S_3)} \sin(N_{q(3)}y) + \sum_{p=1}^{P} C_{p(3)} \frac{\sinh[N_{p(3)}(S_3 - X)]}{\sinh(N_{p(3)}S_3)} \sin(N_{p(3)}y) \\ & + \sum_{r=1}^{R} D_{r(3)} \frac{\cosh[N_{r(3)}(h-y)]}{\cosh(N_{r(3)}h)} \sin(N_{r(3)}X) \\ & + \sum_{m=1}^{M}\sum_{n=1}^{N} A_{mn(3)} \sin(N_{m(3)}X) \sin(N_{n(3)}y) \exp\left[\frac{-(\lambda_{mn(3)})^2 t}{(K_1)^2}\right],\end{aligned} \tag{3.93}$$

where

$$S_3 = \left(\sqrt{\frac{K_y}{K_x}}\right) S_{a(3)}, \tag{3.94}$$

$$N_{m(3)} = \left(\frac{m\pi}{S_3}\right), \tag{3.95}$$

$$N_{n(3)} = \left[\left(\frac{1-2n}{2}\right)\frac{\pi}{h}\right], \tag{3.96}$$

$$N_{p(3)} = \left[\left(\frac{1-2p}{2}\right)\frac{\pi}{h}\right], \tag{3.97}$$

$$N_{q(3)} = \left[\left(\frac{1-2q}{2}\right)\frac{\pi}{h}\right], \tag{3.98}$$

$$N_{r(3)} = \left(\frac{r\pi}{S_3}\right) \tag{3.99}$$

and

$$(\lambda_{mn(3)})^2 = \left(\frac{m\pi}{S_3}\right)^2 + \left[\left(\frac{1-2n}{2}\right)\frac{\pi}{h}\right]^2. \tag{3.100}$$

As may be observed, Eq. (3.93) inherently satisfies boundary condition III by its very definition. We will now evaluate the constants $B_{q(3)}$, $C_{p(3)}$ and $D_{r(3)}$ of Eq. (3.93) by making use of the remaining boundary conditions and the constants A_{mn} utilizing the initial condition I. Transforming first boundary conditions IVa and IVb from the real plane to the computational plane and then applying them to Eq. (3.93), the constants $B_{q(3)}$, like in the previous two cases, can be evaluated as

$$B_{q(3)} = \left(\frac{-2}{h}\right)\left[\frac{\sin(N_q H_3)}{(N_{q(3)})^2}\right]. \tag{3.101}$$

Similarly, applications of boundary conditions IIa and IIb to Eq. (3.93) will give the constants $C_{p(3)}$ as

$$C_{p(3)} = \left(\frac{-2}{h}\right)\left[\frac{\sin(N_p H_1)}{(N_{p(3)})^2}\right]. \tag{3.102}$$

To evaluate the constants D_r, we must first reduce the distances of the inner bunds from the origin O from the real domain to that of the computational domain. This can be easily accomplished by simply adopting the same transformation as has been done in Eq. (3.94); thus, we have

$$S_{vi} = \left(\sqrt{\frac{K_y}{K_x}}\right) S_{vai}, \quad (1 \le i \le N_0 - 1) \tag{3.103}$$

where S_{vi} is the distance of the *i*-th inner bund in the computational plane corresponding to the distance S_{vai} of the *i*-th inner bund in the real plane, all these distances, as mentioned before, are with respect to the origin O of Fig. 3.3. Applying now boundary conditions Va, Vb and Vc, respectively, to Eq. (3.93) in the computational pane and then allowing $R \to \infty$ in the resultant equations, the constants $D_{r(3)}$ then can be evaluated as (by making use of a Fourier series expansion in the range $0 < X < S_3$)

$$D_{r(3)} = \frac{2}{S_3}\left[\int_0^{S_{v1}} (\delta_1)\sin(N_{r(3)}X)dX + \sum_{i=2}^{N_0-1}\int_{S_{v(i-1)}}^{S_{vi}} (\delta_i)\sin(N_{r(3)}X)dX + \int_{S_{v(N_0-1)}}^{S_3} (\delta_{N_0})\sin(N_{r(3)}X)dX\right], \tag{3.104}$$

where $N_0 \geq 3$. After carrying out the integral in Eq. (3.104), we get

$$D_{r(3)} = \frac{2}{S_3}\left\{\left(\frac{\delta_1}{N_{r(3)}}\right)\left[1-\cos(N_{r(3)}S_{v1})\right] + \sum_{i=2}^{N_0-1}\left(\frac{\delta_i}{N_{r(3)}}\right)\left[\cos(N_{r(3)}S_{v(i-1)}) - \cos(N_{r(3)}S_{vi})\right]\right.$$

$$\left. + \left(\frac{\delta_{N_0}}{N_{r(3)}}\right)\left[\cos(N_{r(3)}S_{v(N_0-1)}) - \cos(N_{r(3)}S_3)\right]\right\}. \tag{3.105}$$

There still remain the constants $A_{mn(3)}$ of Eq. (3.93) to be determined. Towards this end, we apply the initial condition I to Eq. (3.93) and arrive at the following expression at $t = 0$

$$\sum_{m=1}^{M}\sum_{n=1}^{N} A_{mn(3)}\sin(N_{m(3)}X)\sin(N_{n(3)}y) = -\sum_{q=1}^{Q} B_{q(3)}\frac{\sinh(N_{q(3)}X)}{\sinh(N_{q(3)}S_3)}\sin(N_{q(3)}y)$$

$$-\sum_{p=1}^{P} C_{p(3)}\frac{\sinh[N_{p(3)}(S_3-X)]}{\sinh(N_{p(3)}S_3)}\sin(N_{p(3)}y)$$

$$-\sum_{r=1}^{R} D_{r(3)}\frac{\cosh[N_{r(3)}(h-y)]}{\sinh(N_{r(3)}h)}\sin(N_{r(3)}X). \tag{3.106}$$

It is clear from the nature of the above equation that, if we let M and N to go to infinity in the above expression, the constants $A_{mn(3)}$ can then be evaluated by running a double Fourier series on the computational plane, i.e., on the area encompassed by $0 < X < S_3$ and $0 < y < h$; the ensuing expression for $A_{mn(3)}$ can then be represented as

$$A_{mn(3)} = -\left(\frac{2}{h}\right)\left(\frac{2}{S_3}\right)\left\{\int_0^h\int_0^{S_3}\sum_{q=1}^{Q} B_{q(3)}\left[\frac{\sinh(N_{q(3)}X)}{\sinh(N_{q(3)}S_3)}\right]\sin(N_{q(3)}y)\sin(N_{m(3)}X)\sin(N_{n(3)}y)dXdy\right\}$$

$$-\left(\frac{2}{h}\right)\left(\frac{2}{S_3}\right)\left\{\int_0^h\int_0^{S_3}\sum_{p=1}^{P} C_{p(3)}\left[\frac{\sinh[N_{p(3)}(S_3-X)]}{\sinh(N_{p(3)}S_3)}\right]\sin(N_{p(3)}y)\sin(N_{m(3)}X)\sin(N_{n(3)}y)dXdy\right\}$$

$$-\left(\frac{2}{h}\right)\left(\frac{2}{S_3}\right)\left\{\int_0^h\int_0^{S_3}\sum_{r=1}^{R} D_{r(3)}\left[\frac{\cosh[N_{r(3)}(h-y)]}{\cosh(N_{r(3)}h)}\right]\sin(N_{r(3)}X)\sin(N_{m(3)}X)\sin(N_{n(3)}y)dXdy\right\}. \tag{3.107}$$

Calling the first integral on the right hand side of the above equation as $I^1_{(3)}$, the second integral as $I^2_{(3)}$, and the last integral as $I^3_{(3)}$, Eq. (3.107) in a condensed form can be represented as

$$A_{mn(3)} = I^1_{(3)} + I^2_{(3)} + I^3_{(3)}. \tag{3.108}$$

Simplifying the above integrals, we get, for $q = n$

$$I^1_{(3)} = \left(\frac{2}{S_3}\right)\sum_{q=1}^{Q} B_{q(3)}\left[\frac{N_{m(3)}\cos(N_{m(3)}S_3)}{(N_{m(3)})^2 + (N_{q(3)})^2}\right] \tag{3.109}$$

and for $q \neq n$

$$I^1_{(3)} = \left(\frac{4}{hS_3}\right)\sum_{q=1}^{Q} B_{q(3)}\left[\frac{N_{m(3)}\cos(N_{m(3)}S_3)}{(N_{m(3)})^2 + (N_{q(3)})^2}\right]\times$$

$$\left\{\frac{1}{2(N_{q(3)} - N_{n(3)})}\sin[(N_{q(3)} - N_{n(3)})h] - \frac{1}{2(N_{q(3)} + N_{n(3)})}\sin[(N_{q(3)} + N_{n(3)})h]\right\}; \tag{3.110}$$

for $p = n$

$$I^2_{(3)} = -\left(\frac{2}{S_3}\right)\sum_{p=1}^{P} C_{p(3)}\left[\frac{N_{m(3)}}{(N_{m(3)})^2 + (N_{p(3)})^2}\right] \tag{3.111}$$

and for $p \neq n$

$$I^2_{(3)} = -\left(\frac{4}{hS_3}\right)\sum_{p=1}^{P} C_{p(3)}\left[\frac{N_{m(3)}}{(N_{m(3)})^2 + (N_{p(3)})^2}\right]\times$$

$$\left\{\frac{1}{2(N_{p(3)} - N_{n(3)})}\sin[(N_{p(3)} - N_{n(3)})h] - \frac{1}{2(N_{p(3)} + N_{n(3)})}\sin[(N_{p(3)} + N_{n(3)})h]\right\}; \tag{3.112}$$

finally, for $r = m$

$$I^3_{(3)} = -\left(\frac{2}{h}\right)\sum_{r=1}^{R} D_{r(3)}\left[\frac{N_{n(3)}}{(N_n)^2 + (N_r)^2}\right] \tag{3.113}$$

and for $r \neq m$

$$I^3_{(3)} = 0. \tag{3.114}$$

All the constants of Eq. (3.93) are thus determined and our boundary value problem is solved.

The quantity of water seeping per unit length into one side of the left hand ditch (i.e., through face *OA* of Fig. 3.3), $Q_{l(3)}$, receiving water from the ponded surface in between the adjacent drains at any instant of time *t* can be calculated as

$$Q_{l(3)}(t) = \sqrt{K_x K_y}\int_0^h \left(\frac{\partial \phi_{(3)}}{\partial X}\right)_{X=0} dy. \tag{3.115}$$

Evaluation of the above integral yields using Eq. (3.93), gives

$$Q_{l(3)}(t) = (\sqrt{K_x K_y})\sum_{q=1}^{Q} B_{q(3)}\left[\frac{1}{\sinh(N_{q(3)}S_3)}\right] - (\sqrt{K_x K_y})\sum_{p=1}^{P} C_{p(3)}\left[\frac{\cosh(N_{p(3)}S_3)}{\sinh(N_{p(3)}S_3)}\right]$$

$$+ (\sqrt{K_x K_y})\sum_{r=1}^{R} D_{r(3)}\left[\frac{\sinh(N_{r(3)}h)}{\cosh(N_{r(3)}h)}\right] + (\sqrt{K_x K_y})\sum_{m=1}^{M}\sum_{n=1}^{N} A_{mn(3)}\left(\frac{N_{m(3)}}{N_{n(3)}}\right)\exp\left[\frac{-(\lambda_{mn(3)})^2 t}{(K_1)^2}\right]. \tag{3.116}$$

In the same way, discharge per unit length into one side of the right hand ditch (i.e., through face *CD* of Fig. 3.3), $Q_{r(3)}$, receiving water from the ponded surface in between the neighboring drains at a desired time *t* can be evaluated as

$$Q_{r(3)}(t) = -\sqrt{K_x K_y}\int_0^h \left(\frac{\partial \phi_{(3)}}{\partial X}\right)_{X=S_3} dy. \tag{3.117}$$

After carrying out the integral of Eq. (3.117) utilizing Eq. (3.93), we get

$$Q_{r(3)}(t) = -(\sqrt{K_x K_y})\sum_{q=1}^{Q} B_{q(3)}\left[\frac{\cosh(N_{q(3)}S_3)}{\sinh(N_{q(3)}S_3)}\right] + (\sqrt{K_x K_y})\sum_{p=1}^{P} C_{p(3)}\left[\frac{1}{\sinh(N_{p(3)}S_3)}\right]$$

$$- (\sqrt{K_x K_y})\sum_{r=1}^{R} D_{r(3)}\left[\frac{\sinh(N_{r(3)}h)}{\cosh(N_{r(3)}h)}\right]\cos(N_{r(3)}S_3)$$

$$- (\sqrt{K_x K_y})\sum_{m=1}^{M}\sum_{n=1}^{N} A_{mn(3)}\left[\frac{N_{m(3)}}{N_{n(3)}}\right]\exp\left[\frac{-(\lambda_{mn(3)})^2 t}{(K_1)^2}\right]\cos(N_{m(3)}S_3). \tag{3.118}$$

The time dependent top discharge function, $Q_{topX(3)}$, per unit length of the ditches at the surface of the soil in between two adjacent drains, can be evaluated by making use of the Darcy's law at the soil surface; $Q_{topX(3)}$ thus, can be evaluated as

$$Q_{topX(3)}(X,t) = -(\sqrt{K_x K_y})\int_{\varepsilon}^{X}\left(\frac{\partial \phi}{\partial y}\right)_{y=0} dX, \tag{3.119}$$

where X is the horizontal distance at the surface of the soil in the transformed domain as measured from the origin O.

Evaluating the integral of Eq. (3.119) using Eq. (3.93), we have

$$\begin{aligned} Q_{topX(3)}(X,t) = & -(\sqrt{K_x K_y})\sum_{q=1}^{Q} B_{q(3)}\left[\frac{1}{\sinh(N_{q(3)}S_3)}\right][\cosh(N_{q(3)}X) - \cosh(N_{q(3)}\varepsilon)] \\ & + (\sqrt{K_x K_y})\sum_{p=1}^{P} C_{p(3)}\left[\frac{1}{\sinh(N_{p(3)}S_3)}\right]\{\cosh[N_{p(3)}(S_3 - X)] - \cosh[N_{p(3)}(S_3 - \varepsilon)]\} \\ & - (\sqrt{K_x K_y})\sum_{r=1}^{R} D_{r(3)}\left[\frac{\sinh(N_{r(3)}h)}{\cosh(N_{r(3)}h)}\right][\cos(N_{r(3)}X) - \cos(N_{r(3)}\varepsilon)] \\ & + (\sqrt{K_x K_y})\sum_{m=1}^{M}\sum_{n=1}^{N} A_{mn(3)}\left[\frac{N_{n(3)}}{N_{m(3)}}\right]\exp\left[\frac{-(\lambda_{mn(3)})^2 t}{(K_1)^2}\right][\cos(N_{m(3)}X) - \cos(N_{m(3)}\varepsilon)]. \end{aligned} \tag{3.120}$$

Eq. (3.120) describes discharge coming from the surface of the soil per unit length of the ditches from a zone extending up to a horizontal distance of X from the origin O in the transformed domain at any instant of time t. Naturally then, to obtain the total transient discharge, $Q_{top(3)}$, from the surface of the soil in between the ditch banks of two neighboring drains per unit length of the drains at any desired time t, we need to simply put $X = S_3 - \varepsilon$ in the above expression; thus, we have

$$\begin{aligned} Q_{top(3)}(t) = & -(\sqrt{K_x K_y})\sum_{q=1}^{Q} B_{q(3)}\left[\frac{1}{\sinh(N_{q(3)}S_3)}\right]\{\cosh[N_{q(3)}(S_3 - \varepsilon)] - \cosh(N_{q(3)}\varepsilon)\} \\ & + (\sqrt{K_x K_y})\sum_{p=1}^{P} C_{p(3)}\left[\frac{1}{\sinh(N_{p(3)}S_3)}\right]\{\cosh(N_{p(3)}\varepsilon) - \cosh[N_{p(3)}(S_3 - \varepsilon)]\} \\ & - (\sqrt{K_x K_y})\sum_{r=1}^{R} D_{r(3)}\left[\frac{\sinh(N_{r(3)}h)}{\cosh(N_{r(3)}h)}\right]\{\cos[N_{r(3)}(S_3 - \varepsilon)] - \cos(N_{r(3)}\varepsilon)\} \\ & + (\sqrt{K_x K_y})\sum_{m=1}^{M}\sum_{n=1}^{N} A_{mn(3)}\left[\frac{N_{n(3)}}{N_{m(3)}}\right]\exp\left[\frac{-(\lambda_{mn(3)})^2 t}{(K_1)^2}\right]\{\cos[N_{m(3)}(S_3 - \varepsilon)] - \cos(N_{m(3)}\varepsilon)\}. \end{aligned} \tag{3.121}$$

For clarity of presentation, the top discharge distribution function, $Q_{topX(3)}$, at any instant of time t can also be expressed as a percentage of the total discharge, $Q_{top(3)}$; naming such a function as $Q^{f}_{topX(3)}$, we get

$$Q^{f}_{topX(3)}(X,t)=\left[\frac{Q_{topX(3)}(X,t)}{Q_{top(3)}(t)}\right]\times 100. \tag{3.122}$$

Eq. (3.122) have been utilized to plot the surface discharge distribution functions of Figs. 3.16, 3.18 and 3.19 corresponding to a few flow situations of Fig. 3.3.

The volume of water entering though the left and right ditches of Fig. 3.3 through the faces OA ($V_{l(3)}$) and CD ($V_{r(3)}$) can now be calculated, like in the earlier cases, by integrating Eqs. (3.116) and (3.118) within the time interval t; carrying out such integrations, we get

$$\begin{aligned}V_{l(3)}=&(\sqrt{K_xK_y})\sum_{q=1}^{Q}B_{q(3)}\left[\frac{1}{\sinh(N_{q(3)}S_3)}\right]t-(\sqrt{K_xK_y})\sum_{p=1}^{P}C_{p(3)}\left[\frac{\cosh(N_{p(3)}S_3)}{\sinh(N_{p(3)}S_3)}\right]t\\&+(\sqrt{K_xK_y})\sum_{r=1}^{R}D_{r(3)}\left[\frac{\sinh(N_{r(3)}h)}{\cosh(N_{r(3)}h)}\right]t\\&-(\sqrt{K_xK_y})\sum_{m=1}^{M}\sum_{n=1}^{N}A_{mn(3)}\left[\frac{N_{m(3)}}{N_{n(3)}}\right]\left[\frac{(K_1)^2}{(\lambda_{mn(3)})^2}\right]\left\{\exp\left[\frac{-(\lambda_{mn(3)})^2t}{(K_1)^2}\right]-1\right\}\end{aligned} \tag{3.123}$$

and

$$\begin{aligned}V_{r(3)}=&-(\sqrt{K_xK_y})\sum_{q=1}^{Q}B_{q(3)}\left[\frac{\cosh(N_{q(3)}S_3)}{\sinh(N_{q(3)}S_3)}\right]t+(\sqrt{K_xK_y})\sum_{p=1}^{P}C_{p(3)}\left[\frac{1}{\sinh(N_{p(3)}S_3)}\right]t\\&-(\sqrt{K_xK_y})\sum_{r=1}^{R}D_{r(3)}\left[\frac{\sinh(N_{r(3)}h)}{\cosh(N_{r(3)}h)}\right]\cos(N_{r(3)}S_3)t\\&+(\sqrt{K_xK_y})\sum_{m=1}^{M}\sum_{n=1}^{N}A_{mn(3)}\left[\frac{N_{m(3)}}{N_{n(3)}}\right]\left[\frac{(K_1)^2}{(\lambda_{mn(3)})^2}\right]\cos(N_{m(3)}S_3)\left\{\exp\left[\frac{-(\lambda_{mn(3)})^2t}{(K_1)^2}\right]-1\right\}.\end{aligned} \tag{3.124}$$

Also, the volume of water entering through the surface GE of Fig. 3.3 in between the adjacent drains in time t, $V_{top(3)}$, can be determined from Eq. (3.121) by integrating it with respect to time within the interval t; performing the integral, we get

$$V_{top(3)} = -(\sqrt{K_x K_y})\sum_{q=1}^{Q} B_{q(3)}\left[\frac{1}{\sinh(N_{q(3)}S_3)}\right]\{\cosh[N_{q(3)}(S_3-\varepsilon)]-\cosh(N_{q(3)}\varepsilon)\}t$$

$$+(\sqrt{K_x K_y})\sum_{p=1}^{P} C_{p(3)}\left[\frac{1}{\sinh(N_{p(3)}S_3)}\right]\{\cosh(N_{p(3)}\varepsilon)-\cosh[N_{p(3)}(S_3-\varepsilon)]\}t$$

$$-(\sqrt{K_x K_y})\sum_{r=1}^{R} D_{r(3)}\left[\frac{\sinh(N_{r(3)}h)}{\cosh(N_{r(3)}h)}\right]\{\cos[N_{r(3)}(S_3-\varepsilon)]-\cos(N_{r(3)}\varepsilon)\}t$$

$$-(\sqrt{K_x K_y})\sum_{m=1}^{M}\sum_{n=1}^{N} A_{mn(3)}\left[\frac{N_{n(3)}}{N_{m(3)}}\right]\left[\frac{(K_1)^2}{(\lambda_{mn(3)})^2}\right]\{\cos[N_{m(3)}(S_3-\varepsilon)]-\cos(N_{m(3)}\varepsilon)\}$$

$$\times\left\{\exp\left[\frac{-(\lambda_{mn(3)})^2 t}{(K_1)^2}\right]-1\right\}. \qquad (3.125)$$

To obtain expressions for the hydraulic head function, the left and the right discharges, the top discharge function and the top discharge corresponding to the steady state situation, we need to simply allow the time variable appearing in these expressions to go to infinity; as can be seen this will make the exponential term of these equations to go to zero and the relevant expressions for the steady state will then turn out to be

$$\phi_{(3)}^{(st)}(X,y) = \sum_{q=1}^{Q} B_{q(3)}\frac{\sinh(N_{q(3)}X)}{\sinh(N_{q(3)}S_3)}\sin(N_{q(3)}y)+\sum_{p=1}^{P} C_{p(3)}\frac{\sinh[N_{p(3)}(S_3-X)]}{\sinh(N_{p(3)}S_3)}\sin(N_{p(3)}y)$$

$$+\sum_{r=1}^{R} D_r\frac{\cosh[N_{r(3)}(h-y)]}{\cosh(N_{r(3)}h)}\sin(N_{r(3)}X), \qquad (3.126)$$

$$Q_{l(3)}^{(st)} = (\sqrt{K_x K_y})\sum_{q=1}^{Q} B_{q(3)}\left[\frac{1}{\sinh(N_{q(3)}S_3)}\right]-(\sqrt{K_x K_y})\sum_{p=1}^{P} C_{p(3)}\left[\frac{\cosh(N_{p(3)}S_3)}{\sinh(N_{p(3)}S_3)}\right]$$

$$+(\sqrt{K_x K_y})\sum_{r=1}^{R} D_{r(3)}\left[\frac{\sinh(N_{r(3)}h)}{\cosh(N_{r(3)}h)}\right] \qquad (3.127)$$

$$Q_{r(3)}^{(st)} = -(\sqrt{K_x K_y})\sum_{q=1}^{Q} B_{q(3)}\left[\frac{\cosh(N_{q(3)}S_3)}{\sinh(N_{q(3)}S_3)}\right]+(\sqrt{K_x K_y})\sum_{p=1}^{P} C_{p(3)}\left[\frac{1}{\sinh(N_{p(3)}S_3)}\right]$$

$$-(\sqrt{K_x K_y})\sum_{r=1}^{R} D_{r(3)}\left[\frac{\sinh(N_{r(3)}h)}{\cosh(N_{r(3)}h)}\right]\cos(N_{r(3)}S_3), \qquad (3.128)$$

$$Q^{(st)}_{topX\,(3)}(X) = -(\sqrt{K_x K_y})\sum_{q=1}^{Q} B_{q(3)}\left[\frac{1}{\sinh(N_{q(3)}S_3)}\right][\cosh(N_{q(3)}X) - \cosh(N_{q(3)}\varepsilon)]$$

$$+(\sqrt{K_x K_y})\sum_{p=1}^{P} C_{p(3)}\left[\frac{1}{\sinh(N_{p(3)}S_3)}\right]\{\cosh[N_{p(3)}(S_3 - X)] - \cosh[N_{p(3)}(S_3 - \varepsilon)]\}$$

$$-(\sqrt{K_x K_y})\sum_{r=1}^{R} D_{r(3)}\left[\frac{\sinh(N_{r(3)}h)}{\cosh(N_{r(3)}h)}\right][\cos(N_{r(3)}X) - \cos(N_{r(3)}\varepsilon)] \qquad (3.129)$$

and

$$Q^{(st)}_{top\,(3)} = -(\sqrt{K_x K_y})\sum_{q=1}^{Q} B_{q(3)}\left[\frac{1}{\sinh(N_{q(3)}S_3)}\right]\{\cosh[N_{q(3)}(S_3 - \varepsilon)] - \cosh(N_{q(3)}\varepsilon)\}$$

$$+(\sqrt{K_x K_y})\sum_{p=1}^{P} C_{p(3)}\left[\frac{1}{\sinh(N_{p(3)}S_3)}\right]\{\cosh(N_{p(3)}\varepsilon) - \cosh[N_{p(3)}(S_3 - \varepsilon)]\}$$

$$-(\sqrt{K_x K_y})\sum_{r=1}^{R} D_{r(3)}\left[\frac{\sinh(N_{r(3)}h)}{\cosh(N_{r(3)}h)}\right]\{\cos[N_{r(3)}(S_3 - \varepsilon)] - \cos(N_{r(3)}\varepsilon)\}, \qquad (3.130)$$

respectively, where the subscript '*st*' under the parenthesis sign is again used to denote that these expressions are applicable to the steady state situation only.

To evaluate the steady stream function, $\psi_{(3)}$, for the flow domain of Fig. 3.3, we apply Eqs. (3.56) and (3.57) to the steady hydraulic head function given by Eq. (3.126); assuming the zero streamline to pass though $(\varepsilon,0)$ in the computational domain, the steady state stream function in the computational domain then works out to be

$$\psi_{(3)}(X,y) = -(\sqrt{K_x K_y})\sum_{q=1}^{Q} B_{q(3)}\frac{\cosh(N_{q(3)}X)}{\sinh(N_{q(3)}S_3)}\cos(N_{q(3)}y)$$

$$+(\sqrt{K_x K_y})\sum_{p=1}^{P} C_{p(3)}\frac{\cosh[N_{p(3)}(S_3 - X)]}{\sinh(N_{p(3)}S_3)}\cos(N_{p(3)}y)$$

$$-(\sqrt{K_x K_y})\sum_{r=1}^{R} D_{r(3)}\frac{\sinh[N_{r(3)}(h-y)]}{\cosh(N_{r(3)}h)}\cos(N_{r(3)}X)$$

$$+(\sqrt{K_x K_y})\sum_{q=1}^{Q} B_{q(3)}\frac{\cosh(N_{q(3)}\varepsilon)}{\sinh(N_{q(3)}S_3)} - (\sqrt{K_x K_y})\sum_{p=1}^{P} C_{p(3)}\frac{\cosh[N_{p(3)}(S_3 - \varepsilon)]}{\sinh(N_{p(3)}S_3)}$$

$$+(\sqrt{K_x K_y})\sum_{r=1}^{R} D_{r(3)} \frac{\sinh(N_{r(3)}h)}{\cosh(N_{r(3)}h)} \cos(N_{r(3)}\varepsilon). \tag{3.131}$$

Further, the stream function can be normalized by dividing the same with the maximum possible value it can attain in the flow domain; thus, denoting the normalized streamline as $\psi^n_{(3)}$, we have

$$\psi^n_{(3)}(X, y) = \frac{\psi_{(3)}(X, y)}{\psi_{(3)}(S-\varepsilon, 0)}. \tag{3.132}$$

Eq. (3.132) has been made use of to plot the normalized streamlines of Figs. 3.10, 3.15, 3.17 and 3.18 corresponding to a few flow situations of Fig. 3.3.

We would like point out here that if ε_a is taken equal to zero (which is the same as saying $\varepsilon = 0$), then δ_1 and δ_{N_0} must also be taken zero, as otherwise the discharge and volume expressions will all diverge. To show that $Q_{topX(3)}$, $Q_{top(3)}$, $V_{top(3)}$ diverge for such a situation, we first substitute D_r of Eq. (3.105) to Eqs. (3.120), (3.121) and (3.125), respectively, and then observe the nature of the resultant expressions. We find that such expressions will be having terms like $(2\delta_1 / SN_{r(3)})\tanh(N_{r(3)}h)$ and $(2\delta_{N_0} / S_3 N_{r(3)})\tanh(N_{r(3)}h)\cos^2(N_{r(3)}S_3)$ under the summation sign; if we assume $\tanh(N_{r(3)}h)$ to reduce to 1 after the summation of the first three terms (see Kirkham, 1950, Barua and Tiwari, 1995)) considering the fact that $\underset{r\to\infty}{Lim}[\tanh(N_{r(3)}h)] = \underset{r\to\infty}{Lim}[\tanh(r\pi h / S_3)] = 1$, then we see that the series

$$\sum_{r=1}^{R\to\infty} \frac{2\delta_1}{S_3 N_{r(3)}} \tanh\left(\frac{r\pi h}{S_3}\right) = \sum_{r=1}^{R\to\infty} \frac{2\delta_1}{r\pi} \tanh\left(\frac{r\pi h}{S_3}\right)$$

after the first three terms, can be represented as

$$\left(\frac{2\delta_1}{\pi}\right)\left(\frac{1}{4}+\frac{1}{5}+\frac{1}{6}+\ldots\right).$$

But the above series diverges to ∞ as $R \to \infty$, and hence we see that $Q_{top(3)}$ overall diverges to $+\infty$ if R is made to increase incessantly. The same argument holds for the term $(2\delta_{N_0} / S_3 N_{r(3)})\tanh(N_{r(3)}h)\cos^2(N_{r(3)}S_3)$ since $\cos^2(N_{r(3)}S_3) = \cos^2(r\pi) = 1$ for any r. In a similar way, we can show that $Q_{l(3)}$, $V_{l(3)}$ go to infinity when $\varepsilon_a = 0$ but $\delta_1 \neq 0$ [since in that case they will be having a term like $\sum_{r=1}^{\infty}(2\delta_1 / S_3 N_{r(3)})\tanh(N_{r(3)}h)]$ and $Q_{r(3)}$, $V_{r(3)}$

go to infinity when $\varepsilon_a = 0$ but $\delta_{N_0} \neq 0$ [since in that case they will be having a term like $\sum_{r=1}^{\infty}(2\delta_{N_0} / S_3 N_{r(3)}) \tanh(N_{r(3)} h) \cos^2(N_{r(3)} S_3)$].

In the same way, we can show that if $\varepsilon_a = 0$ but $\delta_0 \neq 0$, all the discharge and volume expressions derived for the flow problems corresponding to Figs. (3.1) and (3.2) (Q_{side}, V_{stot}, $Q_{top(1)}$, $V_{top(1)}$, $Q_{l(2)}$, $V_{l(2)}$, $Q_{r(2)}$, $V_{r(2)}$, $Q_{top(2)}$, $V_{top(2)}$) will then diverge.

3. 5 Verification of Proposed Model

3.5.1 Comparison with a few available steady state solutions

We will now perform a few checks to ascertain the validity of our developed models. Figs. 3.4, 3.5 and 3.6 show variation of top and side discharges, expressed as ratios with respect to the hydraulic conductivity of soil and thickness of the soil layer, with time for a few flow ponded drainage situations. The plots are for a single ditch drain receiving water from a field having a negligible depth of ponded water over it. The spacing between the adjacent drains is given a very large value, around 100 m (should be theoretically infinite), so that the flow behavior around each ditch can be taken as independent of the flow behavior around neighboring ditches. In all these cases, the ditches are kept empty every time but the magnitude of $h = H_1$ are made to vary from 0.5 m to 3.0 m. As may be observed, both the top and the side discharge fractions converge to a steady state value of around 0.742 in all the plots, irrespective of the depth of the ditches and the anisotropy and specific storage coefficients of the soil. This common value, as obtained from Fukuda's (1957) and Youngs' (1994) (see also Fig. 3.7) steady state solutions of the ponded ditch drainage problem, comes out to be 0.743 and 0.742, respectively – a very good match with the value predicted by our derived solutions thereby showing that the proposed analytical models are correctly developed. Further, from experimental observations, Fukuda (1957) found this ratio to be 0.720, a figure quite close to the analytically predicted value. Thus, this close matching of our results with that of Fukuda's (1957) experimental value can also be considered as an experimental check on our proposed solutions.

It is to be noted that, for the first case, summing $C_{p(1)}$ with P varying from 15 to 20 and $A_{mn(1)}$ with M and N varying from 40 to 50, for the second case, summing $B_{q(2)}$ and $C_{p(2)}$ with P and Q varying from 15 to 20 and $A_{mn(2)}$ with M and N varying from 40 to 50, and for

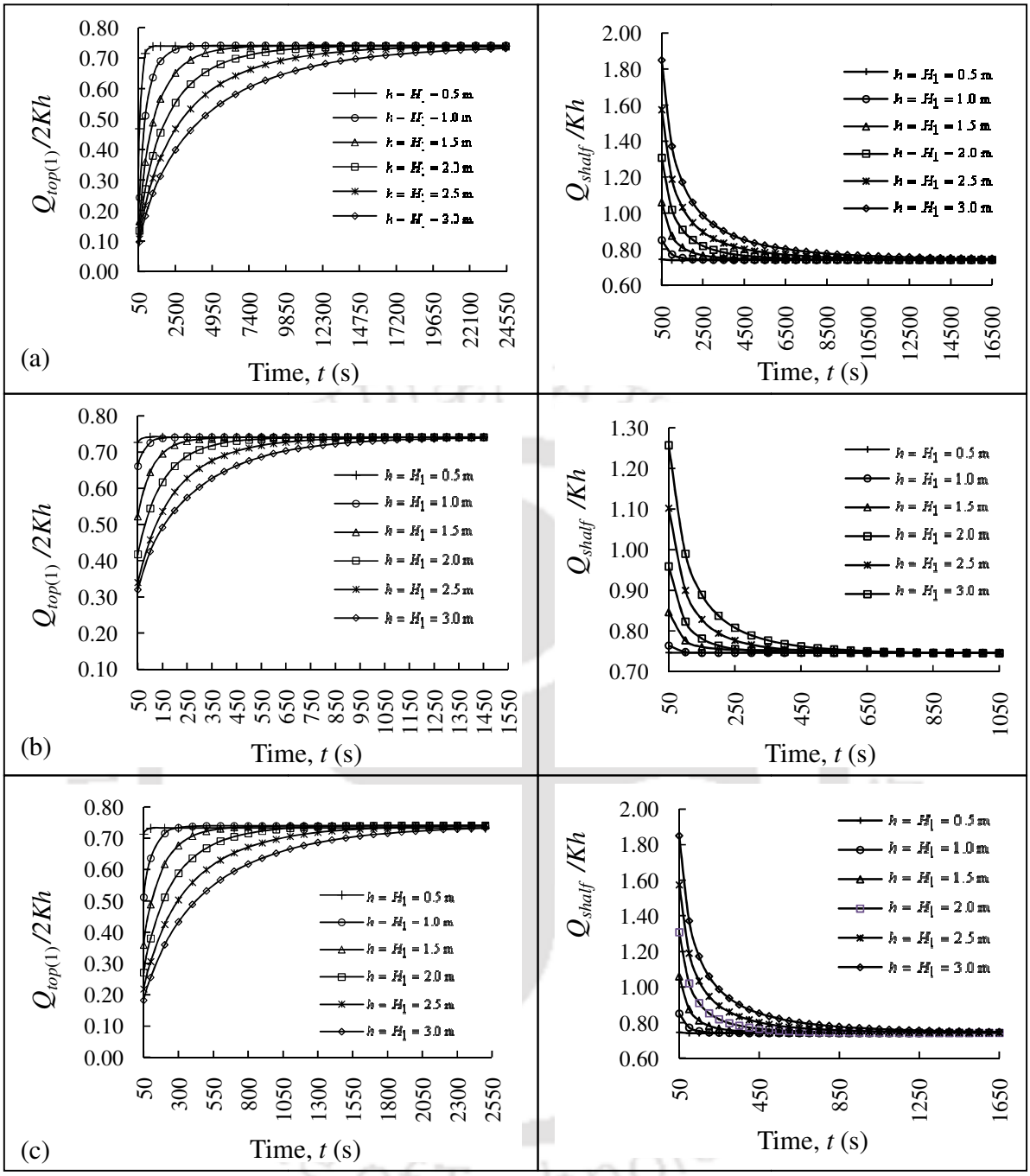

Fig. 3.4. Variation of $Q_{top(1)}/2Kh$ and Q_{shalf}/Kh ratios with time as obtained from the proposed solution of the flow problem of Fig. 3.1 for different $h = H_1$ values (i.e., ditches are running empty) when the other parameters of the flow problem are taken as $S_{a(1)} = 100$ m (theoretically infinite) $\delta_0 = 0$ and (a) $K_x/K_y = 25/1$ ($K_x = 1$ m/day, $K_y = 0.04$ m/day), (b) $K_x/K_y = 1/1$ ($K_x = 1$ m/day, $K_y = 1$ m/day), $S_s = 0.001$ m^{-1} and (c) $K_x/K_y = 25/1$ ($K_x = 1$ m/day, $K_y = 0.04$ m/day), $S_s = 0.0001$ m^{-1}

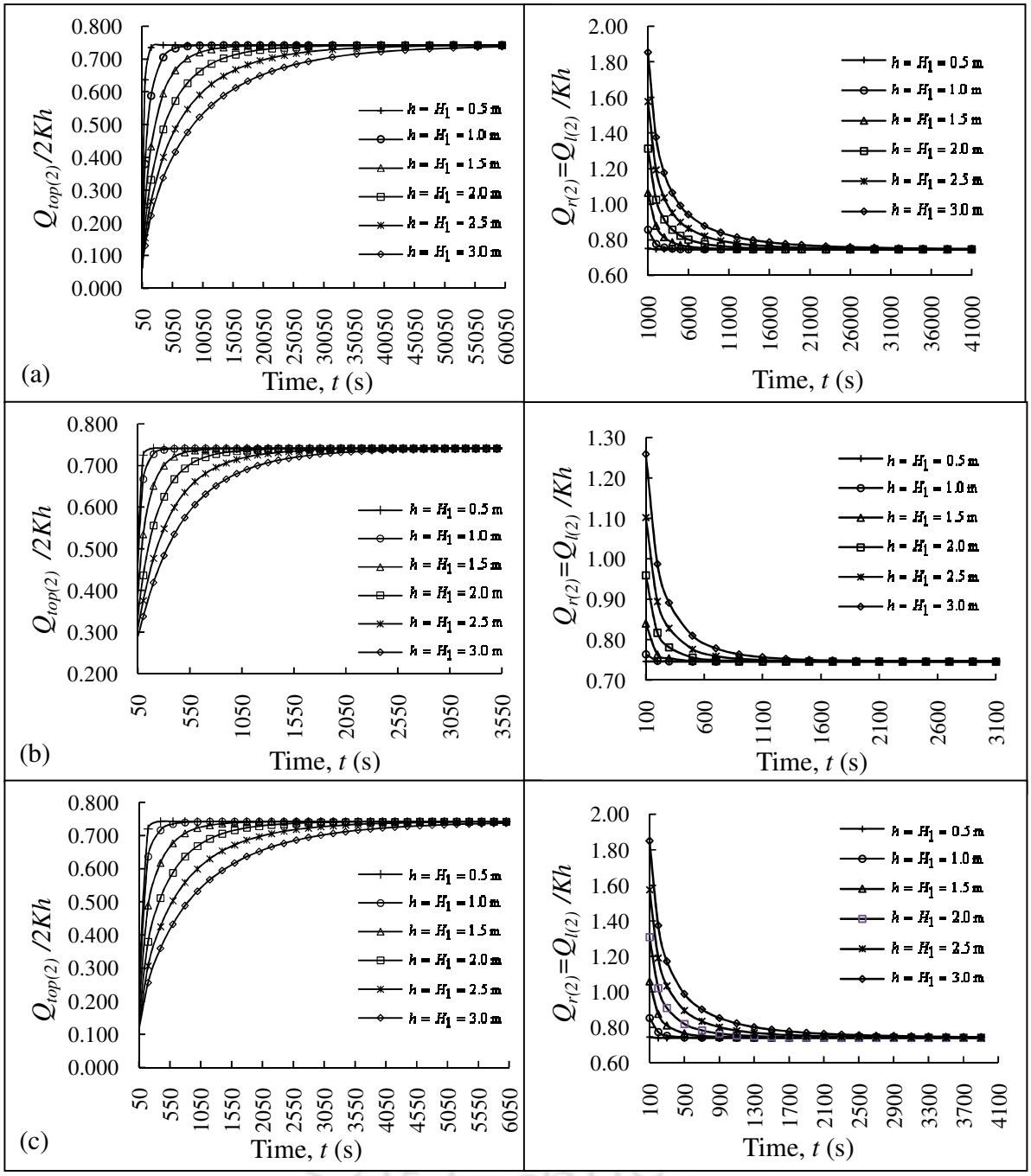

Fig. 3.5. Variation of $Q_{top(2)}/2Kh$ and $Q_{r(2)} = Q_{l(2)}/Kh$ ratios with time as obtained from the proposed solution of the flow problem of Fig. 3.2 for different $h = H_1$ values (i.e., ditches are running empty) when the other parameters of the flow problem are taken as $S_{a(2)} = 100$ m (theoretically infinite), $\delta_0 = 0$ and (a) $K_x/K_y = 25/1$ ($K_x = 0.5$ m/day, $K_y = 0.02$ m/day $S_s = 0.001$ m^{-1}, (b) $K_x/K_y = 1/1$ ($K_x = 0.5$ m/day, $K_y = 0.5$ m/day), $S_s = 0.001$ m^{-1} and (c) $K_x/K_y = 25/1$ ($K_x = 0.5$ m/day, $K_y = 0.02$ m/day), $S_s = 0.0001$ m^{-1}

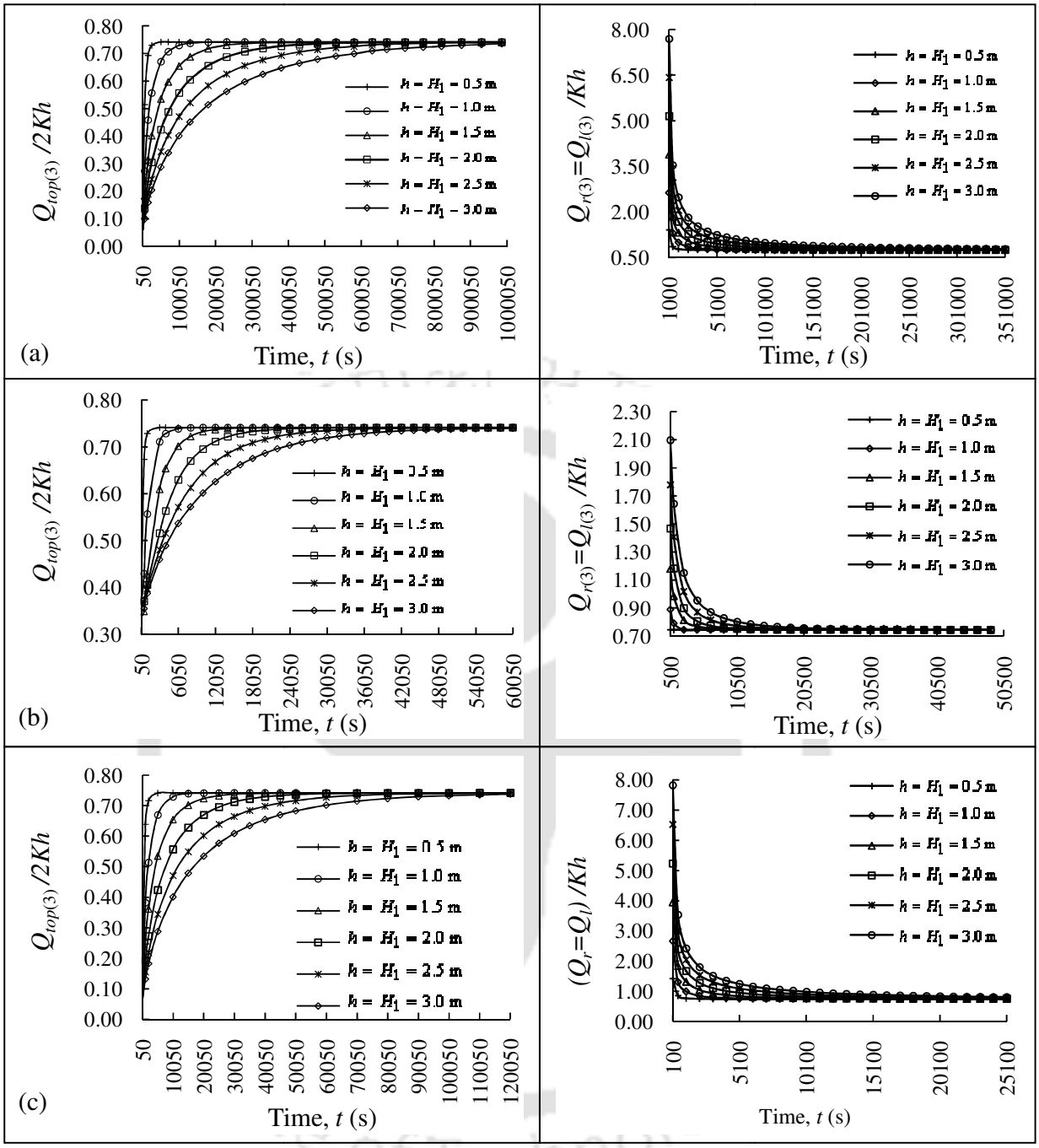

Fig. 3.6. Variation of $Q_{top(3)}/2Kh$ and $Q_{r(3)}=Q_{l(3)}/Kh$ ratios with time as obtained from the proposed solution of the flow problem of Fig. 3.3 for different $h=H_1$ values (i.e., ditches are running empty) when the other parameters of the flow problem are taken as $S_{a(3)}=100$ m (theoretically infinite), $\delta_i=0$ and (a) $K_x/K_y=25/1$ ($K_x=0.0254$ m/day, $K_y=0.001016$ m/day), $S_s=0.001$ m^{-1}, (b) $K_x/K_y=1/1$ ($K_x=0.0254$ m/day, $K_y=0.0254$ m/day), $S_s=0.001$ m^{-1} and (c) $K_x/K_y=25/1$ ($K_x=0.0254$ m/day, $K_y=0.001016$ m/day), $S_s=0.0001$ m^{-1}

the third case, summing $B_{q(3)}$ and $C_{p(3)}$ with P and Q varying from 15 to 20, $D_{r(3)}$ with R varying from 30 to 40 and $A_{mn(3)}$ with M and N varying from 40 to 50, are generally sufficient to achieve a good convergence of our series solutions for most flow situations.

Figs. 3.7(a) and 3.7(b) show variations of $Q_{top(3)}/2Kh$ and $Q_{l(3)} = Q_{r(3)}/Kh$ with water level fraction for an isolated ditch at different times for a few flow situations of Fig. 3.3. As may be observed, our predicted $Q_{top(3)}/2Kh$ versus $(h-H_1)/h$ and $Q_{l(3)} = Q_{r(3)}/Kh$ versus $(h-H_1)/h$ steady state profiles obtained from our analytical model for the flow problem of Fig. 3.3 are found to be matching accurately with the corresponding profiles obtained from the steady state solutions of Youngs (1994), thereby showing, once again, the validity of the proposed analytical model for the variably ponded situation (Case 3). Again the results show the changing water storage with time when the head is reduced on lowering the ditch-water levels. For an incompressible soil, the storage coefficient is zero, and the steady state condition occurs instantaneously. Figs. 3.8(a) and 3.8(b) are similar to that of Fig. 3.7, except that the adjacent ditches are now not separated from each other by an infinite distance but are placed maintaining a ratio of $S_{a(3)}/h = 3.0$; as may be seen, here also our predicted $Q_{top(3)}/2Kh$ versus $(h-H_1)/h$ and $Q_{l(3)} = Q_{r(3)}/Kh$ versus $(h-H_1)/h$ steady state profiles are found to be corresponding exactly with the identical profiles obtained from the steady state analytical solution of Chahar and Vadodaria (2008b), thereby showing again the accuracy of our developed model for the drainage situation of Fig. 3.3.

In Figs. 3.9 and 3.10, we are taking the same ditch drainage examples, one when the field is subjected to zero depth of ponding and the other, when the surface of the soil is covered with a layer of uniform ponded water of thickness one metre, as had been considered by Kirkham (1965), and are comparing the hydraulic heads and the normalized streamlines as predicted by our analytical solutions corresponding to Figs. 3.2 and 3.3, respectively, with the corresponding values obtained from the series solution of Kirkham (1965). From these figures, it is clear that our analytical models could successfully reproduce the steady state

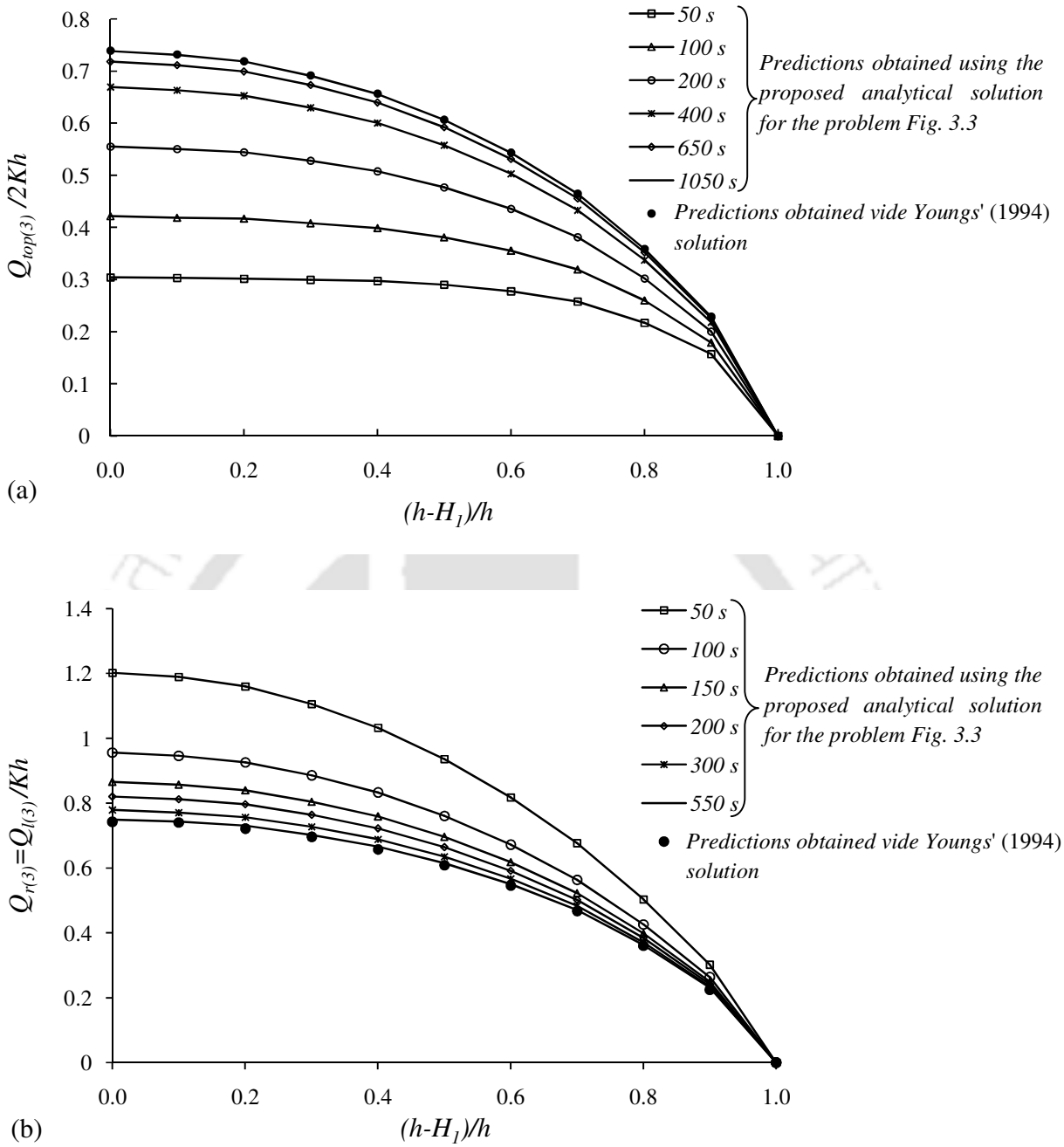

Fig. 3.7. Comparison of $Q_{top(3)}/2Kh$ versus $(h-H_1)/h$ and $Q_{r(3)}=Q_{l(3)}/Kh$ versus $(h-H_1)/h$ profiles as obtained from the proposed solution of the flow problem of Fig. 3.3 at different times with the corresponding steady state profiles obtained from the analytical solution of Youngs' (1994) when the ponding depth is taken as zero and the other parameters of the flow problem are taken as $h=2\,\text{m}$, $S_s=0.001\,\text{m}^{-1}$, $K=K_x=K_y=0.5$ m/day and $S_{a(3)}=100$ m (theoretically infinite)

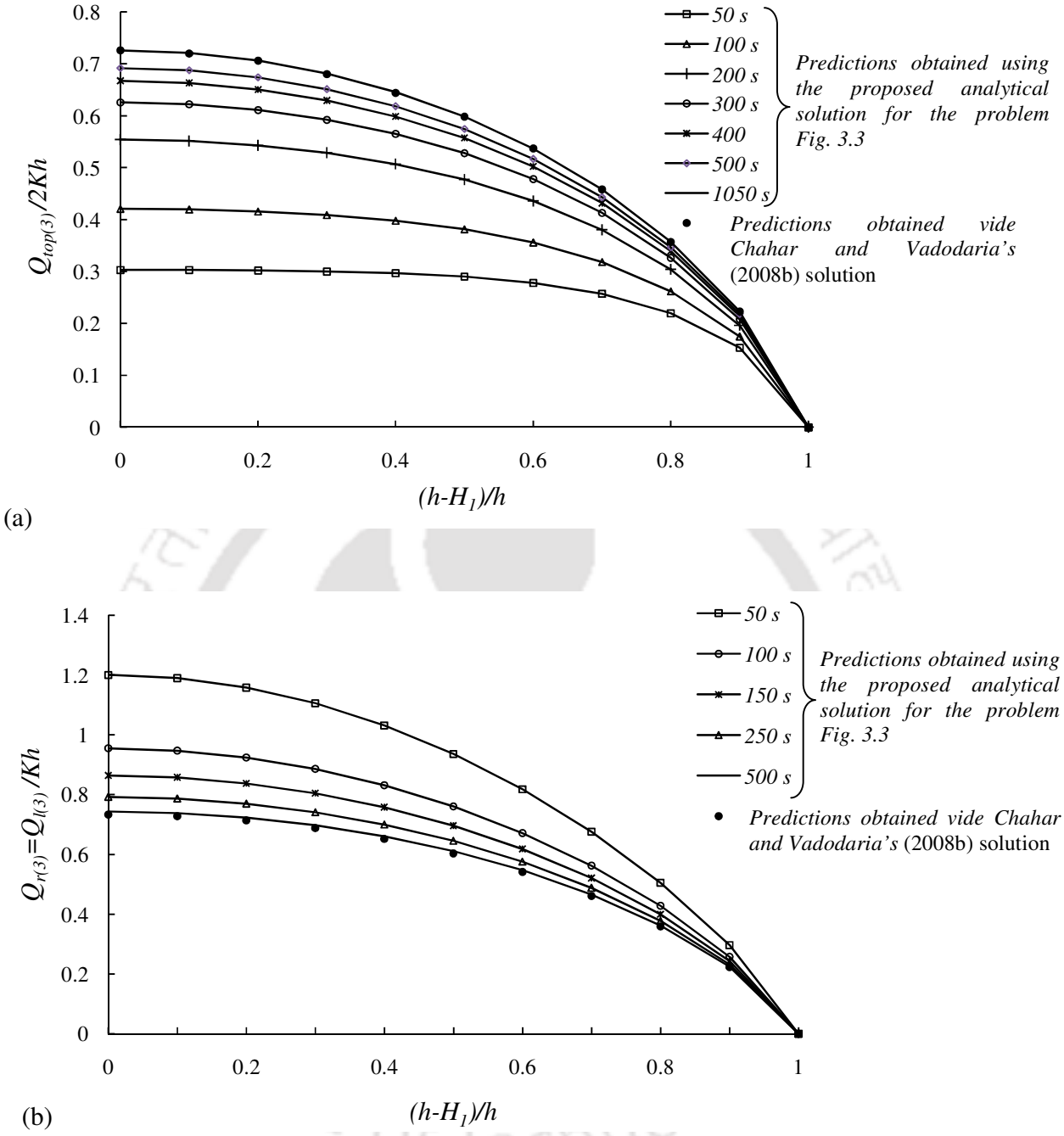

Fig. 3.8. Comparison of $Q_{top(3)}/2Kh$ versus $(h-H_1)/h$ and $Q_{r(3)}=Q_{l(3)}/Kh$ versus $(h-H_1)/h$ profiles as obtained from the proposed solution of the flow problem of Fig. 3.3 at different times with the corresponding steady state profiles obtained from the analytical solution of Chahar and Vadodaria (2008b) when the ponding depth is taken as zero and the other parameters of the flow problem are taken as $h=2$ m, $S_{a(3)}=6$ m ($S_{a(3)}/h=3$), $S_s=0.001$ m^{-1} and $K=K_x=K_y=0.5$ m/day

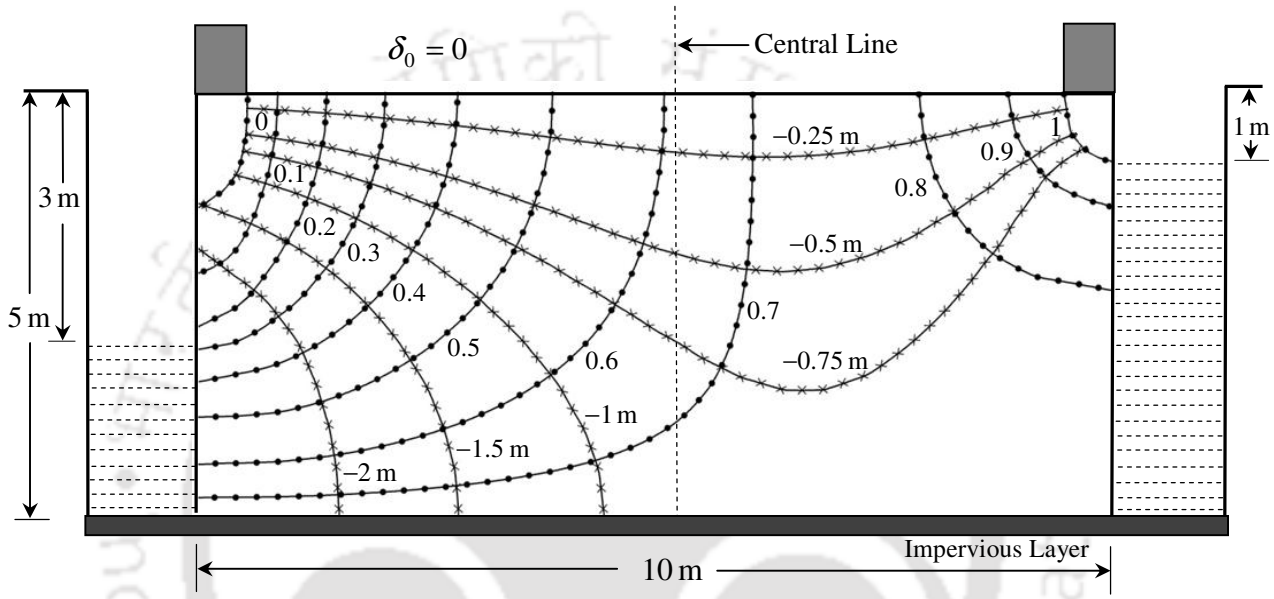

× *Steady state hydraulic head obtained vide Kirkham's (1965) solution*

● *Normalized streamlines obtained vide Kirkham's (1965) solution*

—— *Steady state hydraulic head obtained using the proposed solution for the problem Fig. 3.2*

—— *Steady state normalized streamlines obtained using the proposed solution for the problem Fig. 3.2*

* *Depth of ponding and height of the ditch bunds are not in scale; all other dimensions are in scale*

Fig. 3.9. Comparison of lines of equal hydraulic head and normalized streamlines as obtained from the proposed steady state solution of the flow problem of Fig. 3.2 with corresponding values obtained from the analytical solution of Kirkham (1965) for an isotropic soil when the flow parameters of Fig. 3.2 are taken as $h = 5$ m, $H_1 = 3$ m, $H_3 = 1$ m, $\varepsilon_a = 0.5$ m, $S_s = 0.001$ m^{-1} and $\delta_0 = 0$

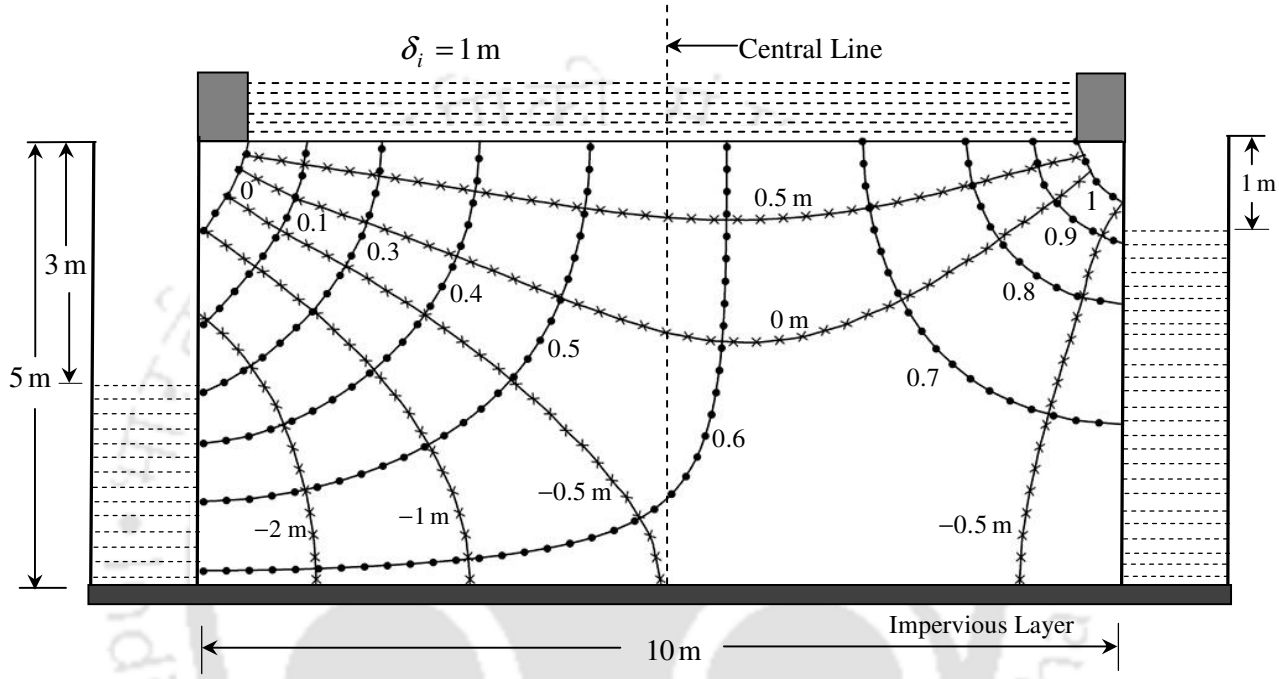

Fig. 3.10. Comparison of lines of equal hydraulic head and normalised streamlines as obtained from the proposed steady state solution of the flow problem of Fig. 3.3 with corresponding values obtained from the analytical solution of Kirkham (1965) for an isotropic soil when the flow parameters of Fig. 3.3 are taken as $h = 5$ m, $H_1 = 3$ m, $H_3 = 1$ m, $\varepsilon_a = 0.5$ m, $S_s = 0.001$ m^{-1} and $\delta_i = 1$ m

hydraulic heads and streamlines as obtained from Kirkham's (1965) steady state analytical solution of the fully penetrating ditch drainage problem, thereby providing us with an check on the truthfulness of our developed solutions for the flow situations of Figs. 3.2 and 3.3, respectively.

3.5.2 Comparison with MODFLOW

As a further check on our analytical solution of the general ditch drainage problem of Fig. 3.3, we also carried out a MODFLOW comparison of the same using Processing Modflow (Chiang and Kinzelbach, 2001) for a particular flow configuration of the problem. An imaginary ponded soil column of surface area 15 m by 10 m and thickness 1 m up to the base of an impervious layer, the soil column on its right and left faces being flanked by two ditch drains extending all the way up to the impervious barrier, was simulated by drawing a grid network of 150 rows, 102 columns and 22 layers. Thus, the size of each grid network used for modeling was 0.1 m$\times$ 0.1 m and the thickness of each grid cell 0.05 m, where it should be noted that two columns were kept aside to represent the left and the right ditches and two layers were also kept reserved to simulate the top soil surface and the bottom impervious layer, respectively. To mimic the ditch banks, the cells of the 2nd and 101th columns in the 1st layer were made inactive in the model for all the rows. The top layer, excluding the cells related to the ditch banks, were assigned a constant cell value of 0.2 m to simulate a uniform ponding depth of 0.2 m over the surface of the soil. The bottom impervious layer was modeled by making all the cells of the 22nd layer ineffective. To simulate a half-filled left ditch having a water level of 0.5 m, constant valued cells were utilized in the first column of the grid network and assigned a value of -0.05 m in the 2nd layer, -0.1 m in the 3rd layer and so on up to the 11th layer, after which a constant value of -0.5 m was assigned to all the cells up to the 21st layer. In the same way, the right ditch having a water level height of 0.75 m was also modeled. The cells belonging to the first and the last rows in all the layers starting from the 2nd and up to the 21st were given a constant value of 0.2 m to simulate the Northern and Southern faces of the model. With the above model structure in place and taking $S_s = 0.001\,\mathrm{m}^{-1}$, a transient MODFLOW simulation was carried out for the considered flow situation for an isotropic soil of hydraulic conductivity 1 m/day and the numerically predicted hydraulic heads at a few time steps compared with

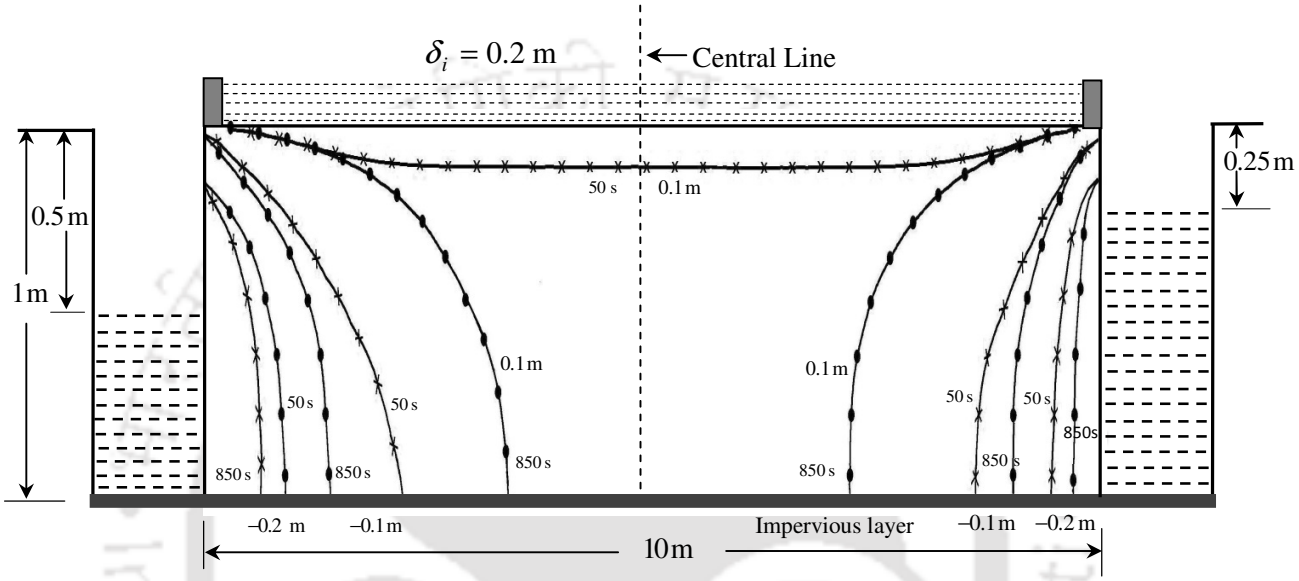

Fig. 3.11. Comparison of hydraulic head contours as obtained from the proposed solution of the flow problem of Fig. 3.3 for a flow situation as shown with the corresponding MODFLOW generated contours at a few time intervals when $\varepsilon_a = 0.1\,\text{m}$ and the soil parameters are taken as $S_s = 0.001\,\text{m}^{-1}$ and $K_x/K_y = 1/1$ $(K_x = 0.5\,\text{m/day}, K_y = 0.5$ m/day)

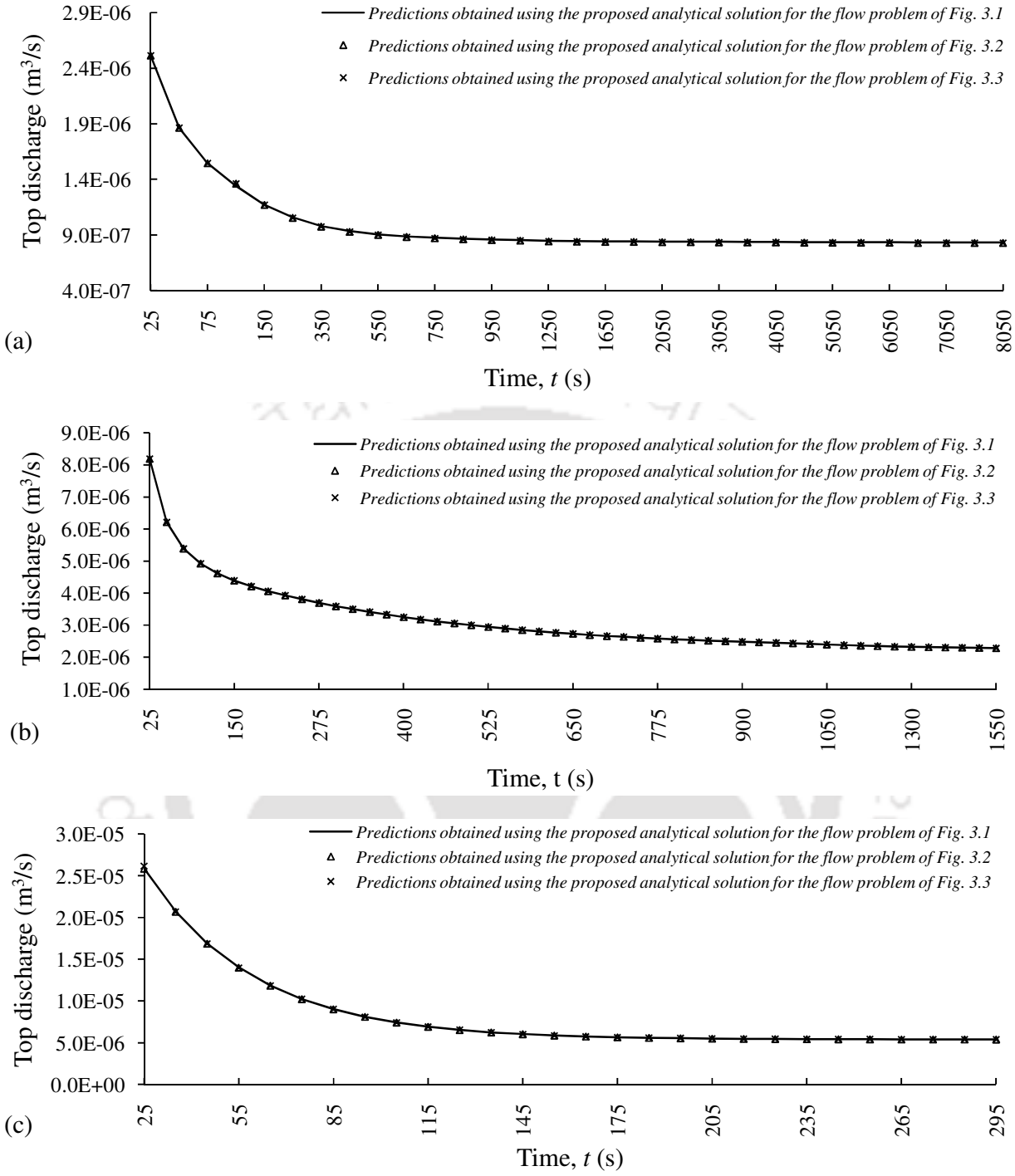

Fig. 3.12. Comparison of top discharge versus time profiles as obtained from the proposed solutions for the flow problems of Figs. 3.1, 3.2 and 3.3 when the flow parameters are taken as $h = 1\,\text{m}$, $H_1 = H_3 = 0.5\,\text{m}$, $S_{a(1)} = S_{a(2)} = S_{a(3)} = 10\,\text{m}$, $S_s = 0.001\ \text{m}^{-1}$, $\delta_0 = \delta_i = 0.2\ \text{m}$, $\varepsilon_a = 0.05\ \text{m}$ and (a) $K_x/K_y = 10/1$ ($K_x = 0.1$ m/day, $K_y = 0.01$ m/day), (b) $K_x/K_y = 1/1$ ($K_x = 0.1$ m/day, $K_y = 0.1$ m/day) and (c) $K_x/K_y = 1/10$ ($K_x = 0.1$ m/day, $K_y = 1\,\text{m/day}$)

their analytical counterparts. Fig. 3.11 shows such a comparison. It should be noted that all the numerical measurements were taken in the 75th row, halfway between the Northern and Southern boundaries of the model, so that the measuring locations were sufficiently away from these boundaries. For two-dimensional flow to prevail in the model, as is being assumed in the development of the analytical model, the distance between the Northern and Southern faces, ideally speaking, should be taken as infinity. However, it was observed that, for the considered flow situation, distance between these faces as low as 10 m was sufficient enough to induce a close approximation of two-dimensional flow in the measuring zone located midway between the faces. As can be seen in Fig. 3.11, the numerically obtained hydraulic heads at all the chosen time steps for the considered flow situation are found to be matching accurately with the corresponding analytical values obtained from our analytical solution for the flow problem of Fig. 3.3, thereby showing that our model predictions are comparing favorably with identical results being generated by MODFLOW.

As mentioned before, the flow problems of Figs. 3.1 and 3.2 can be treated as special cases of the flow problem of Fig. 3.3 and hence, the analytical predictions from this general solution should match with the corresponding values obtained from the other two solutions. To test the veracity of it, a comparison of discharges is carried out from the three analytical models for a few ponded drainage scenarios, as shown in Fig. 3.12. As can be seen, for all the considered flow situations, the discharge versus time curves obtained from all the three analytical models corresponding to the flow situations of Figs. 3.1, 3.2 and 3.3, respectively, are matching accurately with each other. This can also be treated as a validation of the analytical models corresponding to Figs. 3.1 and 3.2, since we have already established the correctness of our general solution of the flow problem of Fig. 3.3 by comparing it with other analytical models for a few simpler situations and also by comparing with time dependent MODFLOW generated outputs corresponding to a ponded drainage situation.

3. 6 Discussions

From Figs. 3.4, 3.5 and 3.6, we see that the time required for a ditch drainage ponded system to go to steady state increases with the increase in depth of the ditch drains and this trend is more pronounced for ditches dug in soils having a high anisotropy ratio and specific storage. The fact that the anisotropy ratio of most sediment deposits is greater than one and that this

value can be as high as 100 (Maasland, 1956; Kruseman and Ridder, 1994; Bair and Lahm, 1996, Schafer, 1996; Zlotnik, 1997 – to name a few) show that anisotropy is an important factor and must be considered while analyzing a ponded ditch drainage system. Further, apart from the anisotropy ratio and specific storage of a soil, the duration of transient state of a ponded ditch drainage situation is also found to be quite sensitive to the absolute values of the directional conductivities of the soil. For example, if the hydraulic conductivity of the isotropic soil for the flow situation corresponding to Fig. 3.5(b) is changed from 0.5 m/day to 0.0254 m/day (1 inch per day, say, glencoe silty soil – see Kirkham, 1949), keeping the other flow parameters same as before, the time required for the top discharge to go to steady state for the $h = H_1 = 3.0\,\text{m}$ scenario will then be about 60,000 seconds [Fig. 3.6(b)], an approximate increase of about 17 times to that of the transient duration obtained when the conductivity is being taken as 0.5 m/day for the concerned flow situation [about 3500 seconds, Fig. 3.5(b)]. It should be noted that for many soils like dense clays, glacial tills and clayey paddy soils, the hydraulic conductivity may be quite low (<0.01 m/day and sometimes even lower than that, Van Hoorn and Van Alphen, 1994; see Table 1, MacDonald et al., 2012; Chen and Liu, 2002; Tabuchi, 2004). Further, since anisotropy of a soil is more of a common phenomenon rather than an exception and the existence of soils with high anisotropy ratios (40 or above, see Maasland, 1957; Schafer, 1996) are also quite common in nature, the time required for a transient ponded ditch drainage system to arrive at the steady state may be quite large for many field situations. Also, similar to Kirkham's (1965) findings, we can also clearly observe in Figs. 3.7 and 3.8 that flow to drains with shallow water is comparatively much quicker than that to drains having a high level of water in them.

Figs. 3.13(a) and 3.13(b) show that the discharges through the sides of a drain and through the top ponded surface in between two adjacent drains are greatly influenced by the anisotropy of the soil for the considered flow situations. For the flow situation of Fig. 3.13(a), the side discharge versus time profile shows a rapid fall at early times when the anisotropy ratio of the soil is taken as 25:1, but for the case when the soil is isotropic [Fig. 3.13(b)], side discharge can be seen not to be getting much affected with time. However, for the considered flow conditions, top discharge can be observed to be less sensitive to time at

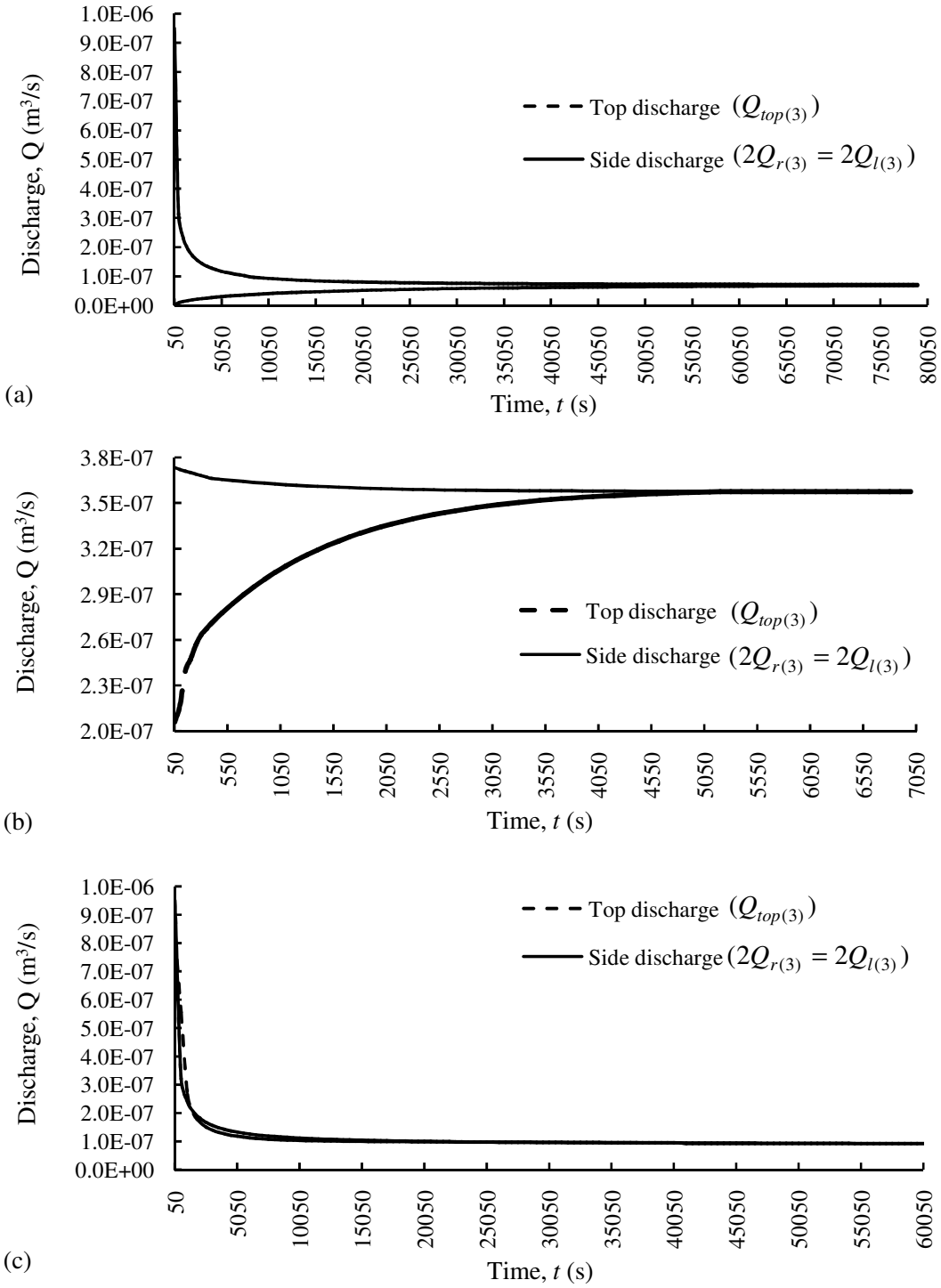

Fig. 3.13. Variation of top and side discharges with time when the flow parameters of Fig. 3.3 are taken as $h = 1$ m, $H_1 = H_3 = 0.5$ m, $S_{a(3)} = 30$ m, $S_s = 0.001$ m^{-1}, $\varepsilon_a = 0.05$ m and (a) $K_x/K_y = 25/1$ ($K_x = 0.0254$ m/day, $K_y = 0.00102$ m/day), $\delta_i = 0$ m, (b) $K_x/K_y = 1/1$ ($K_x = 0.0254$ m/day, $K_y = 0.0254$ m/day), $\delta_i = 0$ m and (c) $K_x/K_y = 25/1$ ($K_x = 0.0254$ m/day, $K_y = 0.00102$ m/day), $\delta_i = 0.1$ m

the early stages of simulation when the anisotropy ratio of the soil is 25:1 than that corresponding to the case when the soil is isotropic. The discharge coming from the top of the field is also found to be quite sensitive to the depth of ponded water over the soil surface; for the flow situations considered in Figs. 3.13(a) and 3.13(b), when the surface of the soil is being subjected to a negligible depth of ponding, top discharge can be seen to be increasing with time, but for the flow situation of Fig. 3.13(c), where the soil surface is being ponded with a uniform water depth of 0.1 m, top discharge can now be observed to be following a reverse trend and decreases with the increase in time. From Fig. 3.13(a), we also observe that the discharge per unit length of a drain at an early time is substantially higher than that corresponding to the state when steady state of the system is being reached. For example, for this flow configuration, the discharge per unit length at the end of 50 seconds is around 0.08209 m^3/day but the equivalent steady state value is only 0.01024 m^3/day. It should be noted that, for the same flow situation, the corresponding figures for $K_x = 0.5$ m/day and $K_x / K_y = 25$ are working out to be 0.40549 m^3/day and 0.12169 m^3/day, respectively. Thus, the steady state drain discharge corresponding to a ponded ditch drainage situation may vary substantially from that of the discharge value at an early time, particularly for situations when the drains are being laid in soils having a high anisotropy ratio. This is an advantage as the available steady state ponded ditch drainage theories (Chahar and Vadodaria, 2008; Kirkham, 1965; Barua and Tiwari, 1995) cannot be used to estimate discharge to a ponded drainage system in the transition zone. The volume of water which has seeped through the surface of the soil for the flow situation of Fig. 3.13(c) in a desired time interval can be determined using Eq. (3.125); for this flow situation, we find the volume for the first 1 hour as 0.00081 m^3 and for the first 5 hours as 0.00256 m^3. If the ponded water is not being maintained constant and allowed to fall, these volumes then can also be used to estimate the upper limits of fall of water during the desired durations. Thus, at the end of the first 1 hour, the upper limit of fall of water level will be about 0.027 mm $(0.00081 \times 1000/30)$ and the corresponding value at the end of first 5 hours will be about 0.085 mm $(0.00256 \times 1000/30)$. These fall of water levels are called as upper limits since they have been calculated based on volumes which have been obtained by assuming that the ponding depth of 0.1 m over the soil surface to be unchanged during the time of simulation;

in reality however, the fall of these water levels would be less than those estimated with the assumption of a constant water ponding depth of 0.1 m owing to the decrease of ponding water level with time. If we perform the same exercise by taking the horizontal hydraulic conductivity of the flow situation of Fig. 3.13(c) as 0.5 m/day, instead of the earlier figure of 0.0254 m/day, and keep the other flow parameters same as before, the volumes of water entering through the surface of the soil at the end of the first 1 and 5 hours will then be 0.00869 m^3 and 0.03984 m^3, respectively, and the consequent upper limits of fall of the surface water level during these periods be 0.2897 mm and 1.328 mm, respectively.

It is interesting to see from the flow situations of Fig. 3.14 that the surface discharge distribution at a very early time is almost uniform and this uniformity can be seen to be getting progressively distorted with the increase of time. Further, from these flow situations we also observe that the high anisotropy ratio of 10:1 is favoring a more uniform distribution of discharge over the soil surface as compared to situations where the soil is isotropic or having a low anisotropy ratio of 1:10. Thus, the nature of anisotropy of a soil alone will have a significant influence on the leaching efficiency of a ponded ditch drainage system in cleaning a salt affected soil; among other factors remaining the same, a high anisotropy ratio of the soil will lead to a relatively better cleaning of the soil profile as compared to the situation where the anisotropy ratio of the soil is low. Since the water transmitting capacity of most of the natural deposits along the bedding plane is generally higher than that perpendicular to the planes (Maasland, 1957; Schafer 1996), the inherent orientation of directional conductivities in soils, in general, assists the cleaning process of a salt affected soil when the desalinization is being brought about by flooding the soil surface with good quality water and then collecting and disposing the salt laden leached water with the help of a series of ditch drains installed for the purpose. Further, from Fig. 3.15(a), we see that if the depth of ponding is maintained uniform over a ponded surface being drained by an array of equally spaced ditch drains, then at the steady state, most of the flows are getting confined within a short distance from the vertical faces of the ditches. This is in line with the observations of Kirkham (1950, 1965), Youngs (1994), Barua and Tiwari (1995), Chahar and Vadodaria (2008) and others who also observed that steady seepage to a ditch drain from a ponded field is mostly limited to a short distance from centre of the ditches.

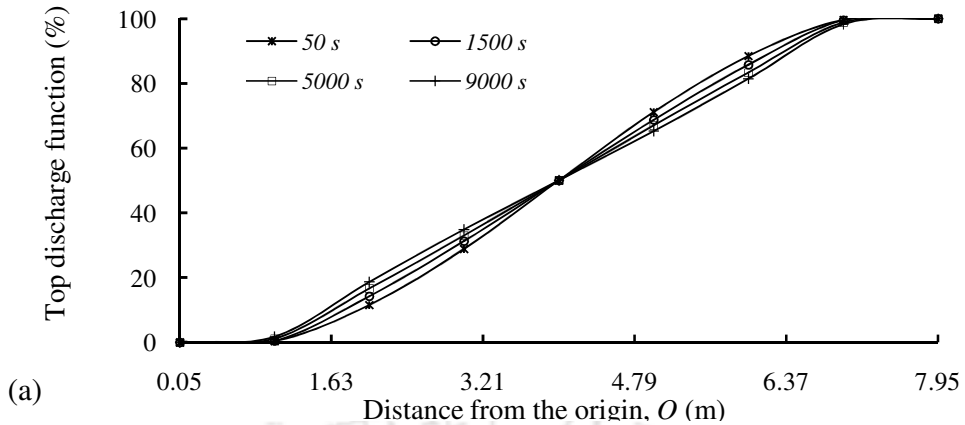

(a)

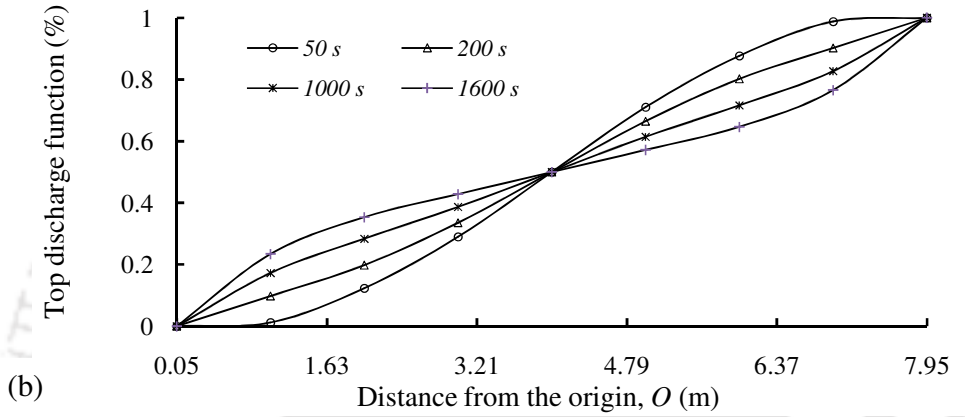

(b)

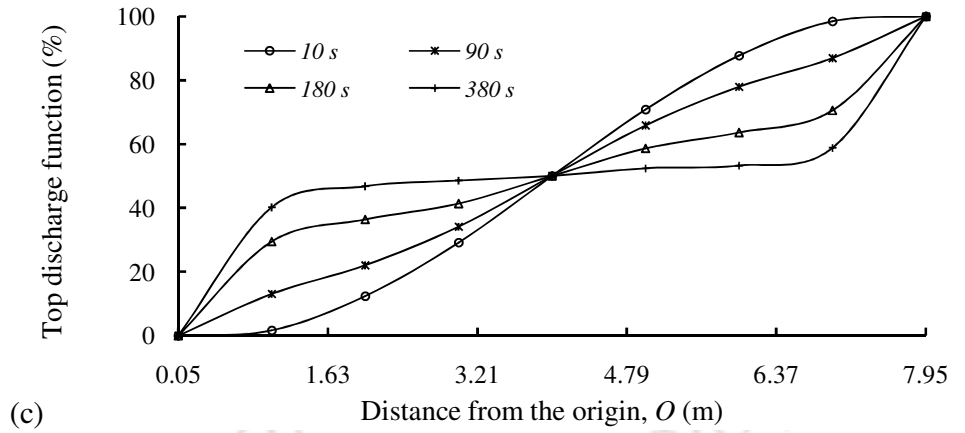

(c)

Fig. 3.14. Variation of top discharge function with distance as measured from the origin O at different times when the flow parameters of Fig. 3.3 are taken as $h = 1\,\text{m}$, $H_1 = 0.5\,\text{m}$, $H_3 = 0.5\,\text{m}$, $\delta_1 = \delta_9 = 0\,\text{m}$, $\delta_2 = \delta_8 = 0.22\,\text{m}$, $\delta_3 = \delta_7 = 0.35\,\text{m}$, $\delta_4 = \delta_6 = 0.4\,\text{m}$, $\delta_5 = 0.45\,\text{m}$, $S_{va1} = 1\,\text{m}$, $S_{va2} = 2\,\text{m}$, $S_{va3} = 3\,\text{m}$, $S_{va4} = 3.5\,\text{m}$, $S_{va5} = 4.5\,\text{m}$, $S_{va6} = 5\,\text{m}$, $S_{va7} = 6\,\text{m}$, $S_{va8} = 7\,\text{m}$, $S_{a(3)} = 8\,\text{m}$, $S_s = 0.001\,\text{m}^{-1}$, $\varepsilon_a = 0.05\,\text{m}$ and (a) $K_x/K_y = 10/1$ ($K_x = 0.1\,\text{m/day}$, $K_y = 0.01\,\text{m/day}$), (b) $K_x/K_y = 1/1$ ($K_x = 0.1$ m/day, $K_y = 0.1$ m/day) and (c) $K_x/K_y = 1/10$ ($K_x = 0.1$ m/day, $K_y = 1$ m/day)

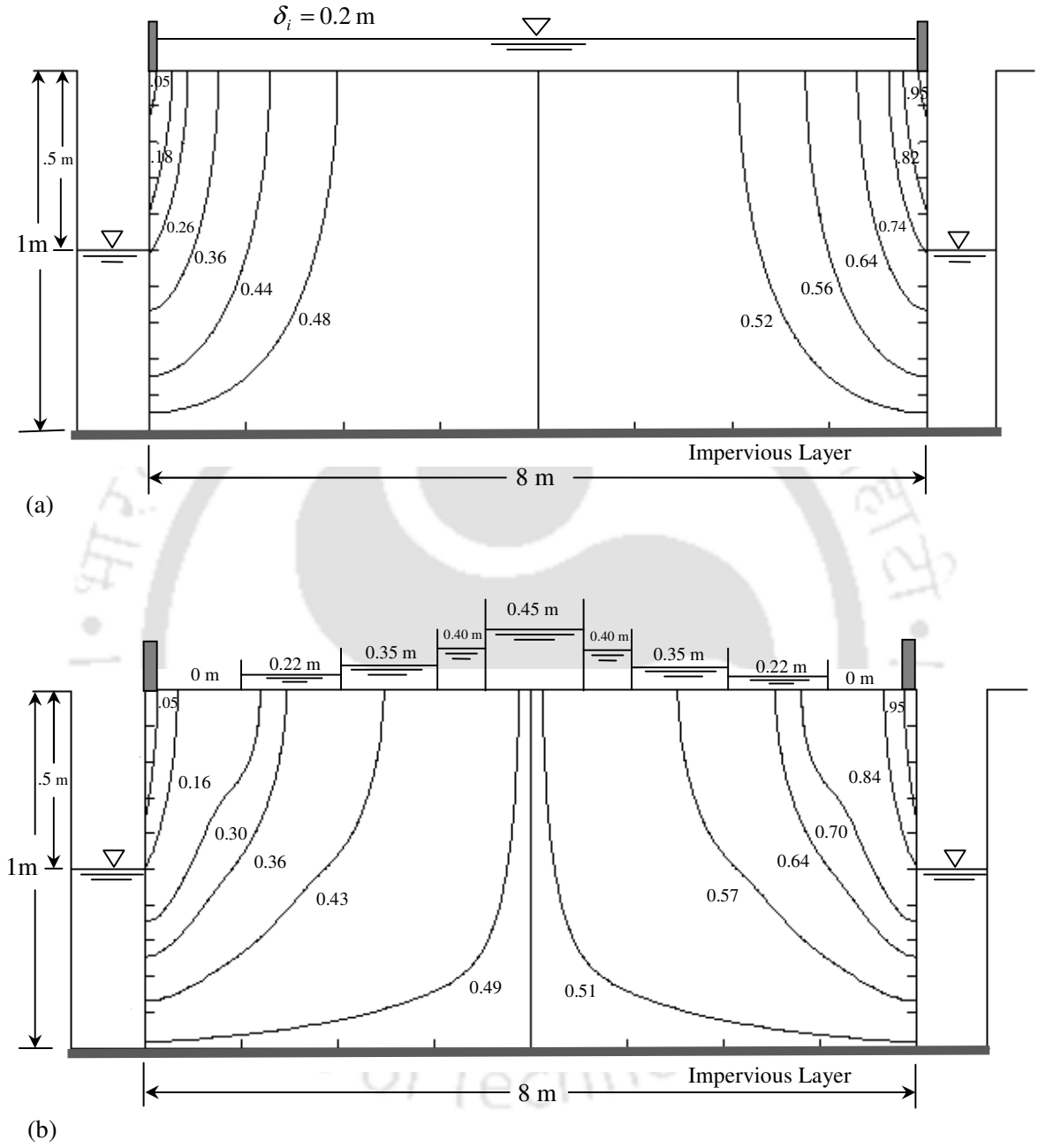

* *Depths of ponding and heights of the ditch bunds are not in scale; all other dimensions are in scale*

Fig. 3.15. Steady state normalized streamlines corresponding to the flow situation of Fig. 3.14(b) when (a) $\delta_i = 0.2$ m and (b) δ_i and S_{vai} are as considered in Fig. 3.14(b).

The uniform distribution of discharge at the surface of the soil at early times as well as during the steady state situation and consequently a uniform distribution of the streamlines in the flow profile, can also be artificially brought about by subjecting the surface of the soil to a variable ponding field. Fig. 3.14 depicts the surface discharge distribution at a few time steps corresponding to a flow geometry of Fig. 3.3 for three different anisotropy ratios of the soil, where, as may be observed, the surface of the soil is subjected to a variable depth of ponding. Fig. 3.15 shows the distribution of the streamlines corresponding to the isotropic flow situation of Fig. 3.14 [i.e., Fig. 3.14(b)] at the steady state and also the steady state orientation of the streamlines should the flow geometry of Fig. 3.15 be subjected to a uniform depth of ponding of magnitude 0.2 m. From Fig. 3.14(b) and 3.15(b), it is apparent that the imposition of a variable ponding field on the soil surface of the nature as mentioned in Fig. 3.14 and shown in Fig. 3.15(b) for the considered flow geometry, has now resulted in a relatively more uniform distribution of discharge at the surface of the soil at all times as compared to a situation when the soil surface is being flooded with only a uniform depth of ponding [Fig. 3.15(a)]. For the flow situation of Fig. 3.15(a), the steady state discharge per unit length of the ditch drains is working out to be 0.2067 m^3/day but, as can be seen, most of this flow is getting concentrated to a narrow zone lying on either side of a ditch, with the 0.49 normalized streamline lying at a distance of only 2.37 m at the surface of the soil from the vertical face of a ditch. For the ponded drainage situation of Fig. 3.15(b), however, where the flow situation considered in Fig. 3.15(a) is now subjected to a variable depth of ponding of the type as shown instead of a uniform depth of ponding of 0.2 m over the surface of the soil, we find the steady discharge to be then 0.1253 m^3/day, a value actually less than that corresponding to the uniform ponding situation of Fig. 3.15(a). But, in this case, as may be observed, the flow is getting more evenly distributed in the entire domain with the 0.49 normalized streamline now being pushed to a surface distance of about 3.90 m on either side of the vertical faces of a ditch. It is to be noted that, in order to provide a non-uniform ponding field over the soil surface, construction of suitable inner bunds at appropriate distances from the ditch faces are required to be done and proper depths of water in between these bunds need be provided.

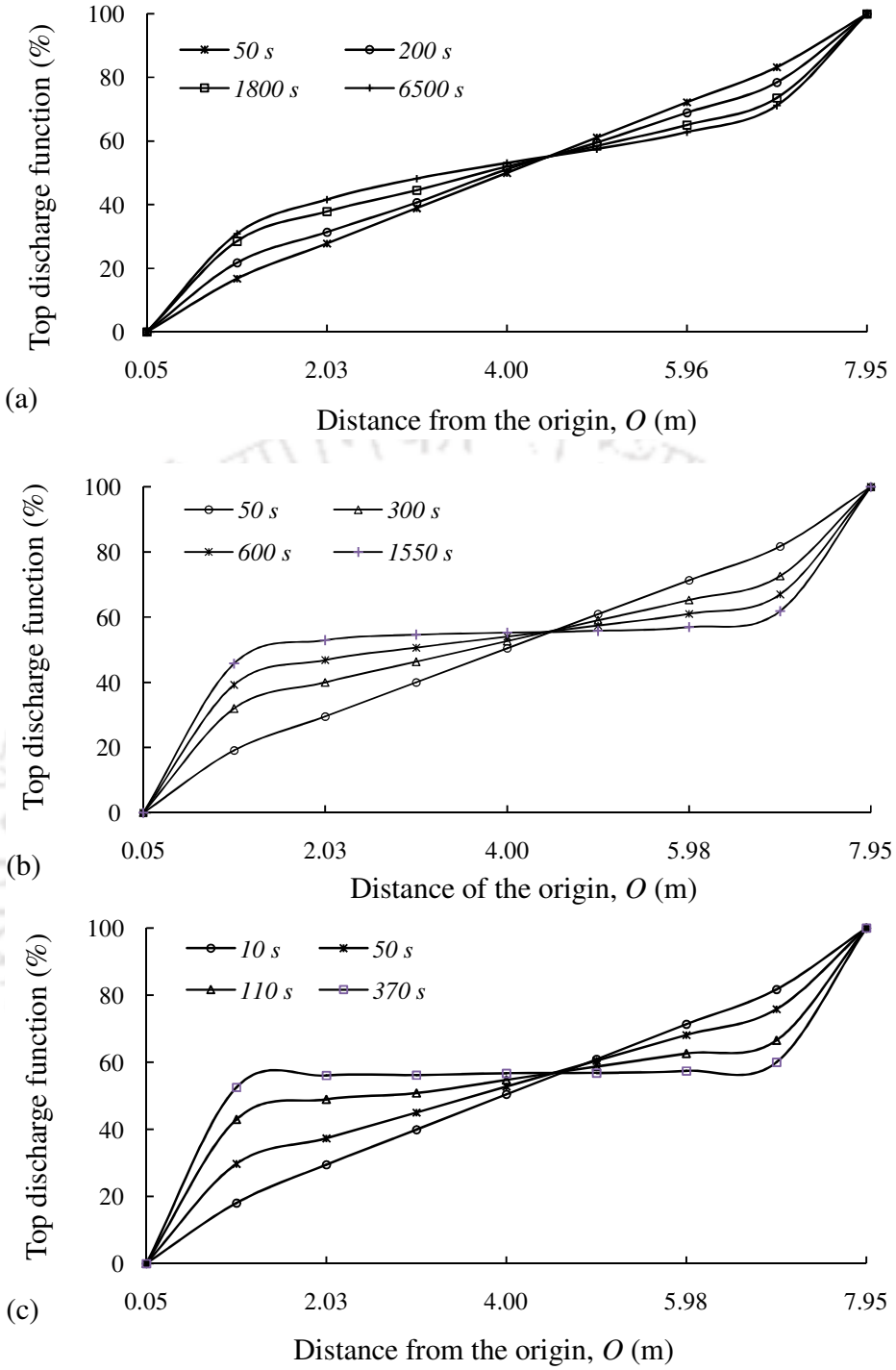

Fig. 3.16. Variation of top discharge function with distance as measured from the origin O at different times when the flow parameters of Fig. 3.3 are taken as $h = 1$ m, $H_1 = 0.5$ m, $H_3 = 0.25$ m, $\delta_i = 0.2$ m, $S_{a(3)} = 8$ m, $S_s = 0.001\,\text{m}^{-1}$, $\varepsilon_a = 0.05$ m and (a) $K_x/K_y = 10/1$ ($K_x = 0.1$ m/day, $K_y = 0.01$ m/day), (b) $K_x/K_y = 1/1$ ($K_x = 0.1$ m/day, $K_y = 0.1$ m/day) and (c) $K_x/K_y = 1/10$ ($K_x = 0.1$ m/day, $K_y = 1$ m/day)

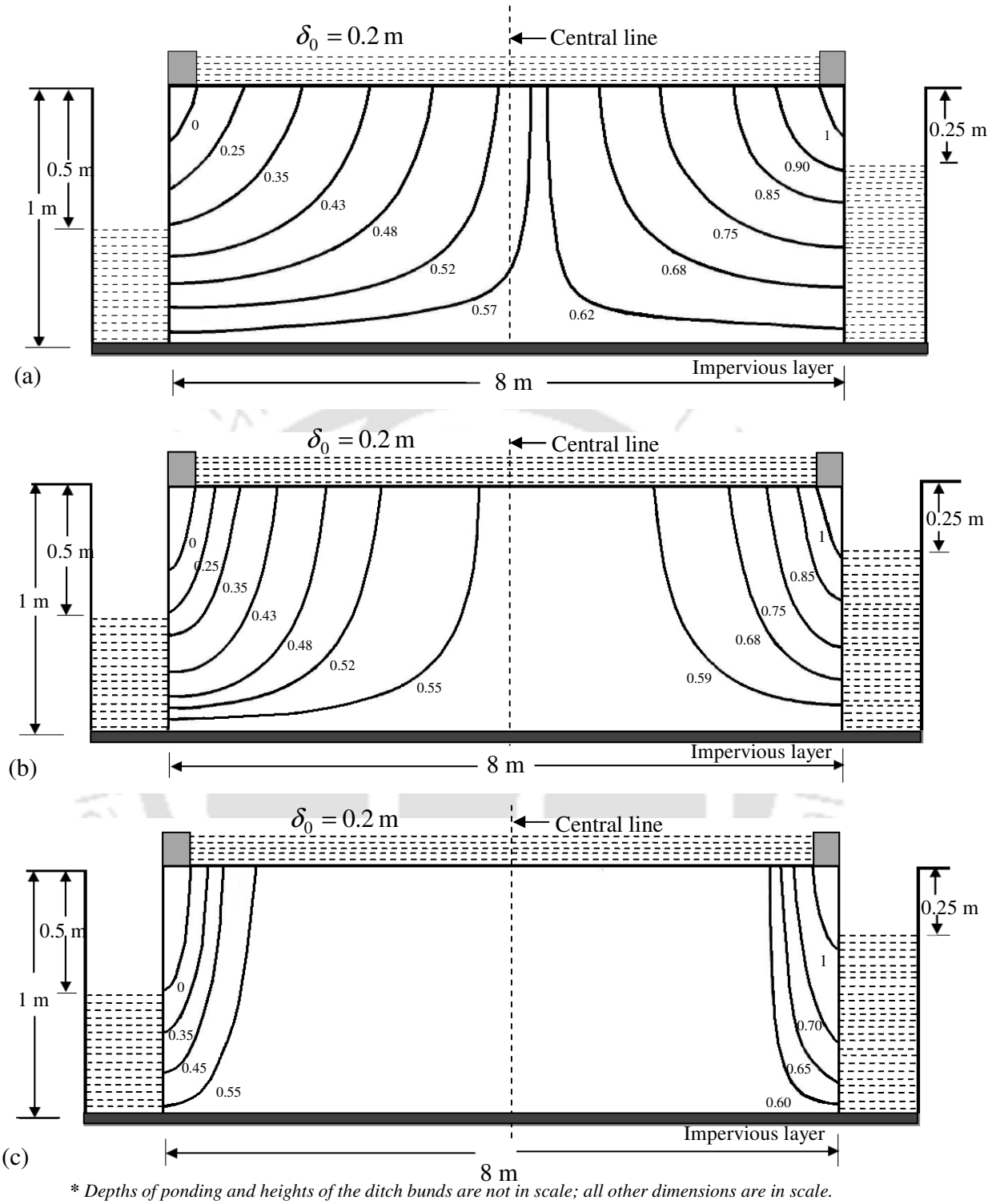

** Depths of ponding and heights of the ditch bunds are not in scale; all other dimensions are in scale.*

Fig. 3.17. Steady state normalized streamlines corresponding to the flow situation of Fig. 3.16 when (a) $K_x/K_y = 10/1$ ($K_x = 0.1$ m/day, $K_y = 0.01$ m/day), (b) $K_x/K_y = 1/1$ ($K_x = 0.1$ m/day, $K_y = 0.1$ m/day) and (c) $K_x/K_y = 1/10$ ($K_x = 0.1$ m/day, $K_y = 1$ m/day)

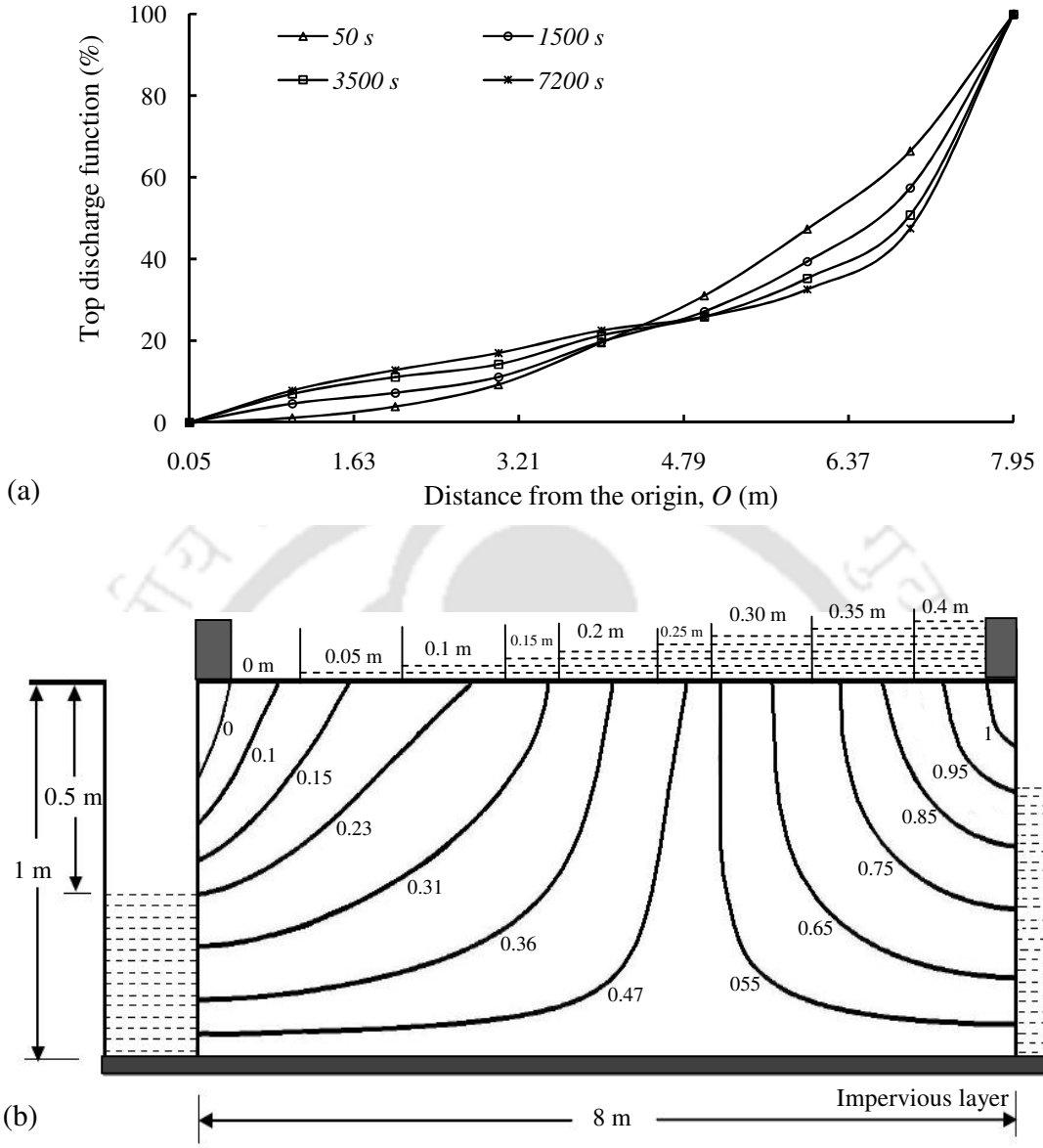

* *Depths of ponding and heights of the ditch bunds are not in scale; all other dimensions are in scale.*

Fig. 3.18. (a) Variation of top discharge function with distance as measured from the origin O at different times when the flow parameters of Fig. 3.3 are taken as $h = 1\,\text{m}$, $H_1 = 0.5\,\text{m}$, $H_3 = 0.25\,\text{m}$, $\delta_1 = 0\,\text{m}$, $\delta_2 = 0.05\,\text{m}$, $\delta_3 = 0.1\,\text{m}$, $\delta_4 = 0.15\,\text{m}$, $\delta_5 = 0.2\,\text{m}$, $\delta_6 = 0.25\,\text{m}$, $\delta_7 = 0.3\,\text{m}$, $\delta_8 = 0.35\,\text{m}$, $\delta_9 = 0.4\,\text{m}$, $S_{va1} = 1\,\text{m}$, $S_{va2} = 2\,\text{m}$, $S_{va3} = 3\,\text{m}$, $S_{va4} = 3.5\,\text{m}$, $S_{va5} = 4.5\,\text{m}$, $S_{va6} = 5\,\text{m}$, $S_{va7} = 6\,\text{m}$, $S_{va8} = 7\,\text{m}$, $S_{a(3)} = 8\,\text{m}$, $S_s = 0.001\,\text{m}^{-1}$, $\varepsilon_a = 0.05\,\text{m}$ (b) Steady state normalized streamlines corresponding to the situation depicted in (a)

Fig. 3.16 is a similar graphical representation of the top discharge distribution function corresponding to a few flow scenarios of Figs. 3.3 when the levels of water in the left and right ditches are kept not the same but are given different values; as can be seen, the left ditch is running with a shallower water level as compared to the right ditch. This, expectedly, has resulted in more water going to the left ditches as compared to the right ones with the groundwater divide shifting towards the right ditch for all the considered flow situations. A similar observation was also made by Kirkham (1965) while analyzing steady seepage of water into equally spaced ditch drains with unequal water level heights, the water to the ditches being originating from a ponded field of zero or uniform depth of ponding. Thus, it is clear that by just adjusting the levels of water in between adjacent ditches, the position of the groundwater divide zone and the fraction of the total flow through the ditches, can be regulated. Further, a still greater control on the water movement to the ditches can be brought about by suitably altering both the ponding depth pyramid over the surface of the soil and the water level heights in between the adjacent ditches, as can be seen in the flow situation as shown in Fig. 3.18.

3. 6 Conclusions

Equations of the hydraulic head functions, and from them expressions for top and side discharges per unit length of a ditch, have been derived for transient groundwater seeping into an array of equally spaced infinitely long parallel ditch drains dug in a homogeneous and anisotropic soil medium receiving water from a ponded field of infinite horizontal extent when (i) the levels of water in the adjacent ditches are equal and the ponding depth over the surface of the soil is uniform, (ii) the levels of water in the adjacent ditches are unequal and the ponding depth over the surface of the soil is uniform and (iii) the levels of water in the adjacent ditches are unequal and the ponding depth over the surface of the soil is non-uniform. In all these problems, the soil has been assumed to be underlain by an impervious barrier and all the drains have been assumed to penetrate all the way up to this barrier. The assumption of an infinitely spread horizontal ponded field along with the assumption of a series of infinitely long parallel trenches collecting seeping water from it, have reduced essentially all the three problems considered for study from a three-dimensional platform to a two-dimensional one. The separation of variable method in conjunction with a judicious

mix of single and double Fourier series – single Fourier series have been utilized to handle the boundary conditions and the double Fourier series has been used to tackle the initial condition of the problem – have been utilized to solve all the three transient boundary value problem. By extending the time variable to go to infinity in the expressions for the hydraulic head, top and side discharges, the corresponding steady state expressions for these quantities have also been evaluated. Using hydraulic head functions thus obtained for the steady state, expressions for the corresponding steady state stream functions have also been worked out. For providing clarity of presentation, the stream functions thus determined have been further normalized for the purpose of plotting. The validity of the developed solutions have been tested by comparing the predictions obtained from the reduced steady state solutions of the problems for a few cases with corresponding predictions obtained from the analytical works of others. A numerical check on the general analytical model for the variable ponding situation has also been carried out for using MODFLOW.

The study shows that the time required for a transient ditch drainage system to go to steady state is dependent on the anisotropy ratio as well as on the absolute values of the directional conductivities of a soil on which the drains are being installed. Further, the depth of the ditch drains and specific storage of a soil mass also affect this time in a substantial way – deeper drains in soils with a high specific storage have a tendency to delay this time whereas shallower ditches in soils with a low specific storage have an inclination to accelerate it being instantaneous when the storage coefficient is zero for an incompressible soil. The general solution provided herein to the ponded ditch drainage problem is a versatile one in the sense that it can account for transient seepage of water into a drainage network from a ponded surface, unequal water level heights in the adjoining trenches and also a non-uniform distribution of ponded water on the surface of the soil. In fact, even for a steady state situation, the authors have not come across any analytical model of the ditch drainage ponded where a variable depth of ponding at the soil surface has been accommodated. It is seen from the study that, by suitably altering the ponding field over the surface of the soil, a substantial improvement on the uniformity of the top discharge as well as uniformity on the steady state streamline distribution on the flow domain can be achieved. Thus, the generalized analytical model given here presents an opportunity to design drainage networks

which may be employed for a better cleaning of a salt affected soil. Further, by playing with both the levels of water in the ditches and the distribution of the ponded pyramid over the surface of the soil, a still better control on the cleaning process in the form of precision cleaning in any desired location of the soil domain may be carried out. If a ditch drainage network is being dug in a ponded waterlogged area with the intention of draining the area, the analytical solutions proposed here can also be utilized to estimate the upper limit of fall of ponded water level in a specified time, providing the directional conductivities of the soil and other design flow parameters of the drainage system are known. Thus, the solutions provided here can also be used for designing efficient ditch drainage networks for reclaiming a waterlogged soil.

3.7 List of Notations

The following notations are used in this chapter

$A_{mn(1)}$, $A_{mn(2)}$, $A_{mn(3)}$, $C_{p(1)}$, $C_{p(2)}$, $C_{p(3)}$, $B_{q(2)}$, $B_{q(3)}$, $D_{r(3)}$ = constants with $m = 1,2,3,\ldots$, $n = 1,2,3,\ldots$, $p = 1,2,3,\ldots$, $q = 1,2,3,\ldots$, $r = 1,2,3,\ldots$

h = depth of the ditch drains as measured from surface of the soil for the flow problems as shown in Figs. 3.1, 3.2 and 3.3, respectively [L];

H_1 = depth of water in the left trench as measured from the surface of the soil for the flow problems as shown in Figs. 3.1, 3.2 and 3.3, respectively [L];

H_3 = depth of water in the right trench as measured from the surface of the soil for the flow problems as shown in Figs. 3.1, 3.2 and 3.3, respectively [L];

$K = \sqrt{K_x K_y}$ = equivalent hydraulic of soil [LT^{-1}];

$(K^a)^2 = K_x / K_y$ = anisotropy ratio of soil (dimensionless);

K_x = horizontal hydraulic conductivity of soil [LT^{-1}];

K_y = vertical hydraulic conductivity of soil [LT^{-1}];

$(K_1) = (S_s / K_y)^{1/2}$ [$T^{1/2}\ L^{-1}$];

M, N, P, Q, R = integers which can take values values 1, 2, 3, …;

N_0 = number of divisions of the ponding surface at the top of the soil;

Q_{shalf} = discharge per unit length through the face *OA* of Fig. 3.1 [$L^3T^{-1}L^{-1}$];

Q_{side} = total discharge per unit length from both the sides of a ditch for the flow problem of Fig. 3.1 [$L^3T^{-1}L^{-1}$];

$Q_{l(2)}$, $Q_{l(3)}$ = discharge per unit length of the ditches through the face *OA* of Figs. 3.2 and 3.3, respectively [$L^3T^{-1}L^{-1}$];

$Q_{top(1)}$, $Q_{top(2)}$, $Q_{top(3)}$ = discharge per unit length of the ditches through the surface *GE* of Figs. 3.1, 3.2 and 3.3, respectively [$L^3T^{-1}L^{-1}$];

$Q_{topX(3)}$ = top discharge function defined on the surface *GE* of Fig. 3.3, [$L^3T^{-1}L^{-1}$];

$Q^f_{topX(3)}$ = top discharge function expressed as a percentage of $Q_{top(3)}$, dimensionless;

$Q^{(st)}_{side}$ = steady state total discharge per unit length from both the sides of a ditch for the flow problem of Fig. 3.1, [$L^3T^{-1}L^{-1}$];

$Q^{(st)}_{l(2)}$, $Q^{(st)}_{l(3)}$ = steady state discharge per unit length of the ditches through face *OA* of Figs. 3.1, 3.2 and 3.3, respectively [$L^3T^{-1}L^{-1}$];

$Q^{(st)}_{r(2)}$, $Q^{(st)}_{r(3)}$ = steady state discharge per unit length of the ditches through face *CD* of Figs. 3.1, 3.2 and 3.3, respectively [$L^3T^{-1}L^{-1}$];

V_{stot} = volume of water seeping through the surface *GE* of Fig. 3.1 per unit length of the ditches in time *t*, [L^3L^{-1}];

$V_{top(1)}$, $V_{top(2)}$, $V_{top(3)}$ = volume of water seeping per unit length of the ditches through the surface *GE* of Figs. 3.1, 3.2 and 3.3, respectively [L^3L^{-1}];

$Q^{(st)}_{top(1)}$, $Q^{(st)}_{top(2)}$, $Q^{(st)}_{top(3)}$ = steady state discharge per unit length of the ditches through the surface *GE* of Figs. 3.1, 3.2 and 3.3, respectively [$L^3T^{-1}L^{-1}$];

$S_{h(1)}$ = semi-spacing between the adjacent ditches in the real plane of Fig. 3.1 [L];

S_h = semi-spacing between the adjacent ditches in the computational plane of Fig. 3.1 [L];

$S_{a(1)}$, $S_{a(2)}$, $S_{a(3)}$ = distance between the adjacent drains in the real plane for the flow problems as shown in Figs. 3.1, 3.2 and 3.3, respectively [L];

S_{vai} = distance of the i^{th} $(1 \le i \le N_0 - 1)$ inner bund from the origin O in the real plane for the flow problem of Fig. 3.3 [L];

$S_{vi} = S_{vai} / K^a$ = distance of the i^{th} $(1 \le i \le N_0 - 1)$ inner bund from the origin O in the computational plane for the flow problem of Fig. 3.3 [L];

S_s = specific storage of soil [L^{-1}];

t = time variable for the flow problems of Figs. 3.1, 3.2 and 3.3, respectively [T];

x = horizontal coordinate as measured from the origin O for the flow problems of Figs. 3.1, 3.2 and 3.3, respectively, in the real plane [L];

X = horizontal coordinate as measured from the origin O for the flow problems of Figs. 3.1, 3.2 and 3.3, respectively, in the computational plane [L];

y = vertical coordinate as measured from the origin O for the flow problems of Figs. 3.1, 3.2 and 3.3, respectively, in the real plane [L];

δ_0 = depth of ponding at the surface of the soil for the flow problems of Figs. 3.1 and 3.2, respectively [L];

δ_i = ponding depth at the i^{th} segment on the surface of the soil for the flow problem of Fig. 3.3 [L];

ε_a = width of the ditch banks in the real plane for the flow problems of Figs. 3.1, 3.2 and 3.3, respectively [L];

$\varepsilon = \varepsilon_a / K^a$ = width of the ditch banks in the computational plane for the flow problems of Figs. 3.1, 3.2 and 3.3, respectively [L];

$\phi_{(1)}, \phi_{(2)}, \phi_{(3)}$ = hydraulic head distribution corresponding the flow domains of Figs. 3.1, 3.2 and 3.3, respectively [L];

$\phi_{(1)}^{(st)}, \phi_{(2)}^{(st)}, \phi_{(3)}^{(st)}$ = steady state hydraulic head distribution corresponding the flow domains of Figs. 3.1, 3.2 and 3.3, respectively [L];

$\psi_{(1)}, \psi_{(2)}, \psi_{(3)}$ = steady state stream function corresponding the flow domains of Figs. 3.1, 3.2 and 3.3, respectively [L^2T^{-1}];

$\psi_{(1)}^{n}, \psi_{(2)}^{n}, \psi_{(3)}^{n}$ = steady state stream normalized function corresponding the flow domains of Figs. 3.1, 3.2 and 3.3, respectively [dimensionless]

CHAPTER 4

SUMMARY AND CONCLUSIONS

Subsurface drainage is provided in many humid areas of the world for reclaiming waterlogged soils and in restoring flooded areas in a desired frame of time. In the irrigated fields in semi-arid and arid areas, drainage is also extensively provided to maintain a proper salt balance in the root zones of plants. Drainage also helps in establishing a suitable air-water balance in soils. One of the methods of cleaning a salt affected soil is to subject the soil to a ponding field at the surface of the soil with the help of embankments so that water is forced though it and in the process wash away a part of the salt present in the soil profile, the salt rich water is then being drained by a series of ditch drains installed for the purpose. Thus, in order to have a better design of a subsurface ditch drainage network for cleaning a salt affected soil, it is essential that the underlying subsurface hydraulics of flow to the drains be thoroughly studied. Further, since subsurface drainage depends greatly on the direction dependent water transmitting capacities of a soil, it is crucial that these properties of soil be accurately estimated in the field. In this study, analytical models for predicting flow into fully and partially penetrating auger holes underlain by an impervious layer have been obtained for an unconfined aquifer of finite horizontal and vertical extents. These solutions have been developed with the intention that the horizontal and vertical saturated conductivities of a phreatic aquifer as well as the horizontal influence of an auger hole test be accurately estimated utilizing experimental data obtained from the test. Further, generalized analytical solutions of the transient ditch drainage problem have also been obtained both for the cases when the flow field over the surface of a ponded field is being subjected to a uniform as well as a variable depth of ponding. The basic objective of obtaining a general solution to the transient ditch drainage problem is to have a mathematical tool which can be utilized to provide better designs of subsurface ditch networks for cleaning salt affected soils as well as for reclaiming waterlogged areas. We now give below, in brief, the rundowns of each of our investigations.

4.1 Hydraulics of an Auger Hole in an Unconfined Aquifer of Finite Horizontal and Vertical Extents

The salient conclusions of this study can be enumerated as below.

1. Analytical models have been obtained for predicting flow into a uniform stressed auger hole in a homogeneous and anisotropic phreatic aquifer of finite horizontal and vertical extents and underlain by an impervious layer. Solutions have been obtained both for the cases when (i) the hole fully penetrates the aquifer and rests on the impervious base and (ii) the hole partially penetrates the aquifer and a finite distance exists between the hole and the impervious base. Equations for the hydraulic head function, the stream function and the discharge rate have been derived for all these cases. Various checks, both by comparing with other analytical models for simpler situations and by comparing with identical MODFLOW generated numerical results, have been carried out to test the accuracy of the developed solutions. The proposed analytical models can be directly utilized to translate the data obtained from a single auger hole test in an unconfined aquifer into the directional conductivities of the aquifer, provided the anisotropy ratio of the aquifer is known beforehand. In case the anisotropy ratio of the aquifer is not known *a priori*, an iterative procedure utilizing experimental data obtained from two auger hole tests of different geometries, may be employed to estimate both the anisotropy ratio as well as the directional conductivities of the aquifer.

2. The study shows that the domain of influence of an auger hole test in a phreatic aquifer of finite vertical extent and bounded below by an impervious layer does not extend to an infinitely large distance in the horizontal plane, as has been commonly assumed in the derivation of the existing auger hole seepage theories (Kirkham and Van Bavel, 1948; Boast and Kirkham, 1971; Dagan, recovery test, 1978; Barua and Tiwari, 1995), but still can be of several metres in the horizontal extent, particularly if the test is being conducted in an aquifer having a high anisotropy ratio (ratio of horizontal to vertical hydraulic conductivity of soil). However, for a test carried out in a low anisotropic aquifer, the situation may be reversed – the extent of the active zone in the horizontal plane may now be considerably small but the domain of influence of the test in the vertical plane may be, at the same time, relatively high. It is also concluded from the study that thickness of an unconfined aquifer, extent of partial penetration and level of water in an auger hole, play an important role in determining flow into the hole and hence due efforts must be made to include these variables in the mathematical analysis of the problem.

4.2 Transient Hydraulics of Flow into Fully Penetrating Ditch Drains Receiving Water from a Ponded Field

The salient findings of this study are as listed below.

1. Analytical expressions for the hydraulic head and from them, expressions for the top and side discharges have been derived for groundwater seeping through a homogeneous and anisotropic saturated soil into an array of equally spaced ditch drains receiving water from a ponded field when (i) the heights of water in the adjacent ditches are equal and the ponding field over the surface of the soil is uniform, (ii) the heights of water in the adjacent ditches are unequal and the ponding field over the surface of the soil is uniform and (iii) the heights of water in the adjacent ditches are unequal and the ponding field over the surface of the soil is non-uniform. In the mathematical derivations, it has been assumed in all the cases that the field is being underlain by an impervious barrier, all the ditches being further assumed to be dug all the way down to this barrier. By extending the time variable to go to infinity in the expressions for the hydraulic head function, top and side discharges, the corresponding steady state expressions for these quantities have also been evaluated. The accuracy of the developed models have been checked by comparing them with existing simpler steady state solutions for a few flow situation; a numerical check on the general analytical solution for the variable ponding depth problem has also been made using MODFLOW. The solutions proposed may be employed to design suitable drainage networks for reclaiming waterlogged as well as salt affected soils. For cleaning a salt affected soil, the general solution provided here can be utilized to work out an appropriate ponding field distribution over the surface of the soil so that a relatively uniform movement of water though the entire soil domain takes place. This is important because, that way, a more uniform cleaning of the soil profile can be ensured. It should be noted that leaching a salt affected soil by an array of ditch drains receiving water from a ponded field of uniform depth may lead to an uneven washing of the soil profile as numerous studies on the uniform ponded drainage problem show that, for such a situation, most of the flow to the drains will be confined to regions close to the drains and at locations faraway from the drains, very less water movement will be observed. Further, by playing with both the water level heights and the distribution of the ponded pyramid over the surface of the soil, precision cleaning in any desired location of a salt affected soil profile can also be carried out.

2. The study shows that the time taken for a transient ponded ditch drainage system to go to steady state may be considerable in a heavy soil, particularly if the anisotropy ratio and specific storage of the soil is high and the installed drains are relatively deep. Thus, among other factors remaining the same, deeper drains in soils with a high specific storage and a high anisotropy ratio have a tendency to delay this time whereas shallower ditches in soils with a low specific storage and low anisotropy ratio have an inclination to accelerate it. Also, as expected, the seepage rate to a drain with a shallower water level is found to be more than that to a drain with a higher water level. The discharges through the sides of the ditch drains as well as through the surface of the soil have also been observed to be influenced by the ponding field over the surface of the soil and also by the specific storage, directional conductivities and anisotropy ratio of the soil.

3. The uniformity of the surface flux as well the steady state streamline distributions are highly influenced by the anisotropy ratio of a soil – considering all other factors to remain as constant, a high anisotropy ratio favors a more equitable distribution of the steady state streamlines as compared to a situation when the anisotropy ratio of the soil is low. As anisotropy ratio of most natural deposits is greater than one and the existence of with anisotropic soils are also quite common in nature, the inherent anisotropy ratio of most soils, in general, favors a more even distribution of steady state streamlines resulting from a ponded ditch drainage situation. The analytical models presented here may also be utilized to work out the upper limit of water required to be pumped for reclaiming a waterlogged soil using an array of ditch drains, provided the directional conductivities as well as other flow parameters of the soil are known. They can also be employed to provide a balanced soil water environment in a crop like paddy, where there exists a standing water level on the surface of the soil. Check on the analytical solutions in this thesis were made by comparing solutions with results obtained using MODFLOW. The analytical solutions are exact whereas models such as MODFLOW are based on numerical solutions and must therefore be considered as approximate. Thus it can be argued that results such as that given in this thesis provide confidence in the model's use in more complex situations.

APPENDIX – A

Table A.1. Shape factors corresponding to a few flow geometries of Fig. 2.2

H_3/a	$(h-H_3)/H_3$	H_1/H_3	Distance of the outer boundary, b, from the centre of the auger hole, expressed as a multiple of H_3						
			$b=0.5H_3$	$b=1H_3$	$b=2H_3$	$b=3H_3$	$b=4H_3$	$b=6H_3$	$b=9H_3$
5	0.1	0.50	36.448	54.944	60.973	61.355	61.378	61.379	61.379
		0.75	28.896	44.378	49.651	49.990	50.010	50.011	50.011
		1.00	26.488	40.977	46.020	46.346	46.365	46.366	46.366
	0.5	0.50	33.423	47.669	53.404	54.167	54.266	54.280	54.280
		0.75	26.081	37.549	42.460	43.125	43.211	43.223	43.224
		1.00	23.467	33.823	38.445	39.078	39.161	39.172	39.172
	2	0.50	34.017	47.328	51.354	52.046	52.274	52.387	52.403
		0.75	26.636	37.298	40.709	41.313	41.513	41.612	41.626
		1.00	24.147	33.823	37.046	37.632	37.827	37.924	37.938
	4	0.50	34.920	48.700	52.763	53.335	53.501	53.610	53.647
		0.75	27.265	38.224	41.641	42.136	42.281	42.377	42.409
		1.00	24.948	35.075	38.371	38.860	39.004	39.099	39.132
	7	0.50	34.930	48.695	52.749	53.311	53.460	53.543	53.575
		0.75	27.307	38.296	41.725	42.214	42.345	42.418	42.445
		1.00	24.964	35.090	38.382	38.863	38.992	39.065	39.090
	10	0.50	35.389	49.099	53.074	53.621	53.765	53.842	53.867
		0.75	28.426	40.017	43.623	44.136	44.272	44.344	44.368
		1.00	25.988	36.620	40.062	40.562	40.695	40.767	40.790
10	0.1	0.50	15.901	21.200	21.478	21.565	21.570	21.570	21.570
		0.75	12.637	17.367	17.443	17.447	17.447	17.447	17.447
		1.00	11.615	14.951	16.078	16.150	16.154	16.155	16.155
	0.5	0.50	14.902	18.124	19.426	19.600	19.623	19.626	19.626
		0.75	11.710	14.340	15.453	15.604	15.623	15.626	15.626
		1.00	10.636	14.103	14.246	14.246	14.265	14.267	14.267
	2	0.50	15.206	18.202	19.107	19.265	19.317	19.342	19.346
		0.75	11.999	14.439	15.210	15.347	15.392	15.415	15.418
		1.00	10.996	13.253	13.989	14.122	14.166	14.188	14.192
	4	0.50	15.605	18.694	19.602	19.731	19.768	19.793	19.802
		0.75	12.277	14.778	15.546	15.658	15.691	15.712	15.719
		1.00	11.362	13.716	14.462	14.573	14.605	14.627	14.634
	7	0.50	15.882	18.928	19.798	19.918	19.950	19.968	19.974
		0.75	12.057	14.528	15.283	15.391	15.419	15.435	15.441
		1.00	11.207	13.502	14.228	14.335	14.364	14.383	14.390
	10	0.50	15.714	18.853	19.793	19.926	19.962	19.981	19.987
		0.75	12.237	14.689	15.428	15.534	15.562	15.577	15.582
		1.00	11.129	13.364	14.043	14.141	14.167	14.181	14.185

H_3/a	$(h-H_3)/H_3$	H_1/H_3	Distance of the outer boundary, b, from the centre of the auger hole, expressed as a multiple of H_3						
			b=0.5H_3	b=1H_3	b=2H_3	b=3H_3	b=4H_3	b=6H_3	b=9H_3
15	0.1	0.50	8.905	10.733	11.324	11.362	11.364	11.364	11.364
		0.75	7.080	8.617	9.127	9.159	9.161	9.161	9.161
		1.00	6.518	7.964	8.449	8.480	8.482	8.482	8.482
	0.5	0.50	8.466	9.859	10.421	10.496	10.506	10.508	10.508
		0.75	6.671	7.813	8.292	8.357	8.365	8.366	8.366
		1.00	6.093	7.147	7.602	7.663	7.671	7.673	7.673
	2	0.50	8.616	9.911	10.301	10.370	10.392	10.403	10.405
		0.75	6.810	7.867	8.199	8.258	8.278	8.287	8.289
		1.00	6.257	7.237	7.553	7.610	7.629	7.638	7.640
	4	0.50	8.761	10.076	10.463	10.518	10.534	10.544	10.548
		0.75	6.933	8.007	8.335	8.383	8.397	8.407	8.410
		1.00	6.408	7.413	7.729	7.775	7.789	7.798	7.801
	7	0.50	8.846	10.159	10.542	10.596	10.610	10.618	10.621
		0.75	7.103	8.210	8.548	8.597	8.610	8.617	8.620
		1.00	6.555	7.584	7.906	7.952	7.965	7.972	7.974
	10	0.50	9.108	10.463	10.851	10.904	10.919	10.926	10.929
		0.75	7.458	8.642	8.997	9.047	9.060	9.068	9.070
		1.00	7.035	8.185	8.538	8.588	8.602	8.609	8.611
20	0.1	0.50	5.768	6.785	7.114	7.135	7.136	7.136	7.136
		0.75	4.588	5.443	5.725	5.743	5.744	5.744	5.744
		1.00	4.230	5.035	5.304	5.321	5.322	5.322	5.322
	0.5	0.50	5.529	6.303	6.614	6.656	6.661	6.662	6.662
		0.75	4.366	5.001	5.266	5.302	5.306	5.307	5.307
		1.00	4.000	4.589	4.841	4.875	4.880	4.880	4.880
	2	0.50	5.628	6.347	6.564	6.601	6.614	6.620	6.621
		0.75	4.458	5.047	5.230	5.263	5.274	5.279	5.280
		1.00	4.110	4.658	4.833	4.864	4.875	4.880	4.881
	4	0.50	5.735	6.465	6.679	6.709	6.718	6.724	6.726
		0.75	4.548	5.146	5.328	5.354	5.362	5.367	5.369
		1.00	4.222	4.785	4.960	4.986	4.993	4.998	5.000
	7	0.50	5.801	6.531	6.743	6.772	6.780	6.785	6.786
		0.75	4.677	5.295	5.482	5.509	5.516	5.520	5.521
		1.00	4.338	4.916	5.094	5.120	5.127	5.131	5.132
	10	0.50	5.943	6.694	6.908	6.937	6.945	6.949	6.951
		0.75	4.875	5.531	5.726	5.753	5.761	5.765	5.766
		1.00	4.613	5.252	5.446	5.473	5.481	5.485	5.486

H_3/a	$(h-H_3)/H_3$	H_1/H_3	Distance of the outer boundary, b, from the centre of the auger hole, expressed as a multiple of H_3						
			b=0.5H_3	b=1H_3	b=2H_3	b=3H_3	b=4H_3	b=6H_3	b=9H_3
25	0.1	0.50	4.077	4.723	4.933	4.946	4.947	4.947	4.947
		0.75	3.243	3.787	3.966	3.978	3.978	3.978	3.978
		1.00	2.994	3.506	3.677	3.688	3.688	3.688	3.688
	0.5	0.50	3.929	4.421	4.618	4.644	4.648	4.648	4.648
		0.75	3.106	3.510	3.678	3.701	3.704	3.704	3.704
		1.00	2.853	3.229	3.389	3.410	3.413	3.413	3.413
	2	0.50	4.000	4.457	4.594	4.618	4.625	4.629	4.630
		0.75	3.173	3.547	3.664	3.684	3.691	3.694	3.695
		1.00	2.932	3.282	3.393	3.413	3.419	3.422	3.423
	4	0.50	4.084	4.549	4.684	4.703	4.709	4.713	4.714
		0.75	3.244	3.625	3.740	3.757	3.761	3.765	3.766
		1.00	3.022	3.382	3.493	3.509	3.514	3.517	3.518
	7	0.50	4.141	4.606	4.739	4.758	4.763	4.766	4.767
		0.75	3.351	3.746	3.864	3.881	3.885	3.888	3.888
		1.00	3.121	3.492	3.605	3.621	3.625	3.628	3.629
	10	0.50	4.221	4.696	4.831	4.850	4.855	4.857	4.858
		0.75	3.467	3.882	4.004	4.021	4.026	4.028	4.029
		1.00	3.287	3.691	3.813	3.830	3.835	3.837	3.838
30	0.1	0.50	3.053	3.500	3.645	3.654	3.655	3.655	3.655
		0.75	2.430	2.805	2.929	2.937	2.938	2.938	2.938
		1.00	2.245	2.599	2.717	2.725	2.725	2.725	2.725
	0.5	0.50	2.954	3.293	3.430	3.448	3.450	3.451	3.451
		0.75	2.338	2.617	2.733	2.749	2.751	2.751	2.751
		1.00	2.151	2.411	2.522	2.537	2.538	2.539	2.539
	2	0.50	3.007	3.323	3.417	3.434	3.439	3.442	3.442
		0.75	2.388	2.647	2.727	2.741	2.746	2.748	2.749
		1.00	2.211	2.453	2.529	2.543	2.548	2.550	2.550
	4	0.50	3.077	3.398	3.491	3.505	3.508	3.511	3.512
		0.75	2.447	2.711	2.790	2.801	2.805	2.807	2.808
		1.00	2.286	2.535	2.612	2.623	2.626	2.629	2.629
	7	0.50	3.128	3.449	3.541	3.554	3.558	3.559	3.560
		0.75	2.539	2.813	2.895	2.906	2.909	2.911	2.912
		1.00	2.374	2.632	2.710	2.721	2.724	2.726	2.727
	10	0.50	3.173	3.500	3.592	3.605	3.609	3.610	3.611
		0.75	2.609	2.894	2.978	2.989	2.993	2.994	2.995
		1.00	2.476	2.755	2.838	2.850	2.853	2.855	2.855

H_3/a	$(h-H_3)/H_3$	H_1/H_3	Distance of the outer boundary, b, from the centre of the auger hole, expressed as a multiple of H_3						
			$b=0.5H_3$	$b=1H_3$	$b=2H_3$	$b=3H_3$	$b=4H_3$	$b=6H_3$	$b=9H_3$
40	0.1	0.50	1.917	2.167	2.248	2.254	2.254	2.254	2.254
		0.75	1.526	1.737	1.806	1.810	1.811	1.811	1.811
		1.00	1.413	1.611	1.677	1.681	1.681	1.681	1.681
	0.5	0.50	1.865	2.055	2.131	2.141	2.142	2.142	2.142
		0.75	1.478	1.634	1.699	1.708	1.709	1.709	1.709
		1.00	1.364	1.510	1.571	1.579	1.581	1.581	1.581
	2	0.50	1.898	2.075	2.128	2.137	2.140	2.141	2.141
		0.75	1.510	1.655	1.699	1.707	1.710	1.711	1.711
		1.00	1.401	1.537	1.580	1.588	1.590	1.591	1.592
	4	0.50	1.876	2.053	2.114	2.125	2.128	2.129	2.129
		0.75	1.488	1.633	1.685	1.695	1.697	1.698	1.698
		1.00	1.377	1.511	1.561	1.571	1.573	1.573	1.573
	7	0.50	1.993	2.173	2.224	2.231	2.233	2.234	2.234
		0.75	1.627	1.782	1.827	1.833	1.835	1.836	1.836
		1.00	1.530	1.677	1.720	1.727	1.728	1.729	1.729
	10	0.50	2.004	2.186	2.237	2.244	2.246	2.247	2.247
		0.75	1.652	1.809	1.855	1.861	1.863	1.864	1.864
		1.00	1.571	1.725	1.770	1.777	1.778	1.779	1.779
50	0.1	0.50	1.328	1.487	1.539	1.542	1.543	1.543	1.543
		0.75	1.058	1.192	1.236	1.239	1.239	1.239	1.239
		1.00	0.980	1.106	1.148	1.151	1.151	1.151	1.151
	0.5	0.50	1.296	1.417	1.465	1.472	1.473	1.473	1.473
		0.75	1.028	1.128	1.169	1.175	1.175	1.175	1.175
		1.00	0.950	1.044	1.083	1.088	1.089	1.089	1.089
	2	0.50	1.319	1.432	1.465	1.471	1.473	1.474	1.474
		0.75	1.050	1.143	1.171	1.176	1.178	1.179	1.179
		1.00	0.977	1.064	1.091	1.096	1.097	1.098	1.098
	4	0.50	1.359	1.474	1.507	1.511	1.513	1.514	1.514
		0.75	1.084	1.178	1.207	1.211	1.212	1.212	1.213
		1.00	1.020	1.110	1.137	1.141	1.142	1.143	1.143
	7	0.50	1.396	1.511	1.543	1.548	1.549	1.550	1.550
		0.75	1.145	1.244	1.273	1.277	1.278	1.279	1.279
		1.00	1.082	1.177	1.205	1.208	1.210	1.210	1.210
	10	0.50	1.396	1.511	1.543	1.548	1.549	1.550	1.550
		0.75	1.145	1.244	1.273	1.277	1.278	1.279	1.279
		1.00	1.082	1.177	1.205	1.208	1.210	1.210	1.210

H_3/a	$(h-H_3)/H_3$	H_1/H_3	Distance of the outer boundary, b, from the centre of the auger hole, expressed as a multiple of H_3						
			b=0.5H_3	b=1H_3	b=2H_3	b=3H_3	b=4H_3	b=6H_3	b=9H_3
75	0.1	0.50	0.673	0.743	0.766	0.768	0.768	0.768	0.768
		0.75	0.536	0.595	0.615	0.616	0.616	0.616	0.616
		1.00	0.498	0.554	0.573	0.574	0.574	0.574	0.574
	0.5	0.50	0.660	0.713	0.735	0.737	0.738	0.738	0.738
		0.75	0.524	0.569	0.587	0.589	0.589	0.589	0.589
		1.00	0.486	0.528	0.545	0.547	0.548	0.548	0.548
	2	0.50	0.672	0.722	0.736	0.739	0.740	0.740	0.740
		0.75	0.536	0.577	0.589	0.592	0.592	0.593	0.593
		1.00	0.500	0.538	0.550	0.552	0.553	0.554	0.554
	4	0.50	0.695	0.746	0.761	0.763	0.763	0.764	0.764
		0.75	0.556	0.598	0.610	0.612	0.612	0.613	0.613
		1.00	0.526	0.566	0.578	0.579	0.580	0.580	0.580
	7	0.50	0.721	0.772	0.786	0.788	0.789	0.789	0.789
		0.75	0.597	0.641	0.654	0.655	0.656	0.656	0.656
		1.00	0.569	0.611	0.624	0.625	0.626	0.626	0.626
	10	0.50	0.715	0.764	0.778	0.779	0.780	0.780	0.780
		0.75	0.593	0.635	0.647	0.649	0.649	0.650	0.650
		1.00	0.566	0.608	0.620	0.621	0.622	0.622	0.622
90	0.1	0.50	0.493	0.542	0.558	0.559	0.559	0.559	0.559
		0.75	0.393	0.434	0.448	0.449	0.449	0.449	0.449
		1.00	0.366	0.404	0.417	0.418	0.418	0.418	0.418
	0.5	0.50	0.485	0.522	0.537	0.538	0.539	0.539	0.539
		0.75	0.385	0.416	0.429	0.430	0.431	0.431	0.431
		1.00	0.358	0.387	0.399	0.400	0.400	0.400	0.400
	2	0.50	0.488	0.522	0.534	0.536	0.537	0.537	0.537
		0.75	0.388	0.417	0.427	0.429	0.429	0.429	0.429
		1.00	0.361	0.388	0.398	0.399	0.400	0.400	0.400
	4	0.50	0.512	0.547	0.557	0.558	0.559	0.559	0.559
		0.75	0.409	0.438	0.447	0.448	0.448	0.449	0.449
		1.00	0.388	0.416	0.424	0.425	0.426	0.426	0.426
	7	0.50	0.501	0.536	0.545	0.547	0.547	0.547	0.547
		0.75	0.400	0.428	0.437	0.438	0.438	0.438	0.438
		1.00	0.376	0.402	0.410	0.411	0.412	0.412	0.412
	10	0.50	0.525	0.561	0.571	0.572	0.573	0.573	0.573
		0.75	0.435	0.467	0.476	0.477	0.477	0.477	0.478
		1.00	0.417	0.448	0.457	0.458	0.458	0.458	0.458

H_3/a	$(h-H_3)/H_3$	H_1/H_3	Distance of the outer boundary, b, from the centre of the auger hole, expressed as a multiple of H_3						
			b=0.5H_3	b=1H_3	b=2H_3	b=3H_3	b=4H_3	b=6H_3	b=9H_3
100	0.1	0.50	0.412	0.451	0.465	0.465	0.465	0.465	0.465
		0.75	0.328	0.362	0.373	0.373	0.373	0.373	0.373
		1.00	0.305	0.337	0.347	0.348	0.348	0.348	0.348
	0.5	0.50	0.405	0.435	0.447	0.449	0.449	0.449	0.449
		0.75	0.322	0.347	0.357	0.359	0.359	0.359	0.359
		1.00	0.299	0.323	0.332	0.334	0.334	0.334	0.334
	2	0.50	0.413	0.441	0.449	0.450	0.451	0.451	0.451
		0.75	0.330	0.353	0.360	0.361	0.361	0.361	0.361
		1.00	0.308	0.330	0.336	0.338	0.338	0.338	0.338
	4	0.50	0.428	0.456	0.464	0.466	0.466	0.466	0.466
		0.75	0.342	0.366	0.373	0.374	0.374	0.374	0.374
		1.00	0.325	0.347	0.354	0.355	0.355	0.356	0.356
	7	0.50	0.426	0.455	0.463	0.464	0.464	0.464	0.464
		0.75	0.341	0.364	0.371	0.372	0.372	0.373	0.373
		1.00	0.323	0.345	0.352	0.353	0.353	0.353	0.353
	10	0.50	0.417	0.445	0.453	0.454	0.455	0.455	0.455
		0.75	0.333	0.357	0.364	0.364	0.365	0.365	0.365
		1.00	0.313	0.334	0.341	0.342	0.342	0.342	0.342

APPENDIX – B

Derivative and integration of zero-order and first order Bessel's functions of first and second kind

$$\frac{d}{dx}[I_0(x)] = I_1(x);$$

$$\frac{d}{dx}[K_0(x)] = -K_1(x);$$

$$\int xI_0(x)dx = xI_1(x);$$

$$\int xK_0(x)dx = -xK_1(x).$$

BIBLIOGRAPHY

Abrol, I. P., Yadav, J. S. P., and Massoud, F. I. (1988). "Salt-affected soils and their management." *FAO Soils Bulletin*, Soil Resources, Management and Conservation Service, FAO Land and Water Development Division, 39, 131.

Amoozegar, A., and Wilson, G. V. (1999). "Methods for measuring hydraulic conductivity and drainable porosity." In R.W. Skaggs & J. Van Schilfgaarde, eds. *Agricultural drainage,* Agronomy Series 38. Madison, USA. 1149-1205**.**

Anderson, E. I. (2000). "The method of images for leaky boundaries." *Adv. Water Resour.,* 23(5), 461-74.

Ataie-Ashtiani, B., Shafei, B., Rashidian-Dezfouli, H., and Mohamadzadeh, M. (2012). "Capture Zone of a Partially Penetrating Well with Skin effects in Confined Aquifers." *Trans. Porous Med.* 91, 437-457.

Bair, E. S., and Lahm, T. D. (1996). "Variation in capture zone geometry of a partially penetrating pumping well in an unconfined aquifer." *Ground Water,* 24(5), 842-852.

Barrett-Lennard, E. G. (2002). "Restoration of saline land through revegetation." *Agric. Water Management,* 53, 213-226.

Barua, G. and Alam, W. (2012) **"**An analytical solution for predicting transient seepage into ditch drains from a ponded field*."* *Adv. Water Resour*., 52, 78-92 http://dx.doi.org/10.1016/j.advwatres.2012.09.002.

Barua, G., and Alam, W. (2012). "An analytical model for predicting transient flow into equally spaced ditch drains receiving water from a uniformly ponded field*."* *4th Int. Conf. Sust. Irrig. Drain.: Mangmt. Technol. and Policy*, WIT, Adelaide, Australia. (*peer-reviewed*).

Barua, G., and Bora, S. N. (2010). "Hydraulics of a partially penetrating well with skin zone in a confined aquifer." *Adv. Water Resour.,* 33, 1575-1587.

Barua, G., and Hoffmann, M. R. (2005). "Theory of seepage into an auger hole in a confined aquifer." *J. Irrig. Drain. Eng.,* 131(5), 440-50.

Barua, G., and Hoffmann, M. R. (2007). "Theory of seepage into an auger hole in a confined aquifer overlying a gravel substratum." *J. Irrig. Drain. Eng.,* 133(4), 330–341.

Barua, G., and Tiwari, K. N. (1995). "Theory of seepage into auger holes in homogeneous anisotropic soil." *J. Hydrol.,* 167, 1-22.

Barua, G., and Tiwari, K. N. (1996a). "Ditch drainage theories for homogeneous anisotropic soil." *J. Irrig. Drain. Eng.,* 122(5), 276 -285.

Barua, G., and Tiwari, K. N. (1996b). "Theories of ditch drainage in layered anisotropic soil." *J. Irrig. Drian. Eng.,* 122(6), 321-330.

Bear, J. (1972). *Dynamics of Fluids in Porous Media*. Elsevier, New York, USA.

Bear, J. (1979). *Hydraulics of Groundwater*. McGraw-Hill, New York, USA

Boast, C. W., and Kirkham, D. (1971). "Auger hole seepage theory." *Soil Sci. Soc. Am. Proc.,* 35, 365-373.

Boast, H., and Langebartel, R. G. (1984). "Shape factors for seepage into pits." *Soil Sci. Soc. Am. Proc.,* 48, 10-15.

Bouwer, H. (1989). "The Bouwer and Rice slug test-An update." *Ground Water,* 27(3), 304-309.

Bouwer, H., and Jackson, R. D. (1974). "Determining Soil Properties." In: Jan Van Schilfgaarde (editor), *Drainage for Agriculture,* Am. Soc. Agron., Madison, WI, 17, 611-672.

Bouwer, H., and Rice, R. C. (1976). "A slug test for determining hydraulic conductivity of unconfined aquifers with completely or partially penetrating wells." *Water Resour. Res.,* 12, 423-428**.**

Bouwer, H., and Rice, R. C. (1983). "The pit bailing method for hydraulic conductivity measurement of isotropic or anisotropic soil." *Trans. Am. Soc. Agric. Eng.,* 26, 1435-1439.

Braester, C., and Thunvik, R. (1984). "Determination of formation permeability by double-packer tests." *J. Hydrol.,* 72, 375-389.

Brahmabhatt, V. S., Dalwadi, G. B., Chhabra, S. B., Ray, S. S., and Dadhwal, V. K. (2000). "Land use/land cover change mapping in Mahi canal command area, Gujarat, using multi-temporal satellite data." *J. Indian Soc. Remote Sens.*, 28 (4), 221-232.

Brown, D. L., Narasimhan, T. N., and Demir, Z. (1995). "An evaluation of the Bouwer and Rice method of slug test analysis." *Water Resour. Res.,* 31(5), 1239-1246.

Cassiani, G., and Kabala, Z. J. (1998). "Hydraulics of a partially penetrating well: solution to a mixed-type boundary value problem via dual integral equations." *J. Hydrol.,* 211, 100-11.

Cassiani, G., Kabala, Z. J., and Medina Jr., M. A. (1999). "Flowing partially penetrating well: solution to a mixed-type boundary value problem." *Adv. Water Resour.,* 23(1), 59-68.

Cavelaars, J. C., Vlotman, W. F., and Spoor, G. (1994). "Subsurface drainage systems." In: *Drainage Principles and Applications,* H.P. Ritzema (ed.). Publ. 16, 2nd ed. (completely revised), ILRI, Wageningen, The Netherlands, 827-929.

Chahar, B. R., and Vadodaria, G. P. (2008a). "Steady subsurface drainage of homogeneous soil by ditches." *Proc. ICE Water Management,* 161(WM6), 303-11.

Chahar, B. R., and Vadodaria, G. P. (2008b). "Drainage of ponded surface by an array of ditches." *J. Irrig. Drain. Eng.,* 134(6), 815-23.

Chahar, B. R., and Vadodaria, G. P. (2010). "Optimal spacing in an array of fully penetrating ditches for subsurface drainage." *J. Irrig. Drain. Eng.,* 136(1), 63-67.

Chahar, B. R., and Vadodaria, G. P. (2011). "Steady subsurface drainage of ponded surface by an array of parallel ditches." *J. Hydrologic Eng.*, ASCE, accepted manuscript posted ahead of print Sept., doi: 10.1061/(ASCE)HE.1943-5584.0000518.

Chang, C. C., and Chen, C. S. (2002). "An integral transform approach for a mixed boundary problem involving a flowing partially penetrating well with infinitesimal well skin." *Water Resour. Res.,* 38(6), 1071.

Chang, C. C., and Chen, C. S. (2003). "A flowing partially penetrating well in a finite-thickness aquifer: a mixed-type initial boundary value problem." *J. Hydrol.,* 271, 101-18.

Chang, Y. C., Yeh, H. D., and Chen, G. Y. (2010). "Transient solution for radial two-zone flow in unconfined aquifers under constant-head tests." *Hydrol. Process.,* 24, 1496-1503.

Chaw, V. T., Maidment, D. R., and Mays, L. W. (1988). *Applied Hydrology*. McGraw-Hill, New York., USA

Chen, S. K., Liu, C. W. (2002). "Analysis of water movement in paddy rice fields (I) experimental studies." *J. of Hydrol.,* 260, 206-215.

Chiang, W., and Kinzelbach, W. (2001). *3D-Groundwater Modeling with PMWIN: A Simulation System for Modeling Groundwater Flow and Pollution,* Berlin, Springer-Verlag.

Childs, E. C. (1952). "The measurement of the hydraulic conductivity of saturated soil in situ. I. Principles of a proposed method." *Proc. Roy. Soc.,* London, A 215, 525-535.

Childs, E. C., Collis-George, N., and Holmes, J. W. (1957). "Permeability measurement in the field as an assessment of anisotropy and structure development." *J. Soil Sci.,* 8(1), 27-41.

Chiu, P. Y., Yeh, H. D., and Yang, S. Y. (2007). "A new solution for a partially penetrating constant-rate pumping well with a finite-thickness skin." *Int. J. Numer. Analy. Meth. Geomech.,* 31, 1659-74.

CSSRI, (2011). "Vision-2030, CSSRI Perspective Plan." Central Soil Salinity Research Institute, Indian Council of Agricultural Research, Karnal, India.

Cushman, J. and Kirkham, D., (1978). "A two-dimensional linearized view of one dimensional unsaturated-saturated flow." *Water Resour. Res*., 14, 319-323.

Dagan, G. (1978). "A note on packer, slug and recovery tests in unconfined aquifers." *Water Resour. Res.,* 14, 929-34.

Dagar, J. C. (2005). "Ecology, management and utilization of halophytes." *Ecology and Environmental Management: Issues and Research Needs*, Bulletin of the National Institute of Ecology, 15, 81-97.

Dane, J. H., and Topp, G.C. (2002). *The Soil Solution Phase. In J.H. Dane and G.C. Topp (eds.), Methods of Soil Analysis, part 4; Physical Methods*, Chapter 3. Soil Sci. of Am., Inc., Madison, WI.

Datta, K. K., and de Jong, C. (2002). "Adverse effect of Waterlogging and soil salinity on crop and land productivity in northwest region of Haryana, India." *Agric. Water Manage.,* 57, 223-238.

Datta, K. K., de Jong, C., and Sing, O. P. (2000). "Reclaiming salt-affected land drainage in Haryana, India." *Agric. Water Manage.,* 46, 55-71.

Datta, K. K., Tewari, L., and Toshi, P. K. (2004). "Impact of subsurface drainage on improvement of crop production and farm income in northwest India." *Irrig. Drain. Sys.*, 18, 43-56.

Dawson, K. J., and Istok, J. D. (1991). *Aquifer Testing: Design and Analysis of Pumping and Slug Tests*. Lewis Publishers, Inc., MI. 344.

Dielman, P. J. (1973). "Reclamation of salt-affected soils in Iraq." Publication no. 11, International Institute for Land Reclamation and Improvement, Wageningen, The Netherlands.

Dils, R. M., and Heathwaite, A. L. (1999). "The controversial role of tile drainage in phosphorus export from agricultural land." *Water Sci. Tech.,* 39, 55-61.

Dorsey, J. D., Ward, A. D., Fausey, N. D., and Bair, E. S. (1990). "A comparison of four field methods for measuring saturated hydraulic conductivity." *Trans. Am. Soc. of Agri. Eng.,* 33, 1925-1931.

Dougherty, D. E., and Babu, D. K. (1984). "Flow to a partially penetrating well in a double-porosity reservoir." *Water Resour. Res.*, 20(8), 1116-22.

Ernst, L. F. (1950*).* "A new formula for the calculation of the permeability factor with the auger hole method." Agricultural Experiment Station T.N.O., Groningen, The Netherlands.

FAO. (2000). "Crops and drops: making the best use of water for agriculture." FAO advance edition. Rome, Italy.

Faures, J. M., Hoogeveen, J., and Bruinsma, J. (2002). *The FAO irrigated area forecast for 2030,* FAO, Rome, Italy.

Faybishenko, B. A., Javandel, A. I., and Witherspoon, P. (1995). "Hydro-dynamics of the capture zone of a partially penetrating well in a confined aquifer." *Water Resour. Res.,* 31(4), 859-866.

Fitts, C. R. (2002). *Groundwater Science*. San Diego, Academic Press. USA.

Fukuda, H. (1957). "Underdrainage into ditches in soil overlying an impervious substratum." *Trans. Am. Geophys. Union,* 38(5), 730-39.

Goswami, D., and Kalita, P. K. (2009). "Simulation of base-flow and tile-flow for storm events in a subsurface drained watershed." *Biosystems Eng.,* 102, 227-235. doi:10.1016/j.biosystemseng.2008.11.004.

Goswami, D., and Kalita, P. K. (2010). "Modeling and simulation of base-flow to drainage ditches during low-flow period." *Water Resour. Mangmt.,* 24, 173-191. doi:10.1007/s11269-009-9443-0

Grisak, G.E., and Cherry, J.A. (1975). "Hydrologic charecteristics and response of fractures till and clay confining a shallow aquifer." *Can. Geotech. J.* 12(23), 23-43.

Gringarten, A. C., and Ramey, H. J. Jr. (1975). "An approximate infinite conductivity solution for a partially penetrating line-source well." *Soc. Pet. Eng. J.,* 259, 140-48.

Grubb, S. (1993). "Analytical model for estimation of steady-state capture zones of pumping wells in confined and unconfined aquifers." *Ground Water,* 31(1), 27-32.

Haitjema, H. M., and Kramer, S. R. (1988). "A new analytic function for modeling partially penetrating wells." *Water Resour. Res.,* 24 (5), 683-690.

Haitjema, H. M. (2006). "The role of hand calculations in ground water flow modeling." *Ground Water,* 44(1), 102-105.

Hantush, M. S. (1964). "Hydraulics of Wells", In Advances in Hydroscience (V.T. Chow editor), Vol. 1, 281-432, Academic Press, New York, USA.

Hathoot, H. M. (1998). "Theory of pipe drainage assisted by mole drainage." *J. Irrig. Drainage,* 124 (2), 102-107.

Healy, K. H., and Laak, R. (1973). "Factors affecting the percolation test." *J. Water Pollut. Control Fed.,* 45, 1508-1516

Heathwaite, A. L., and Dils, R. M. (2000). "Characterising phosphorus loss in surface and subsurface hydrological pathways." *The Sci. of the Tot. Environ.,* 251/252, 523-538.

Hendry, M. J. (1982). "Hydraulic conductivity of a glacial till in Alberta." *Ground Water,* 20(2), 162-169.

Hyder, Z., Butler Jr., J. J., McElvee, C. D., and Liu, W. (1994). "Slug tests in partially penetrating wells." *Water Resour. Res.,* 30(11), 2945-57.

Hyder, Z., and Butler Jr., J. J. (1995). "Slug tests in unconfined formations: An assessment of the Bouwer and Rice technique." *Ground Water,* 33 (1), 16-22.

ICID (International Commission on Irrigation and Drainage), (2003). "Important data of ICID Member Countries." *Int. Comm. Irrig. Drain*., database on website: htt://www.icid.org.

IDNP (Indo-Dutch Network Project), (2002). "Recommendations on Waterlogging and Salinity Control Based on Pilot Area Drainage Research." Indo-Dutch Network Project, Cen. Soil Sal. Res. Inst., Karnal, India, 56 pp.

Ilyinsky, N. B., and Kacimov, A. R. (1992). "Problems of seepage to empty ditch and drain." *Water Resour. Res.,* 28(3), 871-77.

Javandel, I., and Tsang, C. F. (1986). "Capture-zone types curves: A tool for aquifer cleanup." *Ground Water,* 24(5), 616-625.

Jia, X., Dukes, M. D., Jacobs, J. M., and Irmak, S. (2006). "Weighing lysimeters for evapotranspiration research in a humid environment." *Trans ASAE.,* 49(2), 401-412.

Johnson, H. P., Frevert, R. K., and Evans, D. D. (1952). "Simplified procedure for the measurement and computation of soil permeability below water table." *Agricultural Engineering*, 283-286.

Kacimov, A. R. (1997). ''Optimization of seepage rate through a triangular core.'' *Int. J. for Numer. Analy. Meth. Geomech.,* 21, 443-451.

Kacimov, A. R. (2000). "Analytical solution for transient flow into hemispherical auger hole." *J. Hydrol.,* 228, 1-9.

Kacimov, A. R. (2006). "Seepage to a drainage ditch and optimization of its shape." *J. Irrig. Drain. Eng.,* 132(6), 619-22.

Kessler, J., and Oosterbaan, R. J. (1980). "Determining hydraulic conductivity of soils." In: *Drainage Principles and Applications*. Second Ed., Publication 16, III, ILRI, Wageningen, The Netherlands, 254-296.

Khan, M.Y., and Kirkham, D. (1971). "Steady-state flow around a well in a two-layered aquifer." *Water Resour. Res.,* 7, 155-165.

Kirkham, D. (1940). "Artificial drainage of land: Streamline experiments. The artesian basin – II." *Trans. Am. Geophys. Union,* 21, 587-93.

Kirkham, D. (1945). "Artificial drainage of land: Streamline experiments. The artesian basin – III." *Trans. Am. Geophys. Union,* 26(III), 393-406.

Kirkham, D. (1949). "Flow of ponded water into drain tubes in soil overlying an impervious layer." *Trans. Am. Geophys. Union,* 30(3), 369-385.

Kirkham, D. (1950). "Seepage into ditches in the case of a plane water table and an impervious substratum." *Trans. Am. Geophys. Union,* 31(3), 425-30.

Kirkham, D. (1951). "Seepage into drain tubes in stratified soil." *Trans. Am. Geophys. Union,* 32(3), 433-42.

Kirkham, D. (1954). "Seepage of artesian and surface water into drain tubes in stratified soil." *Trans. Am. Geophys. Union,* 35(5), 775-90.

Kirkham, D. (1957). "Theory of land drainage: The ponded water case." In: Luthin JN, editor, *Drainage of agricultural lands*, Vol. 7, Madison, Wisconsin.

Kirkham, D. (1958). "Theory of seepage into an augur hole above an impermeable layer." *Soil Sci. Soc. of Am. Proc.,* 22 (3), 204-208.

Kirkham, D. (1959). "Exact theory of flow into a partially penetrating well." *J. Geophys. Res.,* 64(9), 1317-1327.

Kirkham, D. (1960). "Seepage into ditches in the case of a plane water table overlying a gravel substratum." *Trans. Am. Geophys. Union,* 65(4), 1267-72.

Kirkham, D. (1964). "Exact theory for the shape of the free water surface about a well in a semiconfined aquifer." *J. Geophysical Res.,* 69, 2537-2549.

Kirkham, D. (1965). "Seepage of leaching water into drainage ditches of unequal water level height." *J. Hydrol.,* 3, 207-24.

Kirkham D. (1967). "Explanation of paradoxes in Dupuit–Forchheimer seepage theory." *Water Resour. Res.,* 1967; 3(2), 609-622.

Kirkham, D., and Powers, W. L. (1972). *Advanced Soil Physics.* Wiley-Interscience, New York.

Kirkham, D., and Sotres, M.O. (1978). "Casing depths and solute travel times to wells." *Water Resour. Res.,* 14, 237-243.

Kirkham, D., and Sotres, M.O. (1979). "Influence of cover slab diameter on solute travel time to wells." *Water Resour. Res.,* 15(4), 941-948.

Kirkham. D., Toksoz, S., and Van Der Ploeg, R. R. (1974). "Steady flow to drains and wells." In: Schilfgaarde JV, editor, *Drainage for agriculture*, Am. Soc. of Agron., Vol. 17, Madison, Wisconsin.

Kirkham, D., and Van Bavel, C. H. M. (1948). "Theory of seepage into auger holes." *Soil Sci. Soc. Am. Proc.,* 13, 75-82.

Kirkham, D., van der Ploeg, R. R., and Horton, R. (1997). "Potential theory for dual-depth subsurface drainage of ponded land." *Water Resour. Res.,* 33: 1643-1654.

Kresic, N. (1997). *Quantitative Solution in Hydrogeology and Groundwater Modeling*. Lewis Publishers, New York, USA.

Kresic, N. (2007). *Hydrogeology and Groundwater Modeling.* Second Edition, CRO Press, New York. USA.

Kroger, R., Cooper, C. M., and Moore, M. T. (2008). "A preliminary study of an alternative controlled drainage strategy in surface drainage ditches: low-grade weirs." *Agric. Water Management,* 95, 678-684.

Lee, T. C., and Damiata, B. N. (1995). "Distortion in resistivity logging as shallow depth." *Geophys.,* 60, 1058-69.

Liu, S., Xingguo, M., Haibin, L., Gongbing, P., and Alan, R. (2001). "Spatial variation of soil moisture in China: Geostatistical characterization." *J. Meteorol. Soc. Japan,* 79, 555-574.

Lomen, D. O., Warrick, A. W., and Zhang, R. (1987). "Determination of hydraulic conductivity from auger holes and pits – an approximation." *J. Hydrol.,* 90, 219-229.

Luthin, J. N., and Gaskell, R. E. (1950). "Numerical solutions for the tile drainage of layered soils." *Trans. Am. Geophys. Union,* 31(4), 595-602.

Luthin, J. N. (1957). *Drainage of Agricultural Lands*. Am. Soc. Agron., Vol. 7, Madison, WI, 420-432.

Maasland, M. (1957). "Soil anisotropy and land drainage." In Luthin, J.N., *Drainage of Agricultural Lands*. Am. Soc. Agron., Madison, Wisconsin, 216-285.

MacDonald, A. M., Maurice, L., Dobbs, M. R., Reeves, H. J., and Auton, C. A. (2012). "Relating in situ hydraulic conductivity, particle size and relative density of superficial deposits in a heterogeneous catchment." *J. Hydrol.,* 434-435.

Manjunatha, M. V., Oosterbaan, R. J., Gupta, S. K., Rajkumar, H., and Jansen, H. (2004). "Performance of subsurface drains for reclaiming waterlogged saline under rolling topography in Tungabhadra irrigation project in India." *Agric. Water Management,* 69, 69-82.

Martinez-Beltran, J. (1978). "Drainage and reclamation of salt affected soils in the Bardenas area, Spain." ILRI Publication 24, Wageningen, The Netherlands.

Martinez-Beltran, J., and Manzur, C. L. (2005). "Overview of salinity problems in the world and FAO strategies to address the problem." In: *Proceedings of the International Salinity Forum*, Riverside, California, 311-313.

Melvile, J. G., Molz, F. J., Guven, O., and Widdowson, M. A. (1991). "Multi-level slug tests with comparisons to tracer data." *Ground Water,* 29(6), 897-907.

Milne-Thomson, L. M. (1960). *Theoretical Hydrodynamics.* Macmillan, New York.

Mohanty, B. P., Kanwar, R. S., and Everts, C. J. (1994). "Comparison of saturated hydraulic conductivity measurement methods for a glacial till soil." *Soil Sci. Soc. Am. J.,* 58, 672-677.

Muskat, M. (1937). *The flow of homogeneous fluids through porous media*. McGraw-Hill, New York. (second printing by J. W. Edwards, Ann Arbor, Michigan, 1946, p.763).

Neuman, S. P., (1975). "Analysis of pumping test data from anisotropic unconfined aquifers considering delayed gravity response." *Water Resour. Res.* 11(2), 329-342.

Nunes, L. M., Dill, C. A., Riberiro, L., and Vieira, J. (2002). "Mixed analytical and numerical modeling of an oceanic peninsula using the Dupuit-Ghyben-Herzberg approach." *Proc. of Model Calibration and Reliability in Groundwater Modeling: A Few Steps Closer to Reality*, IAHS Publ. no. 277, Prague. Czech. Republic, 239-246.

Odhiambo, L. O., and Murty, V. V. N. (1996). "Modeling water balance components in relation to field layout in lowland paddy fields I. Model development." *Agric. Water Management,* 30, 185-199.

Olson, R. E., and Daniel, D. E., (1981). "Measurment of the Hydraulic Conductivity of Fine-Grained Soils". *Permeability and Groundwater Contamination Transport*, ASTM STP 746, 18-64.

Oosterbaan, R. J., and Nijland, H. J. (1994). "Determining the saturated hydraulic conductivity." *Drainage Principles and Applications,* H.P. Ritzema, ed., 2nd ed., ILRI Publ. 16, Wageningen, The Netherlands, 435-476.

Papadopulos, A. S., and Copper Jr., H. H. (1967). "Drawdown in a well of large diameter." *Water Resour. Res.*, 8(1), 241-244.

Pasandi, M., Samani, N., and Barry, D. A. (2008). "Effect of wellbore storage and finite thickness skin on flow to a partially penetrating well in a phreatic aquifer." *Adv. Water Res.,* 31(2), 383-98.

Perina, T., and Lee, T. C. (2006). "General well function for pumping from a confined, leaky, or unconfined aquifer." *J. Hydrol.*, 317, 239-60.

Rao, K. V. G. K., and Leeds-Harrison, P. B. (1991). "Desalination with subsurface drainage." *Agric. Water Management,* 19, 303-11.

Reeve, R. C., and Kirkham, D. (1951). "Soil anisotropy and some field methods for measuring permeability." *Trans. Am. Geophys. Union,* 32, 582-590.

Rengasamy, P. (2006). "World saliization with emphasis on Australia." *J. Exp. Botany,* 57(5), 1017-1023.

Reynolds, W. D., and Zebchuk, W. D. (1996). "Hydraulic Conductivity in a clay soil: Two measurement techniques and Spatial Charectization." *Soil. Sci. Soc. of Am. J.* 60(6), 1679-1685.

Rhoades, J. D. (1974). "Drainage for salinity control." Chap. 16, pages 433-461 in J. van Schilfgaarde, ed. *Drainage for Agriculture*, Agronomy Monograph 17, Am. Soc. of Agron., Madison, WI.

Rhodes, J. D., Kandiah, A., and Mashali, A. M. (1992). "The use of saline waters for crop production, water conservation and environmental protection: Guidelines on water, soil and crop management." *FAO Irrigation and Drainage*, paper no. 48, FAO, Rome, 133.

Ritzema, H. P., Satyanarayana, T. V., Raman, S., and Boonstra, J. (2008). "Subsurface drainage to combat water logging and salinity in irrigated lands in India: Lessons learned in farmer's field." *Agric. Water Management,* 95, 179-189.

Ruud, N. C., and Kabala, Z. J. (1997). "Response of a partially penetrating well in a heterogeneous aquifer: Integrated well-face flux vs. uniform well-face flux boundary conditions." *J. Hydrol.,* 194, 76-94.

Scarborough, J. B. (1966). *Numerical Mathematical Analysis.* 6th ed. New Delhi: Oxford and IBH Publishing Company Private Limited, 203-207..

Schafer, D. C. (1996). "Determining capture zones in homogeneous anisotropic aquifers." *Ground Water,* 34(4), 628-639.

Selim, M. S., and Kirkham, D. (1974). "Screen theory for wells and soil drain pipes." *Water Resour. Res.,* 10(5), 1019-30.

Shan, C. (1999). "An analytical solution for the capture zone of two arbitrarily located wells." *J. Hydrol.,* 222, 123-128.

Sharp, J. M. (1984). "Hydrogeologic characteristics of shallow glacial drift aquifers in dissected till plains (North-central Missouri), *Ground Water*, 22(6), 683-689.

Shaver, R. B. (1998). "The determination of Glacial till specific storage in North Dakota." *Ground Water*, 36(4). 552-557.

Sharma, D. P., and Gupta, S. K. (2006). "Subsurface drainage for reversing degradation of waterlogged saline lands." *Land Degradation and Development,* 17(6), 605-614.

Sharma, R. C., Rao, B. R. M., and Saxena, R. K. (2004). "Salt Affected soils in India-Current Assessment." *In: Advances in Sodic Land Reclamation,* International Conference on Sustainable Management of Sodic Lands, Lucknow, India, 1-26.

Skaggs, R.W. and Van Schilfgaarde J.,(eds.) (1999). "Agricultural drainage." Number 38 in the series Agronomy, *Am. Soc. of Agron., Crop Science Soc. America, Soil Sci. Soc. Am.*, Madinson, Wisconsin, USA

Smedema, L. K., and Rycroft, D. W. (1983). "Land drainage: planning and design of Agricultural Drainage Systems." Batsford, London, p.376.

Smith, A. S., and Mullins, C. E., (2000). *Soil and Environmental Analysis: Physical Method,. Revised and Expanded (2d ed.)*, Marcel Dekker, Inc., CRC press, New York, USA.

Stibinger, J. (2009). "Terrain experimental measurement of saturated hydraulic conductivity on paddy fields in Taoyuan (Taiwan) during the cycle of flooded period." *Agricultura. Tropica. et subtropica.,* 42(2), 82-89.

Tabuchi, T. (2004). "Improvement of paddy field drainage for mechanization." *Paddy Water Environ.,* 2004, 2:5-10, doi:10.1007/s10333-004-0034-7.

Talsma, T. (1960). "Measurement of soil anisotropy with piezometers." *J. Soil. Sci.,* 11(1), 159-1711.

Topp, G. C., Zebchuk, W. D. (1986). "An evaluation of screening tests for soil conditioners." *Can. J. Soil Sci.,* 66, 45-49.

Van Bavel, C. H. M., and Kirkham, D. (1948). "Field measurement of permeability using auger holes." *Soil Sci. Soc. Am. Proc.,* 13, 90-96.

Van Beers, W. F. J. (1958). "The Auger-Hole Method: A field measurement of the hydraulic conductivity of soil below the water table." International Institute for Land Reclamation and Improvement, Bull. 1. Wageningen, The Netherlands.

Van Beers, W. F. J. (1983). "The auger-hole method; a field measurement of the hydraulic conductivity of soil below the water table." 6th edition. ILRI Bulletin 1. Wageningen, The Netherlands, ILRI.

Van Hoorn, J. W., and Van Alphen, J. G. (1994). "Salinity control." In H.P. Ritzema, ed. *Drainage Principles and Applications*, 2nd edition. ILRI Publication 16, Wageningen, The Netherlands, 533-600.

Van Rooy, D. (1988). "A note on the computerized interpretation of slug test data." *Progress Report 66,* Institute of Hydrodynamics and Hydraulic Engineering, Technical University of Denmark.

Walton, W. C. (1979). "Progress in analytical groundwater modeling." *J. of Hydrol.,* 43, 149-159.

Walton, W. C. (1989). *Analytical Ground Water Modeling*. Lewis Publishers, Chelsea, Michigan, USA.

Wang, J. F., and Anderson, M. P. (1982). *Introduction to Groundwater Modeling*. Freeman, San Francisco, CA, p.237..

Warrick, A. W., and Kirkham, D. (1969). "Two-dimensional seepage of ponded water to full ditch drains." *Water Resour. Res.,* 5(3), 685-93.

Wesseling, J., Wijk, W. R., Fireman, M., Van't Woudt, B. D. and Hagan, R. M. (1957). "Land drainage in relation to soils and crops." In J.N Luthin (ed.) 1957, *Drainage of Agriculture Lands*, Am. Soc. Agron. Monograph 7, Chapter 5, Madison, Wisc., U.S.A.

Widdowson, M. A., Molz, F. J., and Melville, J. G. (1990). "An analysis technique for multilevel and partially penetrating slug test data." *Ground Water,* 28(6), 937-45.

Wild, A. (2003). *Soils, land and food: managing the land during the twenty-first century*. Cambridge, UK, Cambridge University Press.

Yang, S. Y., and Yeh, H. D. (2002). "Solution for flow rates across the wellbore in a two-zone confined aquifer." *J. Hydraul. Eng.,* 128(2), 175-83.

Yang, S. Y., and Yeh, H. D. (2004). "A simple approach using Bouwer and Rice's method for slug test data analysis." *Ground Water,* 42(5), 781-84.

Yeh, H. D., Yang, S. Y., and Peng, H. Y. (2003). "A new closed-form solution for a radial two-layer drawdown equation for groundwater under constant-flux pumping in a finite-radius well." *Adv. Water Res.,* 26(7), 747-57.

Yeo, W., and Lee, Kang-Kun. (2003). "Analytical solution for arbitrarily located multiwells in an anisotropic homogeneous confined aquifer." *Water Resour. Res.,* 39(5), 1133, doi: 10.1029/2003WR002047.

Youngs, E. G. (1968). "Shape factors for Kirkham's piezometer method for determining the hydraulic conductivity of soil overlying an impermeable floor or infinitely permeable stratum." *Soil Sci.,* 106, 235-237.

Youngs, E. G. (1982). "Calculations of ponded water drainage for flow regions of various geometries to demonstrate effect of disturbed soil-zone shape on drain performance." *J. Agric. Eng. Res.,* 27. 441-54.

Youngs, E. G. (1986). "Water-table heights in drained anisotropic homogeneous soils". *Agric. Water Management*. 11 (1), 1-11.

Youngs, E. G. (1988). "Soil physics and hydrology." *J. of Hydrol.,* 100, 411-431.

Youngs, E. G. (1994). "Seepage to ditches from a ponded surface." *J. Hydrol.,* 161, 145-54.

Youngs, E. G., and Leeds-Harrison, R. B. (2000). "Improving efficiency of desalinization with subsurface drainage." *J. Irrig. and Drain. Eng.,* 126(6), 375-80.

Zaslavsky, D. (1979). "Drainage for salt leaching." In: Wesseling J, editor. *Proceedings of the international drainage workshop*, International Institute for Land Reclamation and Improvement, Vol 25, Wageningen.

Zlotnik, V. A. (1994). "Interpretation of slug and packer tests in anisotropic aquifers." *Ground Water,* 32(5), 761-766.

Zlotnik, V. A. (1997). “Effect of anisotropy on the capture zone of a partially penetrating well in a confined aquifer.” *Ground Water,* 35(5), 842-847.

Zlotnik, V. A., Goss, D., and Duffield, G. M. (2010). “Generally steady-state shape factor for a partially penetrating well.” *Ground Water,* 48(1), 111-116.